

MYCOBACTERIUM TUBERCULOSIS VIRULENCE FACTOR MPT64 TARGETS THE
ENDOPLASMIC RETICULUM

APPROVED BY SUPERVISORY COMMITTEE

Michael Shiloh, M.D., Ph.D.

Vanessa Sperandio, Ph.D.

Neal Alto, Ph.D.

Sebastian Winter, Ph.D.

ACKNOWLEDGEMENTS

I must first thank my mentor, Michael Shiloh. While I am not his first student to graduate, I was the first to join after rotating and it has been wonderful to go through the entire process with him. I have appreciated both Michael's willingness to be directly involved with experimental design and interpretation and, more recently, his encouragement for my developing scientific independence. I'm grateful for all Michael's positive encouragement including much needed pep-talks and his unwavering support towards my scientific career. Finally, it has been fulfilling to grow as a scientist as the lab itself grew and changed.

I would like to acknowledge the members of the Shiloh Lab past and present. While this work was presented as an individual accomplishment, science is strongest when it is performed in collaboration. Thank you for training me, being willing to lend a hand towards any experiments and for providing helpful advice at lab meetings and during stressful situations. I must especially thank Breanna, Vidhya and Luis for their help with animal experiments, Sujitra, Molly and Patrick for collecting vital screening data and Haaris for being willing to listen and provide insightful scientific and professional advice.

Thank you to my graduate committee, Vanessa Sperandio, Neal Alto, and Sebastian Winter. I always left committee meetings feeling rejuvenated and excited for the next phase of my graduate career. Thank you especially for each providing unique perspectives to the interpretation and design of my experiments, and more recently for echoing Michael's positivity towards my scientific career. Finally, this study was borne out of a fantastic collaboration with Neal Alto's lab and I would like to extend my gratitude to

him and his lab for their willingness to provide reagents and resources anytime I requested them.

Lastly, I would like to thank my family and friends. To my parents and grandmothers, thank you for always supporting my educational endeavors even when they took me a thousand miles away. I wouldn't be half the woman and scientist without their constant love and encouragement. I'm grateful to Katie and "Chef" Lucas for their positive thoughts and comic relief. They are my reminder to appreciate the relationships we make outside of family. I would like to extend the most gratitude to my best friends Brett and Breanna for always providing a shoulder to lean on and reminding me to have fun throughout graduate school. We have a special connection that cannot be broken by distance. Finally, I am eternally thankful for my boyfriend, my anchor, Stephen. He has provided me with steadfast understanding and patience throughout this journey.

MYCOBACTERIUM TUBERCULOSIS VIRULENCE FACTOR MPT64 TARGETS THE
ENDOPLASMIC RETICULUM

by

CHELSEA ELIZABETH STAMM

DISSERTATION

Presented to the Faculty of the Graduate School of Biomedical Sciences

The University of Texas Southwestern Medical Center at Dallas

In Partial Fulfillment of the Requirements

For the Degree of

DOCTOR OF PHILOSOPHY

The University of Texas Southwestern Medical Center at Dallas

Dallas, Texas

May, 2019

Copyright

by

Chelsea Elizabeth Stamm, 2019

All Rights Reserved

MYCOBACTERIUM TUBERCULOSIS VIRULENCE FACTOR MPT64 TARGETS THE
ENDOPLASMIC RETICULUM

Chelsea Elizabeth Stamm, Ph.D.

The University of Texas Southwestern Medical Center at Dallas, 2019

Supervising Professor: Michael U. Shiloh, M.D., Ph.D.

Mycobacterium tuberculosis, the causative agent of tuberculosis, is one of the most successful human pathogens. One reason for its success is that *M. tuberculosis* can reside within host macrophages, a cell type that normally functions to phagocytose and destroy infectious bacteria. However, *M. tuberculosis* is able to evade macrophage defenses in order to survive for prolonged periods of time. Many intracellular pathogens secrete virulence factors targeting host membranes and organelles to remodel their intracellular environmental niche. I hypothesized that *M. tuberculosis* secreted proteins that target host membranes are vital for *M. tuberculosis* to adapt to and manipulate the host environment for survival. Thus, I characterized nearly 200 secreted proteins from *M.*

tuberculosis for their ability to associate with eukaryotic membranes using a live-dead, temperature sensitive yeast screen and to manipulate host trafficking pathways using a modified inducible secretion screen. I identified five *M. tuberculosis* secreted proteins that both associated with eukaryotic membranes and altered the host secretory pathway. One of these secreted proteins, Mpt64, localized to the endoplasmic reticulum during *M. tuberculosis* infection of murine and human macrophages and impaired the unfolded protein response in macrophages. These data highlight the importance of secreted proteins in *M. tuberculosis* pathogenesis and provide a basis for further investigation into their molecular mechanisms.

TABLE OF CONTENTS

PREFACE	vi
TABLE OF CONTENTS	viii
PRIOR PUBLICATIONS	xi
LIST OF FIGURES	xii
LIST OF TABLES	xiv
LIST OF APPENDICES	xv
LIST OF DEFINITIONS	xvi
CHAPTER 1: INTRODUCTION AND REVIEW OF THE LITERATURE	1
<i>Mycobacterium tuberculosis</i>	1
Intracellular survival of <i>M. tuberculosis</i>	2
Secretion systems of other bacterial pathogens are required for survival	2
<i>M. tuberculosis</i> secretion systems and substrates	7
Summary of results	8
CHAPTER 2: MATERIALS AND METHODS	10
CHAPTER 3: IDENTIFICATION AND SCREENING OF MYCOBACTERIAL SECRETED PROTEINS	28
INTRODUCTION	28
RESULTS	29
Categorization of putative effector-like proteins from Mtb	29
Mtb encodes secreted proteins that interact with eukaryotic membranes ...	30
Subcellular localization of membrane-localizing MSP	34
Mycobacterial secreted proteins do not affect yeast sensitivity to calcofluor	

white	37
A subset of mycobacterial secreted proteins alters eukaryotic vesicular transport	40
DISCUSSION	42
CHAPTER 4: CHARACTERIZATION OF MPT64 MEMBRANE BINDING AND VIRULENCE FUNCTIONS	44
INTRODUCTION	44
RESULTS	45
Mpt64 does not interact with lysozyme from two species	45
Mpt64 N-terminus is important for ER localization and inhibition of vesicular trafficking	47
Mpt64 ER localization depends on its N-terminus	50
Probing Mpt64 protein-protein interactions through yeast two hybrid	53
Mpt64 interacts with phosphatidylinositol phosphates in vitro	57
Mpt64 ER localization in yeast is dependent on PI3P and PI(3,5)P ₂	57
Secreted Mpt64 localizes to the ER during infection	61
Mpt64 does not inhibit cytokine secretion during macrophage infection	65
Mpt64 inhibits the unfolded protein response	67
Mpt64 contributes to the Mtb modulation of the unfolded protein response during infection	69
Mpt64 contributes to early Mtb growth after aerosol infection of mice	71
Mpt64 localized to the ER in primary human macrophages but is dispensable for Mtb survival	73

DISCUSSION	77
CHAPTER 5: CONCLUSIONS AND RECOMMENDATIONS	80
DISCUSSION OF RESULTS	80
Identification and screening of mycobacterial secreted proteins	80
Characterization of mpt64 membrane binding and virulence functions	82
DISCUSSION OF CONTINUING EXPERIMENTS	86
Characterization of MSP through novel screening	85
Unbiased approaches to uncover the function of Mpt64	86
BIBLIOGRAPHY.....	102

PRIOR PUBLICATIONS

Nair VR, Franco LH, Zacharia VM, Khan HS, **Stamm CE**, You W, Marciano DK, Yagita H, Levine B, Shiloh MU. Microfold Cells Actively Translocate *Mycobacterium tuberculosis* to Initiate Infection. *Cell Rep.* 2016. 16(5):1253-58.

Scharn CR, Collins AC, Nair VR, **Stamm CE**, Marciano DK, Graviss EA, Shiloh MU. Heme Oxygenase-1 Regulates Inflammation and Mycobacterial Survival in Human Macrophages during *Mycobacterium tuberculosis* Infection. *J. Immunol.* 2016. 196(11):4641-9.

Collins AC, Cai H, Li T, Franco LH, Li XD, Nair VR, Scharn CR, **Stamm CE**, Levine B, Chen ZJ, Shiloh MU. Cyclic GMP-AMP Synthase Is an Innate Immune DNA Sensor for *Mycobacterium tuberculosis*. *Cell Host Microbe.* 2015. 17(6):820-8.

Stamm CE, Collins AC, Shiloh MU. Sensing of *Mycobacterium tuberculosis* and consequences to both host and bacillus. *Immunol. Rev.* 2015. 264(1):204-19.

West JD, **Stamm CE**, Brown HA, Justice SL, Morano KA. Enhanced toxicity of the protein cross-linkers divinyl sulfone and diethyl acetylenedicarboxylate in comparison to related monofunctional electrophiles. *Chem. Res. Toxicol.* 2011. 24(9):1457-9.

West JD, **Stamm CE**, Kingsley PJ. Structure-activity comparison of the cytotoxic properties of diethyl maleate and related molecules: identification of diethyl acetylenedicarboxylate as a thiol cross-linking agent. *Chem. Res. Toxicol.* 2011. 24(1):81-8.

LIST OF FIGURES

FIGURE 1. INTERACTION OF BACTERIAL PATHOGENS WITH THE HOST ENDOMEMBRANE SYSTEM	6
FIGURE 2. <i>M. TUBERCULOSIS</i> SECRETED PROTEINS INTERACT WITH YEAST MEMBRANES	32
FIGURE 3. HOST SUBCELLULAR LOCALIZATION OF MEMBRANE-BINDING MSP	35
FIGURE 4. MYCOBACTERIAL SECRETED PROTEINS DO NOT ALTER YEAST SENSITIVITY TO CALCOFLUOR WHITE	38
FIGURE 5. <i>M. TUBERCULOSIS</i> SECRETED PROTEINS ALTER hGH RELEASE	41
FIGURE 6. RECOMBINANT MPT64 DOES NOT INTERACT WITH LYSOZYME	46
FIGURE 7. hGH RELEASE INHIBITION IS DEPENDENT ON MEMBRANE LOCALIZATION OF MPT64.....	48
FIGURE 8. MPT64 LOCALIZES TO THE ENDOPLASMIC RETICULUM DURING HETEROLOGOUS EXPRESSION IN YEAST AND HeLa CELLS	51
FIGURE 9. MPT64 DOES NOT INTERACT WITH THE SODIUM/POTASSIUM ATPASE BETA CHAIN	56
FIGURE 10. MPT64 BINDS PHOSPHATIDYLINOSITOL PHOSPHATES TO MEDIATE ITS ER LOCALIZATION.....	59
FIGURE 11. MPT64 ER LOCALIZATION IS ESX1-DEPENDENT DURING <i>M.</i> <i>TUBERCULOSIS</i> INFECTION.....	63

FIGURE 12. MPT64 DOES NOT INHIBIT CYTOKINE SECRETION IN MACROPHAGES	66
FIGURE 13. MPT64 INHIBITS THE UNFOLDED PROTEIN RESPONSE	68
FIGURE 14. MPT64 CONTRIBUTES TO THE MTB MODULATION OF THE UNFOLDED PROTEIN RESPONSE DURING INFECTION	70
FIGURE 15. MPT64 CONTRIBUTES TO EARLY MTB GROWTH AFTER AEROSOL INFECTION OF MICE	72
FIGURE 16. MPT64 LOCALIZATION AND IMPACT ON SURVIVAL IN PRIMARY HUMAN MACROPHAGES	75
FIGURE 17. EXPRESSION AND PURIFICATION OF RECOMBINANT MPT64 TRUNCATIONS	98
FIGURE 18. CONSTRUCTION AND PHENOTYPIC ANALYSIS OF MTB Δ MPT64	99
FIGURE 19. SECRETED MPT64 CO-LOCALIZES WITH CALRETICULIN IN MURINE MACROPHAGES	100
FIGURE 20. SECRETED MPT64 CO-LOCALIZES WITH CALRETICULIN IN HUMAN MACROPHAGES	101

LIST OF TABLES

TABLE 1. PRIMERS USED IN THIS STUDY	27
TABLE 2. CHARACTERIZATION OF MYCOBACTERIAL SECRETED PROTEINS	88
TABLE 3. MTB PROTEINS THAT RESCUED YEAST GROWTH IN RAS RESCUE ASSAY	94
TABLE 4. MTB PROTEINS THAT EXCEEDED CUT-OFFS IN hGH RELEASE ASSAY	96

LIST OF APPENDICES

APPENDIX A: CHARACTERIZATION OF MYCOBACTERIAL SECRETED PROTEINS	88
APPENDIX B: SUMMARY OF HITS FROM RAS RESCUE ASSAY	94
APPENDIX C: SUMMARY OF HITS FROM hGH RELEASE ASSAY	96
APPENDIX D: PURIFICATION OF RECOMBINANT MPT64	98
APPENDIX E: CHARACTERIZATION OF MPT64 DELETION MUTANT.....	99
APPENDIX F: LOCALIZATION OF MPT64 IN MURINE MACROPHAGES	100
APPENDIX G: LOCALIZATION OF MPT64 IN PRIMARY HUMAN MACROPHAGES	101

LIST OF DEFINITIONS

Mtb – *Mycobacterium tuberculosis*

BCG – *Mycobacterium bovis* Bacille-Calmette-Guérin

PAMP – pathogen associated molecular pattern

DC – Dendritic cell

PI – phosphatidylinositide

PIP – phosphatidylinositol phosphates

PI3P – phosphatidylinositol 3-phosphate

PI4P – phosphatidylinositol 4-phosphate

PI5P – phosphatidylinositol 5-monophosphate

PI(4,5)P₂ – phosphatidylinositol 4,5-bisphosphate

PI(3,4,5)P₃ – phosphatidylinositol (3,4,5)-trisphosphate

TTSS – Type III Secretion System

SCV – Salmonella containing vacuole

ESX – ESAT-6 system

ESCRT – endosomal sorting complex required for transport

PMA – phagosome maturation arrest

G6PDH – glucose-6-phosphate dehydrogenase

HRP – horse radish peroxidase

OADC – oleic acid-albumin-dextrose-catalase

LiAc – lithium acetate

SD – synthetically defined medium

SD/-HIS – synthetically defined medium lacking histidine

SD/-LEU – synthetically defined medium lacking leucine

Gal/Raf – galactose/raffinose base medium

Y2H – yeast two hybrid

DDO – synthetically defined medium lacking leucine and tryptophan

DDO/X/A – DDO supplemented with α -gal and Aureobasidin A

QDO – synthetically defined medium lacking leucine, tryptophan, histidine and adenine

QDO/X/A – QDO supplemented with α -gal and Aureobasidin A

BLAST – basic local alignment search tool

ELISA – enzyme-linked immunosorbent assay

BSA – bovine serum albumin

PFA – paraformaldehyde

CFU – colony forming units

ANOVA – analysis of variance

TLR – Toll-like receptor

PLC – phospholipase C

MSP – Mycobacterial secreted proteins

Ras^{mut} – non-lipidated, constitutively-activated Ras

GFP – green fluorescent protein

ER – endoplasmic reticulum

CAD – conditional aggregation domain

hGH – human growth hormone

RD2 – region of difference 2

ATPase β 1 – sodium/potassium ATPase, beta chain 1

ATPase β 3 – sodium/potassium ATPase, beta chain 3

PGM1 – phosphoglucomutase 1

EB – empty bait vector

EP – empty prey vector

WCL – whole cell lysate

Dox – doxycycline

PM – plasma membrane

UPR – unfolded protein response

CHOP – CCAAT-enhancer-binding protein homologous protein

BiP – immunoglobulin heavy-chain-binding protein

sXbp-1 – spliced variant of the transcription factor X-box binding protein 1

H&E – hematoxylin and eosin

MS – mass spectrometry

CLEM – correlative light and electron microscopy

CHAPTER ONE

Introduction and Review of the Literature

Mycobacterium tuberculosis

Tuberculosis caused by *Mycobacterium tuberculosis* (Mtb) is a persistent, global epidemic. While the number of deaths due to Mtb fell below 2 million in 2015, there were over 9 million new cases [1] and the incidence of multidrug-resistant Mtb is increasing [1], highlighting the need for new anti-tuberculosis therapies. In addition, the only currently available vaccine, *Mycobacterium bovis* Bacille-Calmette-Guérin (BCG), is ineffective in preventing pulmonary tuberculosis infection [2]. Thus, understanding the intracellular survival mechanisms employed by Mtb is vital to developing new anti-tuberculosis treatments and vaccines.

Mtb is spread through the inhalation of aerosolized droplets that are released in to the air when an infected individual coughs or sneezes [3]. The bacteria are ingested by resident alveolar macrophages that recognize specific pathogen associated molecular patterns (PAMPs) [4, 5]. Following phagocytosis of mycobacteria, infected macrophages release pro-inflammatory cytokines that recruit additional immune cells to the lung, including neutrophils, naïve monocytes, and dendritic cells (DCs). DCs that have ingested Mtb leave the lung and migrate to regional lymph nodes, where they drive induction of the adaptive immune response [4]. Therefore, the ability to manipulate the host response to infection is vital to Mtb survival.

Intracellular survival of *M. tuberculosis*

Macrophages, phagocytic innate immune cells that are generally competent for bacterial killing, represent the primary intracellular niche for Mtb. Some of the antimicrobial mechanisms utilized by macrophages include acidification of the phagosome, production of reactive oxygen and nitrogen species, fusion of lysosomes to bacteria containing phagosomes and autophagy [6-9]. However, despite these robust defenses, Mtb survives inside macrophages during its infectious life cycle. To facilitate its survival Mtb has evolved to resist macrophage defenses, either by directly protecting the bacterial cell from damage [10-12] or by modulating the macrophage's ability to shuttle the bacteria through the traditional phagolysosome maturation process [13]. In that way, Mtb prevents its intracellular compartment from acidifying [14] and fusing [15] with the destructive lysosome (Figure 1). Genetic studies have identified several Mtb proteins important for remodeling host membrane trafficking [16-18]. For example, Mtb *Rv3310* encodes SapM, a secreted acid phosphatase [19] that converts phosphatidylinositol 3-phosphate (PI3P) to phosphatidylinositol. Loss of PI3P from the phagosome membrane is sufficient to prevent fusion of phagosomes with late endosomes [20, 21]. Importantly, many genes reported to be important for Mtb survival inside macrophages remain uncharacterized [16, 17, 22] and the manipulation of the host cell by Mtb remains poorly understood.

Secretion systems of other bacterial pathogens are required for survival

The problem of intracellular survival faced by Mtb is also shared by other bacterial pathogens, and many of these organisms utilize specialized secretion systems to deliver molecules into the host cell to establish a unique intracellular niche [23]. For example, some Gram-negative pathogens with both extracellular and intracellular life cycles use needle-like machines encoded by Type III Secretion Systems (TTSS) that span the bacterial and host cell membranes to inject protein cargo into the host [24-27]. Another specialized secretion machine called a Type IV Secretion System is found in Gram-positive and Gram-negative bacteria and can be used by many human and plant pathogens such as *Legionella pneumophila*, *Coxiella burnetii* and *Agrobacterium tumefaciens* to transport effector proteins that promote bacterial survival [28, 29]. Finally, Mtb encodes multiple Type VII secretion systems, discussed below, that are important in pathogenesis [30-32]. However, the identity and functions of the Type VII dependent secreted proteins remain poorly characterized. Despite structural differences, a common theme is that these elaborate secretion systems aid in pathogenesis by delivering virulence proteins called “effectors” to the host cell.

Effectors are proteins that promote bacterial survival by manipulating vital cellular processes including signal transduction, vesicular trafficking and the cytoskeleton [33-35]. Like the secretion systems themselves, the repertoire of effectors expressed by each pathogen can differ, adapted specifically for each unique life cycle. However, major common characteristics of effectors include that they are targeted to host membranes and interact with membrane-associated proteins (Figure 1). Furthermore, some effectors can also function by directly modifying membranes. A common target of bacterial pathogens is PI3P which is required for the progression of early endosomes to late

endosomes and eventually lysosomes [36]. Thus, effector proteins such as VipD and SidP from *L. pneumophila* respectively hydrolyze [37] or dephosphorylate [38] PI3P on endosomes to avoid degradation of the bacteria by the lysosome. Interestingly, the PI3 kinase OpiA from *Francisella tularensis* enriches PI3P on late endosomes to facilitate escape to the cytosol [39]. Similarly, the PM is a common target for bacterial effectors from both plant and animal pathogens. Myristoylation of HopZ4 from *Pseudomonas syringae* localizes it to the PM where it inhibits the proteasome and influences the secretory pathway [40], whereas the phospholipase ExoU from *Pseudomonas aeruginosa* uses PM-specific PIPs to for localization [41]. Furthermore, PIPs in the PM are enzymatic substrates of bacterial proteins to promote invasion such as IpgD from *Shigella flexneri* that hydrolyzes phosphatidylinositol 4,5-bisphosphate (PI(4,5)P₂) to phosphatidylinositol 5-monophosphate (PI5P) leading to membrane blebbing and bacterial uptake into host cells [42].

Many effectors are localized to pathogen-specific vacuolar compartments. For example, SifA from *Salmonella enterica* serovar Typhimurium (*S. Typhimurium*) is prenylated inside the host cell and localizes to the Salmonella containing vacuole (SCV) [43]. SifA interacts with SifA kinesin interacting protein (SKIP) to recruit lysosomes to maintain SCV membrane integrity and its membrane interaction is vital to Salmonella pathogenicity [43, 44]. The *Legionella pneumophila* Type IV secreted effector SidM is anchored to the Legionella containing vacuole and disrupts host vesicle trafficking by sequestering and modifying Rab1 [45].

Organelles central to secretory and signaling events such as the Golgi apparatus, ER and mitochondria are often target of effector localization and activity. The *S. flexneri*

effectors IpaB and IpaJ use distinct mechanisms to disrupt the Golgi network to inhibit recycling and secretion of protein cargo [46, 47]. Similarly, the enterohemorrhagic *Escherichia coli* (EHEC) effectors NleA and EspG target the Golgi to inhibit vesicular trafficking [48, 49]. Mitochondrial localization of effectors is more rare, but the enteropathogenic *Escherichia coli* protein Map disrupts mitochondrial membrane potential [50]. Finally, the vacuoles of intracellular pathogens are trafficked to specific localizations such as near the Trans-Golgi network for the SCV and *Chlamydia* inclusion or require membranes from the ER such as *L. pneumophila* and *Brucella abortus* [51]. Not surprisingly, these processes are carried out by bacterial effector proteins [52-54]. Thus, both host membranes themselves and membrane-dependent processes represent valuable targets for bacterial effectors [33, 35, 55] as was recently shown for a variety of bacterial pathogens [56].

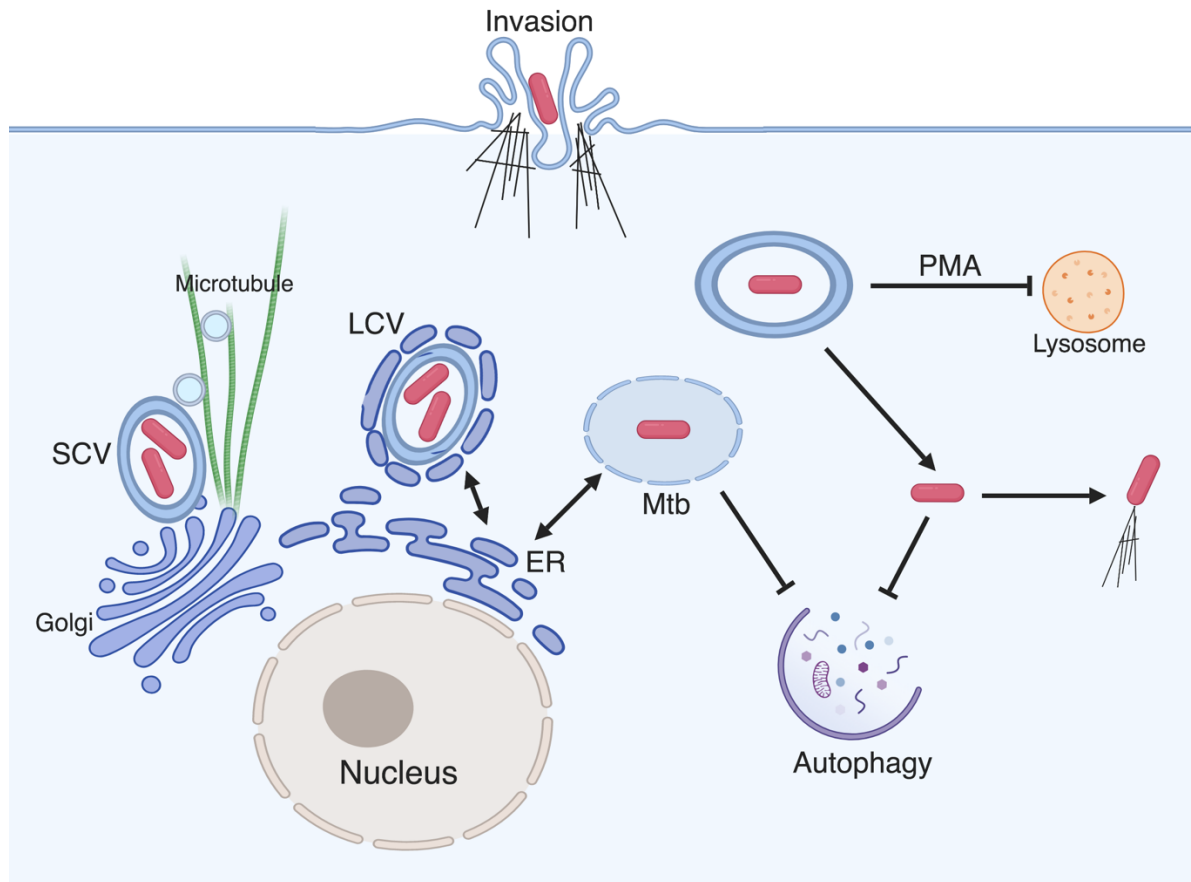


Figure 1. Interaction of bacterial pathogens with the host endomembrane system. Bacteria can induce invasion of non-phagocytic cells by modulating membrane ruffling and actin dynamics. Intracellular bacterial pathogens must avoid fusion of their compartments with the lysosome, either by modification of that vacuole as employed by *M. tuberculosis*, *S. Typhimurium* and *L. pneumophila*, or escape to the cytosol like *S. flexneri*. Bacteria that have damaged the vacuole or entered the cytoplasm must avoid detection by autophagy. Finally, bacteria maintain their vacuoles by manipulating intracellular trafficking among the ER, Golgi and endosomes. SCV, Salmonella containing vacuole; LCV, Legionella containing vacuole; ER, endoplasmic reticulum; PMA, phagosome maturation arrest.

M. tuberculosis secretion systems and substrates

The virulence functions of most Mtb secreted proteins are poorly understood. Although Mtb does not encode a TTSS, it does contain the conserved general secretion systems Sec and Tat [57], an accessory SecA2 system [58], as well as multiple Type VII (also called ESX) secretion systems [31]. The ESX-1 system is required for Mtb virulence in macrophages and mouse models of infection [30] through modulation of immune functions such as induction of Type I interferon via the secreted effectors ESAT-6 (EsxA) and CFP-10 (EsxB) [59, 60]. In contrast, the functions of other Esx-1 substrates such as EspA, EspB, EspC, PE35, and PPE68 are not well understood [31]. The ESX-3 system is required for iron acquisition and is essential for growth *in vitro* [61]. However, ESX-3 also secretes iron-independent virulence proteins [62]. For example, EsxH interacts with a component of the host endosomal sorting complex required for transport (ESCRT) machinery, leading to decreased co-localization of Mtb with lysosomes [63] and inhibition of antigen presentation in infected macrophages [64]. In addition, ESX-5 is required for the secretion of a majority of the PE/PPE family of proteins [65, 66] and disruption of the ESX-5 secretion system [67] or PPE10 [68] leads to attenuation of Mtb virulence *in vivo*. PE/PPE proteins are named for conserved Proline-Glutamate (PE) or Proline-Proline-Glutamate (PPE) N-terminal motifs and the genes encoding this family of proteins comprise 7% of the coding capacity of Mtb [69]. The vast genetic space donated to PE/PPE genes originally caused speculation that the proteins participated in immunomodulation through antigenic variation, which is still controversial [69, 70]. However, a subset of PE/PPE proteins are known to be important for full virulence of Mtb

[71, 72]. Finally, the SecA2 system is also required for Mtb growth in macrophages, possibly by dampening the host immune response [73]. Substrates of the accessory SecA2 system such as the protein kinase PknG and the esterase LipO are also important for Mtb virulence by contributing to phagosome maturation arrest (PMA) [16, 21, 74, 75]. Although there is still much to uncover, it is clear that the survival of Mtb relies heavily on its secretion systems, and therefore the secreted protein substrates.

Summary of results

Because membrane processes are high value targets of many bacterial effectors [56, 76], and Mtb has a large repertoire of secreted proteins of unknown function [77-81], I hypothesized that some of the Mtb secreted proteins are membrane-binding effectors with virulence activities. To test my hypothesis, I generated a library of 200 secreted proteins from Mtb, tested whether they individually bound yeast membranes in a life or death assay, and characterized their ability to alter host protein secretion in an inducible secretion assay. I also determined the subcellular localization of membrane-binding proteins using fluorescence microscopy. By combining data from the cell biological screens, I identified five Mtb secreted proteins that localized to eukaryotic membranes and disrupted the host secretory pathway in a model system. One protein, Mpt64 (Rv1980c), localized to the ER during both heterologous expression in HeLa cells and Mtb infection of macrophages. Though Mpt64 is a Sec substrate, its access to the macrophage cytoplasm was dependent on the ESX-1 secretion system. Although Mpt64 was not required for virulence of Mtb in either a macrophage or murine model of infection,

Mpt64 alone was sufficient to partially inhibit the UPR suggesting a possible role for Mpt64 in regulating the macrophage response to infection.

CHAPTER TWO Methodology

MATERIALS AND METHODS

Antibodies

To generate an antibody against native Mpt64, two rabbits were immunized with recombinant 6xHIS-tagged Mpt64 Δ SP purified from *E. coli* in incomplete Freund's adjuvant (Pacific Biosciences). The polyclonal rabbit antibody to Antigen 85 (NR-13800) and mouse anti-GroEL2 CS-44 (NR-13813) are from BEI Resources. Chicken (ab94935), mouse (ab22683) and rabbit (ab2907) anti-calreticulin were purchased from Abcam and anti-GM130 (610822) was purchased from BD Biosciences. Mouse anti-Tom20 F-10 (sc-17764), Na⁺/K⁺-ATPase β 1 Antibody M17-P5-F11 (sc-58627) and anti- β -Actin C4 (sc-47778) were purchased from Santa Cruz. Rabbit anti-Ras (3965S) and rabbit anti-glucose-6-phosphate dehydrogenase (G6PDH, A9521) were purchased from Cell Signaling Technology and Sigma, respectively. Mouse anti-PMP70 CL2524 (MA5-31368), anti-CHOP 9C8 (MA1-250) and horse radish peroxidase (HRP)-conjugated secondary antibodies were purchased from Thermo Scientific. Alexa fluor-conjugated secondary antibodies were from Life Technologies.

Molecular Biology

Unless otherwise stated, all Mtb proteins were cloned from the BEI resources Gateway Mtb ORF library using Gateway cloning technology (Life Technologies). The Mpt64

truncation mutants were PCR amplified (Table 1) and cloned into pENTR (Life Technologies) prior to cloning into subsequent destination vectors.

Bacterial Strains and Growth Conditions

M. tuberculosis Erdman and mutants were grown in Middlebrook 7H9 broth or on Middlebrook 7H11 agar (Difco) supplemented with 10% oleic acid-albumin-dextrose-catalase (OADC, Remel). Liquid medium was also supplemented with 0.05% Tween 80.

Yeast Strains and Growth Conditions

The *Saccharomyces cerevisiae* strain INVSc1 (Invitrogen) was grown at 30°C in histidine drop out media (SD/-HIS) or agar plates (Clontech). The construction of *cdc25^{ts}* was previously described [82]. *cdc25^{ts}* was grown at 25°C in leucine drop out media or agar plates (SD/-LEU) (Clontech). Yeast knock out strains Δ FAB1, Δ LSB6 and Δ VPS34 are on the *S. cerevisiae* BY4741 background and were grown in YPD (Difco) prior to transformation. The tetracycline off strains (MSS4, PIK1 and STT4, Thermo Scientific) are on the genetic background of R1158 and were grown in YPD supplemented with 300ug/mL G418 (Millipore, 345810) prior to transformation.

Yeast Transformation

Yeast strains were transformed using a lithium acetate (LiAc) protocol. Yeast were grown to high density overnight at the appropriate temperature, shaking. The cultures were diluted to an $OD_{600}=0.2$ in 50mL YPD and allowed to reach mid-log phase. Cells were washed, resuspended in 0.1M LiAc and incubated 10 minutes at room temperature. The

sample DNA was mixed with an equal volume of pre-boiled Yeastmaker Carrier DNA (Clontech). To the DNA was added 100 μ L yeast and 500 μ L of a solution of LiAc+PEG (40% PEG w/v, 0.1M LiAc). This solution was incubated 30 minutes at 25°C (*cdc25^{ts}*) or 30°C with agitation every 10 minutes. DMSO was added and the cells were heat shocked at 42°C for 15 minutes. The cells were pelleted, washed in TE (10mM Tris, pH 7.4, 1mM EDTA) and resuspended in 500 μ L TE. The transformed cells were plated on selective agar plates and incubated at the appropriate temperature for 2-4 days.

Yeast Screening Assays

To perform the Ras rescue assay, 3-4 fresh colonies were combined in 30 μ L SD/-LEU and 3 μ L was spotted onto duplicate plates that were subsequently incubated at either 25°C or at 37°C for 2 days.

INVSc1, deletion mutants and tetracycline off yeast were transformed with a galactose-inducible vector (p413GALGFP) containing GFP-Mtb fusion proteins and selected on SD/-HIS. To induce GFP fusion protein expression in WT and deletion mutant strains, yeast were inoculated in 5mL galactose/raffinose (Gal/Raf) base lacking histidine (Clontech) and allowed to grow 16-20 hours at 30°C, shaking. Cultures were pelleted, resuspended in 3mL Gal/Raf/-HIS and incubated another 4 hours at 30°C, shaking. Yeast were pelleted and resuspended in 30-50 μ L PBS and immobilized on an agar pad prior to visualization. For tetracycline off strains, yeast were inoculated into 5mL SD/-HIS supplemented with 300 μ g/mL G418 and 50 μ g/mL (PIK1 and STT4) or 300 μ g/mL (MSS4) doxycycline (Millipore, 324385) and incubated overnight at 30°C, shaking. Yeast were washed in TE buffer and resuspended in Gal/Raf/-HIS (to induce GFP fusion protein

expression) with 300µg/mL G418 and 50ug/mL (PIK1 and STT4) or 300µg/mL (MSS4) doxycycline. After overnight incubation, yeast were immobilized on agar pads as above.

To screen for calcofluor white sensitivity, yeast expressing GFP-MSP fusion proteins under a galactose-inducible promoter were inoculated in 100µL Gal/Raf/-HIS in 96-well plates and incubated overnight at 30°C, 250rpm. Cultures were back diluted to OD₆₀₀=0.2 in fresh Gal/Raf/-HIS media and allowed to grow 4 hours. Cultures were diluted tenfold prior to replica plating on Gal/Raf/-HIS agar containing 0, 20 or 40µg/mL calcofluor white (Sigma, F3543) using a pin replicator, or manually by spotting 3µL to each plate. Plates were incubated at 30°C for 2-3 days prior to visualization.

Yeast Two Hybrid

The Matchmaker Gold Yeast Two Hybrid (Y2H) protocols were followed and all reagents were purchased from Clontech unless otherwise stated. Mpt64ΔSP was cloned into the bait vector pGBKT7 and transformed into *S. cerevisiae* Y2H Gold. To mate 4mL of bait yeast (1x10⁸cfu/mL) were mixed with 1mL Normalized Mate and Plate Library for 24 hours at 30°C and 75rpm. cDNA libraries used were a universal human (630481), HeLa (630479), or universal mouse (630483). Primary selection for protein interactions was achieved by plating the entire mating on synthetically defined agar lacking leucine and tryptophan (DDO) supplemented with x-α-gal (40µg/mL 630463) and Aureobasidin A (200ng/mL, 630499) (DDO/X/A). Blue colonies from DDO/X/A plates were individually selected and patched on agar plates lacking leucine, tryptophan, histidine and adenine

(QDO) supplemented with $x\text{-}\alpha\text{-gal}$ and Aureobasidin A (QDO/X/A) and subsequently segregated by quadrant streaking back on DDO/X/A.

To identify protein interaction partners, individual colonies were lysed in 50 μL zymolase (0.12U/ μL , Zymo Research, E1005-A) for 30 minutes at 37°C and genes inserted into the prey vector (pGADT7) were PCR amplified using primers flanking the cDNA insertion (Table 1). PCR products were purified, sequenced (Table 1) and identified by the basic local alignment search tool (BLAST, NCBI).

To confirm interactions, directed yeast two hybrid assays were carried out. Plasmids were isolated directly from positive colonies by zymolase treatment followed by purification through a standard miniprep kit. To enrich, the isolated plasmids were transformed into *E. coli* (Mach-1) and selected for on LB agar containing ampicillin (100 $\mu\text{g}/\text{mL}$). Then Y2H Gold yeast were co-transformed with the resulting pGADT7 vectors and Mpt64 Δ SP-pGBKT7 and selected on DDO/X/A and QDO/X/A. Alternatively, cDNAs were amplified, cloned into pGADT7 and resultant plasmids were transformed into Y187 yeast. To confirm interactions, Y2H Gold containing Mpt64 Δ SP-pGBKT7 (or empty vector) were mixed with Y187 containing pGAD constructs in 2x YPD supplemented with adenine and incubated 24 hours at 28dC, 150rpm. Interactions were selected for on DDO/X and QDO/X/A.

Yeast Lysis and Western Blotting

Yeast (*cdc25^{ts}*) were inoculated into 5mL SD/-Leu and incubated overnight at room temperature, shaking (250rpm). To lyse, 1.5mL of each culture was centrifuged at

14,000rpm for one minute. Each pellet was resuspended in 100 μ L 2.0M LiAc and incubated on ice for five minutes. Samples were centrifuged at 14,000 for one minute to pellet, resuspended in 100 μ L 0.4M NaOH and incubated on ice for five minutes. Samples were pelleted as before, resuspended in 75 μ L 1x SDS Laemmli sample buffer and boiled at 100°C for five minutes. Lysates were centrifuged 14,000rpm for one minute to remove debris, separated by SDS- polyacrylamide gel electrophoresis and transferred to polyvinylidene difluoride membrane for Western blotting. Fusion proteins were detected by rabbit anti-Ras (1:100) and equal loading was confirmed by detection with rabbit anti-G6PDH (1:10,000).

Cell Culture

HeLa cells (ATCC CCL-2) were cultured in Dulbecco's modified Eagle medium (DMEM, Gibco) supplemented with 10% fetal bovine serum (FBS, Gibco), 100 I.U./mL penicillin, 100 μ g/mL streptomycin, 292 μ g/mL L-glutamine (Corning). RAW267.4 macrophages (ATCC TIB-71) were cultured in RPMI 1640 (Gibco) supplemented with 10% heat-inactivated FBS, 100 I.U./mL penicillin, 100 μ g/mL streptomycin, 292 μ g/mL L-glutamine, and 10mM HEPES (Hyclone).

To isolate primary human macrophages, 50mL of blood from each donor was added to an equal volume of PBS then separated by centrifugation over a Ficoll-Paque Plus (Sigma, GE17-1440-03) gradient at 750 x g for 20 minutes with no brake. The lymphocyte/monocyte layer was collected and incubated 1-2 minutes with 1mL ACK lysing buffer (Gibco, A10492-01) to remove red blood cells. The cells were diluted to 50mL in PBS and centrifuged 350 x g for 10 minutes at 4°C. The supernatant was removed and

cells were washed in 25mL PBS and pelleted at 160 x g for 15 minutes at 4°C. Cells were washed again in 25 mL PBS but centrifuged at 300 x g for 10 minutes at 4°C. This final pellet was resuspended in 5-10 mL of RPMI 1640 supplemented with 10% human AB serum (Corning, 35-060-CI). To differentiate into macrophages, cells were cultured in RPMI 1640 supplemented with 10% human AB serum for at least 4 hours to allow for attachment. Cells were washed in PBS then replaced with RPMI 1640 +10% human AB serum + 50ng/mL human M-CSF (R&D Systems, (R&D Systems, 216-MC-025) for 7 days with media changes every 1-2 days.

hGH Release Assay and Quantification

HeLa cells were plated in 24-well plates to achieve approximately 50,000 cells/well 24h prior to transfection. Cells were co-transfected with 1 µg hGH-CAD and 1µg GFP-Mtb effector or GFP alone using FuGene 6 (Promega) per manufacturer instructions. Cells were transfected 16-18h at 37°C 5% CO₂. The transfection media was then aspirated and replaced with DMEM containing 2µM D/D Solubilizer (Clontech, 635054) and incubated for 2 h at 37°C 5% CO₂. The plates were centrifuged at 1500 RPM for 5 minutes to pellet debris and the culture supernatants were saved at -80°C prior to hGH quantification.

Released hGH was quantified by enzyme-linked immunosorbent assay (ELISA) (Roche, 11585878001). Briefly, samples were thawed on ice and 20µL was transferred to each well containing 180µL sample buffer (1:10). The plate was incubated 1h at 37°C, washed 5 times in 250µL wash buffer and incubated 1h at 37°C with a polyclonal antibody to hGH conjugated to digoxigenin (α-hGH-DIG). The plate was washed as described and incubated 1 h at 37°C with a polyclonal antibody to digoxigenin

conjugated to peroxidase (α -DIG-POD). The plate was washed and developed in peroxidase substrate (2,2'-Azinobis [3-ethylbenzothiazoline-6-sulfonic acid]-diammonium salt). The absorbance was read on a Biotek plate reader at 405nm.

PIPs strips membrane binding

6xHIS-Mpt64_24-228 and 6xHIS-Mpt64_24-143 were codon optimized for *E. coli* prior to cloning into pJ401T5 for recombinant protein expression. Protein expression was induced in cultures of exponential growth phase bacteria by addition of 1mM isopropyl β -D-1-thiogalactopyranoside (IPTG). Bacteria were lysed by sonication and proteins were purified by cobalt TALON affinity resin per manufacturer's instructions (Clontech). Proteins were dialyzed into Tris buffered saline (20mM Tris, pH 7.4, 150mM NaCl) for use in biochemical assays.

PIPs strips membranes (Invitrogen, P23751) were blocked for one hour at room temperature in 3% fatty-acid free bovine serum albumin (BSA)(Sigma, A7030) in TBST. Mpt64_24-228 or Mpt64_24-143 was diluted to 1.5ug/mL in 3mL 3% fatty-acid free BSA and incubated with the PIP strips for 3h at room temperature with agitation. Membranes were washed three times in 3% fatty-acid free BSA prior to incubation with anti-Mpt64 or pre-immune serum (1:3,000) overnight at 4°C, with agitation. Membranes were washed three times in 3% fatty-acid free BSA then incubated with HRP-conjugated donkey anti-rabbit (1:2000) for 30 minutes at room temperature. Membranes were washed three times before detection of Mpt64 lipid interactions by chemiluminescence.

Transfection and co-localization of MSPs in HeLa cells

HeLa cells were transfected overnight with GFP fusion proteins using FuGene 6 transfection reagent (Roche). Cells were fixed in 4% paraformaldehyde (PFA) for 15 minutes, washed in PBS and permeabilized in 0.25% Triton X-100 for 3 minutes at room temperature or in 100% methanol for 10 minutes at -20°C when using Tom20 antibody. Cells were stained with organelle-specific antibodies for 1h at room temperature. Antibodies were visualized by secondary antibodies conjugated to Alexa Fluor 594. Cells were mounted in ProLong Gold + DAPI (Invitrogen, P36931) and z-stacks were collected on an AxioImager M2 microscope (Zeiss).

Sodium/Potassium ATPase pull down

E. coli lysates containing overexpressed 6xHIS-Mpt64dSP or 6xHIS-MBP were incubated with TALON affinity resin for 15 minutes at room temperature to bind histidine-tagged proteins. Confluent plates of HEK293T and HeLa cells were lysed in wash buffer (50nM NaH₂PO₄ + 300mM NaCl) with 0.1% Tween 20 and EDTA-free protease inhibitor cocktail (Roche, 11836170001). Beads containing 6xHIS-Mpt64dSP or 6xHIS-MBP were washed four times in wash buffer then incubated with 1mL cell lysates for 20 minutes at room temperature with nutation. Beads were washed 4 times in wash buffer and eluted for 15 minutes at room temperature in wash buffer supplemented with 300mM imidazole. To better visualize the membrane protein, fractions were combined with SDS sample buffer and heated to 70°C for 10 minutes prior to separation by SDS-PAGE and Western blotting. Na⁺/K⁺-ATPase β1 was used at 1:500.

Detection of CHOP accumulation in macrophages

RAW267.4 cells stably expressing Mpt64 Δ SP under a CMV promoter or control cells transduced with an empty lentivirus were seeded in 12-well plates at 5×10^5 cells/well. To induce UPR, culture media was replaced with media supplemented with 50nM thapsigargin (Sigma, T9033) or an equal volume of vehicle (DMSO) and cells were incubated for 4 hours. Cells were washed twice in PBS and lysed in ice cold RIPA buffer supplemented with protease inhibitor tablets (Roche, 11836153001). Lysates (15-25ug) were separated by SDS-polyacrylamide gel electrophoresis and transferred to polyvinylidene difluoride membrane for Western blotting. Accumulation of CHOP was detected by mouse anti-CHOP (1:2000) and band density was normalized to bands detected by the loading control mouse anti-Actin (1:3000).

Construction of the Mtb mpt64 deletion mutant and complementation

An in-frame mpt64 deletion in Mtb was made using mycobacteriophage as previously described [83]. Briefly, 500-bp 5' to the mpt64 start codon and 500-bp 3' to the mpt64 stop codon were amplified from Erdman genomic DNA (Table 1) and sequentially cloned into the multiple cloning sites of pMSG360HYG. This vector was linearized with AflIII and DraI (NEB, R0520 and R0129) and transformed into EL350/phAE87 *E. coli* by electroporation. Phagemid DNA was isolated from pooled colonies and transformed into *M. smegmatis* by electroporation. Plaques were isolated and pooled from *M. smegmatis* lawns and high titer phage was produced. Log phase Mtb Erdman was transduced with phage at 42°C for 4h. Mutants were selected on 7H11+Hygromycin (100 μ g/mL). Wild-type mpt64 and mpt64 lacking its secretion signal were cloned into an integrating vector

containing a constitutive promoter (pMV306_MSP), conferring zeocin resistance. The *Mtb*Δmpt64 was transformed by electroporation and complements were selected on 7H11 + zeocin (25µg /mL).

To confirm expression and secretion of Mpt64 complements, *Mtb* strains were grown to late-log phase and pelleted by centrifugation. The culture supernatants were saved and passed twice through 0.22 µm filters. Bacterial pellets were boiled 30 minutes in lysis buffer (50mM Tris, pH 7.4, 150mM NaCl) supplemented with Complete Mini protease inhibitor, then subjected to bead beating to lyse the cells. Protein content in lysates was determined by Bradford assay. Mpt64 expression in the lysates and culture supernatants was detected by Western blotting using a rabbit polyclonal antibody to Mpt64 (1:10,000). Equal loading of samples in the lysates and supernatants was confirmed by Western blotting with anti-GroEL2 (1:500) and anti-antigen 85 (1:1000) respectively.

Infection and co-localization of Mpt64 in macrophages

Bacteria were washed repeatedly in PBS, then sonicated to create a single cell suspension. RAW267.4 cells were infected in DMEM+10% horse serum (Invitrogen 26050088) at MOI 20:1 with mycobacteria expressing mCherry. Cells were centrifuged at 1500 rpm for 10 minutes to permit bacterial attachment, then allowed to phagocytose for 1.5h at 37°C 5% CO₂. Cells were fixed after 4 hours post-infection in 4% PFA for 60 minutes. Cells were permeabilized in 0.25% Triton X-100 for 3 minutes at room temperature then blocked in 5% normal donkey serum (Sigma). Mpt64 was detected with rabbit anti-Mpt64 antibody (1:500) and an HRP-conjugated goat-anti rabbit secondary

antibody (1:1000, Santa Cruz). Antibody signal was amplified by addition of biotinylated Tyramide (1:50, PerkinElmer) with detection by Alexa fluor 488-conjugated streptavidin (1:250, Jackson ImmunoResearch) or Cyanine 5 Tyramide (1:50, PerkinElmer). Z-stack slices were acquired with an AxioImager M2 microscope (Zeiss).

Primary human macrophages were infected in RPMI + 10% human AB serum at a MOI 10:1 with mycobacteria expressing mCherry for 2h at 37°C 5% CO₂ to allow for phagocytosis. Cells were washed and fixed at 4 hours post-infection in 4% PFA for 45-60 minutes. Cells were permeabilized in 100% ice cold methanol for 10 minutes at -20°C and blocked in 5% normal goat serum (Sigma). Mpt64 was detected with rabbit anti-Mpt64 antibody (1:500) and an HRP-conjugated donkey-anti rabbit secondary antibody (1:500, Thermo Scientific) followed by amplification with cyanine 5 Tyramide (1:50, PerkinElmer). Co-localization of Mpt64 with the ER was detected with chicken anti-calreticulin (1:100), followed by goat anti-chicken-488 (Abcam).

Macrophage infections for CFU

Primary human macrophages were seeded in low-evaporation 24-well plates at approximately 5×10^5 cells/well. Bacteria were washed repeatedly in PBS, then sonicated to create a single cell suspension. Macrophages were infected in RPMI + 10% human AB serum at MOI 0.1:1. Cells were centrifuged at 1500 rpm for 10 minutes to permit bacterial attachment, then allowed to phagocytose for 15 minutes at 37°C 5% CO₂. The cells were washed in PBS then replaced with RPMI + 10% human AB serum and cells were washed every day between time points. The cells were lysed at time zero and subsequent time

points in 500 μ L 0.5% Triton X-100 in PBS. Serial dilutions were plated on 7H11 plates and colonies were enumerated after 2-3 weeks.

Infection of macrophages for multiplex ELISA

RAW267.4 macrophages were seeded into 24-well plate at about 50,000 cells per well. Bacteria were washed repeatedly in PBS, then sonicated to create a single cell suspension. Cells were infected in DMEM+10% horse serum at MOI 5:1 and allowed to phagocytose for 3 hours. Cells were washed and incubated at 37°C, 5% CO₂ for 24 hours. Supernatants were passed through 0.22 μ m centrifugal filters twice to sterilize and stored at -80°C. A Novex murine 4-plex kit (LMC0003M) was used to quantify cytokines per manufacturer's instructions. Supernatants were diluted 1:20 with sample diluent and standards were reconstituted in 50:50 sample diluent:RPMI. ELISAs were analyzed by the Luminex MAGPIX machine with xPonent software.

For acute infections of primary human macrophages, cells were infected and samples collected as above but supernatants were collected 6 hours after the phagocytosis step. Cytokines were quantified by a Bio-Rad human 17-plex kit (M5000031YV) on undiluted supernatants.

Infection and detection of UPR induction in macrophages

RAW267.4 cells were seeded in 12-well plates at 3-5 x10⁵ cells/well. Bacteria were washed repeatedly in PBS, then sonicated to create a single cell suspension. Macrophages were infected in DMEM+10% horse serum at a MOI of 1:1 or 10:1. Cells

were centrifuged at 1500 rpm for 10 minutes to permit bacterial attachment, then allowed to phagocytose for 15 minutes at 37°C 5% CO₂. The cells were washed in PBS then replaced with RPMI + 10% FBS or RPMI +10%FBS supplemented with 50nM thapsigargin or DMSO for 4 hours. After 4 hours, cells were washed twice in PBS and fixed in TRIzol reagent (Life Technologies) for downstream qPCR analysis or lysed in ice cold RIPA buffer supplemented with protease inhibitor tablets (Roche) for Western blot analysis. Lysates were sterilized by centrifugation through 0.22µM PES filters twice. Samples were stored at -20°C prior to Western blotting and -80°C prior to RNA extraction.

Detection of CHOP accumulation in infected macrophages

Lysates were thawed on ice prior to protein quantification by BCA assay. Lysates (15-25ug) were separated by SDS-polyacrylamide gel electrophoresis and transferred to polyvinylidene difluoride membrane for Western blotting. Accumulation of CHOP was detected by mouse anti-CHOP (1:100) and band density was normalized to bands detected by the loading control mouse anti-Actin (1:2000).

Preparation of RNA and cDNA for qPCR

To extract RNA, samples in 1mL TRIzol were mixed with 200uL chloroform and shaken vigorously. The phases were separated by centrifugation at 12,000xg at 4dC for 15 minutes. The aqueous layer was saved and added to 400uL isopropanol. Samples were incubated at room temperature for 30 minutes and nucleic acids were pelleted at 12,000xg for 10 minutes at 4dC. Pellets were washed once in 1mL 75% ethanol. RNA

was pelleted at 7,500xg for 10 minutes at 4°C and allowed to dry before reconstitution in nuclease free water.

cDNA was prepared using the iScript Reverse Transcription Supermix kit (Bio-Rad, 1708841) according to manufacturer's instructions. Fast SYBR Green Master Mix (Thermo Fisher Scientific, 4385612) was used for qPCR. The primers used for qPCR are listed in Table 1. Data were analyzed by the $\Delta\Delta CT$ method.

Mouse infections

Female BALBc mice (The Jackson Laboratory) were infected via aerosol as described previously [84]. Briefly, mid-log phase Mtb were washed in PBS repeatedly then sonicated to create a single-cell suspension. Bacteria were resuspended to yield an $OD_{600}=0.1$ in PBS. This suspension was transferred to the nebulizer of a GlassCol aerosolization chamber calibrated to infect mice with ~100 bacteria per animal. On the day of infection, whole lungs were collected from 5 mice per group, homogenized and plated on 7H11 to determine initial inoculum. At subsequent time points, the left lung, spleen and left lobe of the liver were used to determine CFU, while the right lung was insufflated with 10% neutral buffered formalin for histopathology.

Lysozyme pull down

E. coli lysates containing 6x-histidine (6xHIS) tagged Mpt64 or an unrelated protein Cor were incubated with cobalt affinity resin (TALON, Clontech) to bind histidine-tagged proteins. After extensive washing, 1mg/mL either hen egg white lysozyme (Fisher

Scientific, BP535) or human lysozyme (Sigma, L1667) was flowed over the immobilized beads and incubated 5 minutes. Beads were washed two more times before proteins were eluted with 300mM imidazole.

Mtb genomic DNA isolation

Late exponential phase Mtb was collected by centrifugation and washed once in PBS. Pellets were boiled 20-30 minutes to sterilize. Pellets were washed once in GTE (25mM Tris, pH 8.0; 10mM EDTA; 50mM glucose) and incubated overnight in lysozyme solution (10mg/mL in GTE) at 37°C. Samples were incubated in 10% SDS and 10mg/mL proteinase K for 40 minutes at 55°C followed by incubation in NaCl and CTAB (2.4M NaCl, 274mM cetrimonium bromide (Sigma, H9151)) at 60°C for 10 minutes. Genomic DNA was then isolated using a phenol-chloroform extraction followed by ethanol precipitation.

Extraction of apolar lipids and PDIM analysis

Log phase Mtb or Mtb Δ mpt64 were synchronized to OD₆₀₀=0.2 in 7H9 supplemented with 0.01% Tween 80 and grown 24 hours. Bacteria were collected by centrifugation at 1,600xg for 10 minutes, resuspended in 1mL 15% isopropanol and transferred to a glass tube containing 5mL chloroform: methanol (17:1, v/v) and incubated 24 hours at room temperature. Samples were centrifuged at 1,600xg for five minutes and the apolar lipids were collected from the bottom, organic layer and dried. Apolar lipids were resuspended in 1.5mL 100% methanol. Tween 80 was removed by addition of cobalt/thiocyanate solution and vortexed. Remaining lipids were extracted by addition of 4mL hexane. After

centrifugation the organic layer was saved and the aqueous layer was re-extracted with 4mL hexane. Both hexane fractions were combined, dried and resuspended in 1mL chloroform: methanol (2:1, v/v). PDIM standard was similarly resuspended. PDIM standard, or apolar lipids extracted from Mtb or Mtb Δ mpt64 were infused into an AbSciex TripleTOF 5600/5600+ mass spectrometer. Samples were analyzed in the positive mode.

Statistical analysis

Statistical analysis was performed using GraphPad Prism software. For *in vitro* studies, one-tailed Analysis of Variance (ANOVA) tests were used for experiments with multiple comparisons using Dunnett's test. For experiments with single comparisons, two-tailed unpaired student's t-test was used. For experiments containing samples with non-normal distributions such as *in vivo* CFU measurements and area of lung inflammation the Kruskal-Wallis non-parametric test was used with Dunn's correction for multiple comparison. Analysis of survival studies was performed by Kaplan-Meier test.

Ethics Statement

Primary human macrophages were isolated from buffy coats from anonymous donors provided by a local blood bank (Carter Bloodcare). This study was reviewed by the UT Southwestern Institutional Review Board and deemed to be exempt.

Animal experiments were reviewed and approved by the Institutional Animal Care and Use Committee at the University of Texas Southwestern (protocol #2017-102086) and followed the Eighth Edition of the *Guide for the Care and Use of Laboratory Animals*. The

University of Texas Southwestern is accredited by American Association for Accreditation of Laboratory Animal Care (AAALAC).

Table 1. Primers used in this study. DNA primers are listed in 5' to 3' orientation. Primers paired together are labeled F for forward and R for reverse. Non-contiguous primer pairs are listed in the last column.

Yeast Two Hybrid Analysis			
Name	Sequence	Use	
CES084	CTATTTCGATGATGAAGATACCCACCAAACCC	PCR and sequencing upstream MCS pGADT7	
CES085	GTGAACTTGCGGGGTTTTTCAGTATCTACGAT	PCR and sequencing downstream MCS pGADT7	
Mpt64 Truncation Analysis			
Name	Sequence	Use	Pairs With
CES005-F	5' caccgcgccaagacctactg	Mpt64 lacking signal peptide	CES005-R
CES005-R	5' ctaggccagcatcgagtcgatc	Mpt64 full length	
CES013-R	5' gattggcttgcatagggcctg	Mpt64 N-terminal domain (Truncate at amino acid 143)	CES005-F
CES014-F	5' caccacctatgacacgctgtggcag	Mpt64 C-terminal domain (Begins at amino acid 144)	CES005-R
mpt64 Knock Out Construction			
Name	Sequence	Use	
CES109-F	5' cttCTCGAGccaccgcgaatacacctgcg	mpt64 5' flank with XhoI	
CES109-R	5' gggAAGCTTgtcgaaattcctccgggagtagttgcagcac	mpt64 5' flank with HindIII	
CES110-F	5' cttTCTAGAactcgcgaggaccgcgcggt	mpt64 3' flank with XbaI	
CES110-R	5' gaaGGTACCcaacaccccccaagcgaatg	mpt64 3' flank with KpnI	
mpt64 Complementation			
Name	Sequence	Use	Pairs With
CES114-F	5' cttTCTAGAgtcgcatcaagatcttcatgctgg	mpt64 with XbaI	
CES114-R	5' gaaGAATTCctaggccagcatcgagtcgatcg	mpt64 with EcoRI	
CES115-F	5' cttTCTAGAgcgcaccaagacctactg	mpt64 lacking signal peptide with XbaI	CES114-R
Unfolded Protein Response qPCR			
Name	Sequence	Use	
Actin-F	5' GCAAGTGCTTCTAGGCGGAC	Amplifies murine gene	
Actin-R	5' AAGAAAGGGTGTAACGACGAGC	Amplifies murine gene	
BiP-F	5' TTCAGCCAATTATCAGCAAACCTCT	Amplifies murine gene	
BiP-R	5' TTTTCTGATGTATCCTCTCACCAGT	Amplifies murine gene	
CHOP-F	5' CCACCACCTGAAAGCAGAA	Amplifies murine gene	
CHOP-R	5' AGGTGAAAGGCAGGGACTCA	Amplifies murine gene	
sXbp1-F	5' CTGAGTCCGAATCAGGTGCAG	Amplifies murine gene	
sXbp1-R	5' GTCCATGGGAAGATGTTCTGG	Amplifies murine gene	

CHAPTER THREE

Results

IDENTIFICATION AND SCREENING OF MYCOBACTERIAL SECRETED PROTEINS

Introduction

Lipids, membrane-bound proteins and membrane-dependent processes are targets of bacterial pathogens

The lipid bilayers of the PM and subcellular organelles are distinct in curvature, asymmetry, and fluidity. These attributes are modulated, in part, by the lipid composition of each membrane. The formation of stable microdomains (lipid rafts), the binding of adaptor molecules directly to membrane lipids, as well as the conversion of resident lipids to second messenger molecules are all vital to signaling events from the PM [85]. In immune cells, the lipid second messengers created by phospholipase C γ (PLC γ) can mediate the respiratory burst, cell migration and Toll-like receptor (TLR) signaling [85, 86]. Cellular cargo is transported within cells and to the extracellular space in dynamic vesicular trafficking pathways through intimate lipid-protein interactions [87, 88]. Lipid composition and curvature are vital to the formation of isolation membranes during the early stages of autophagy as well as autophagosome-lysosome fusion [89]. Finally, these events are governed by the non-homogenous distribution of phosphatidylinositol phosphates (PIPs) among different organelles [36].

Both host membranes themselves and membrane-dependent processes represent valuable targets for bacterial effectors [33, 35, 55] as was recently shown for a

variety of bacterial pathogens [56]. Indeed, Mtb is known to target and manipulate trafficking pathways through incompletely understood mechanisms [63, 90, 91] and Mtb secreted proteins can exploit PM signaling from the pattern recognition receptor TLR2 [92-94]. Considering the large repertoire of Mtb secreted proteins of unknown function [77-81], I hypothesized that some of the Mtb secreted proteins are membrane-binding effectors with virulence activities.

I used published literature to guide directed identification of putative effectors from Mtb with an emphasis on proteins that may interact with membranes and that are important for Mtb pathogenesis. I performed four cell-biological screens to characterize mycobacterial secreted proteins: Ras rescue assay for membrane binding, immunofluorescence for subcellular localization, calcofluor white for alterations in yeast vesicular trafficking and hGH release assay for alterations in mammalian vesicular trafficking. By combining data from the cell biological screens, I identified five Mtb secreted proteins that localized to eukaryotic membranes and disrupted the host secretory pathway in a model system.

Results

Categorization of putative effector-like proteins from Mtb

Through the analysis of published datasets, I identified Mtb proteins that may function as secreted effectors (Appendix A). For simplicity, I define these putative effectors as Mycobacterial secreted proteins (MSPs), as this encompasses proteins that may be secreted to the mycobacterial surface, into the exoproteome (i.e. the extracellular milieu),

or delivered into the host cell [95-98]. I used the following criteria to assemble a library of MSPs: 1) Mtb proteins identified via unbiased proteomic approaches that are either in the cell wall or the exoproteome [78-81, 99, 100], 2) Mtb proteins known to be involved in manipulation of host vesicular trafficking pathways, such as ones that induce mammalian cell entry (MCE) [101-103] or phagosome maturation arrest [16, 17, 104], 3) a subset of PE/PPE proteins and proteins related to those encoded by Type VII (ESX-1) loci [67, 70, 105], and 4) proteins involved in virulence, ranging from defined to unknown functions [22, 106-109]. I then used Gateway recombination cloning to subclone MSPs from the freely available Mtb ORFome Gateway compatible library (BEI) into destination vectors for a variety of subsequent assays. The comprehensive list of MSPs is shown in Appendix A.

Mtb encodes secreted proteins that interact with eukaryotic membranes

To identify membrane binding Mtb proteins, I used a system that leverages the signal transduction of the essential yeast GTPase Ras to promote growth and division [110]. Ras is lipidated at a unique sequence called the CaaX box that promotes its localization to the plasma membrane, where it can be activated by Cdc25, a guanine nucleotide exchange factor [82, 110]. In a yeast strain with a temperature sensitive *CDC25* allele, yeast can only grow at the permissive temperature (25°C) but not the restrictive temperature (37°C) because Ras activation requires interaction with Cdc25. Heterologous expression of a non-lipidated, constitutively-active Ras whose activity is independent of Cdc25 (Ras^{mut}) can rescue yeast growth at the restrictive temperature when Ras is recruited to intracellular membranes by fusion to a membrane binding protein

(Figure 2A). This system has been used to successfully identify membrane binding effectors from Gram negative pathogens [56]. To identify membrane-localizing proteins from Mtb, I subcloned MSPs into a destination vector for yeast expression that generates an in-frame fusion of the MSP to Ras^{mut}. I transformed *S. cerevisiae cdc25^{ts}* [56, 110] individually with each of the 200 MSP fused to Ras^{mut} and incubated them at both permissive and restrictive temperatures (Figure 2B). Shown are 20 examples of yeast growth at 25°C and 37°C when expressing individual Ras^{mut}-MSP fusion proteins. All strains grew when incubated at 25°C. However, at the restrictive temperature only some yeast strains were rescued. For example, I observed yeast growth rescue in yeast expressing a Ras^{mut} fusion to SapM (Rv3310), as expected due to its PI3P phosphatase activity [19, 21], but not for yeast expressing Ras^{mut} to the protein tyrosine phosphatase PtpA (Rv2234)[91, 111] which did not grow at 37°C (Figure 2B). I identified 52 Mtb proteins that rescued *S. cerevisiae cdc25^{ts}* growth at the restrictive temperature (Figures 2B and 2C and Appendix B).

I confirmed expression of the Ras^{mut}-MSP fusion proteins by Western blotting (Figure 2D). In addition, I determined the membrane localization of each MSP by fluorescence microscopy of GFP-MSP fusion proteins in yeast (Figure 2E). It has been established that Ras can function from membranes other than the plasma membrane [112, 113] and Ras^{mut} maintains this function [56]. Thus, using fluorescence microscopy I observed GFP-MSP fusion proteins localizing to distinct subcellular compartments including vacuoles, ER and plasma membrane (Figure 2E). Together these results show that 25% of the MSPs tested could associate with the membranes of a variety of organelles in *S. cerevisiae*.

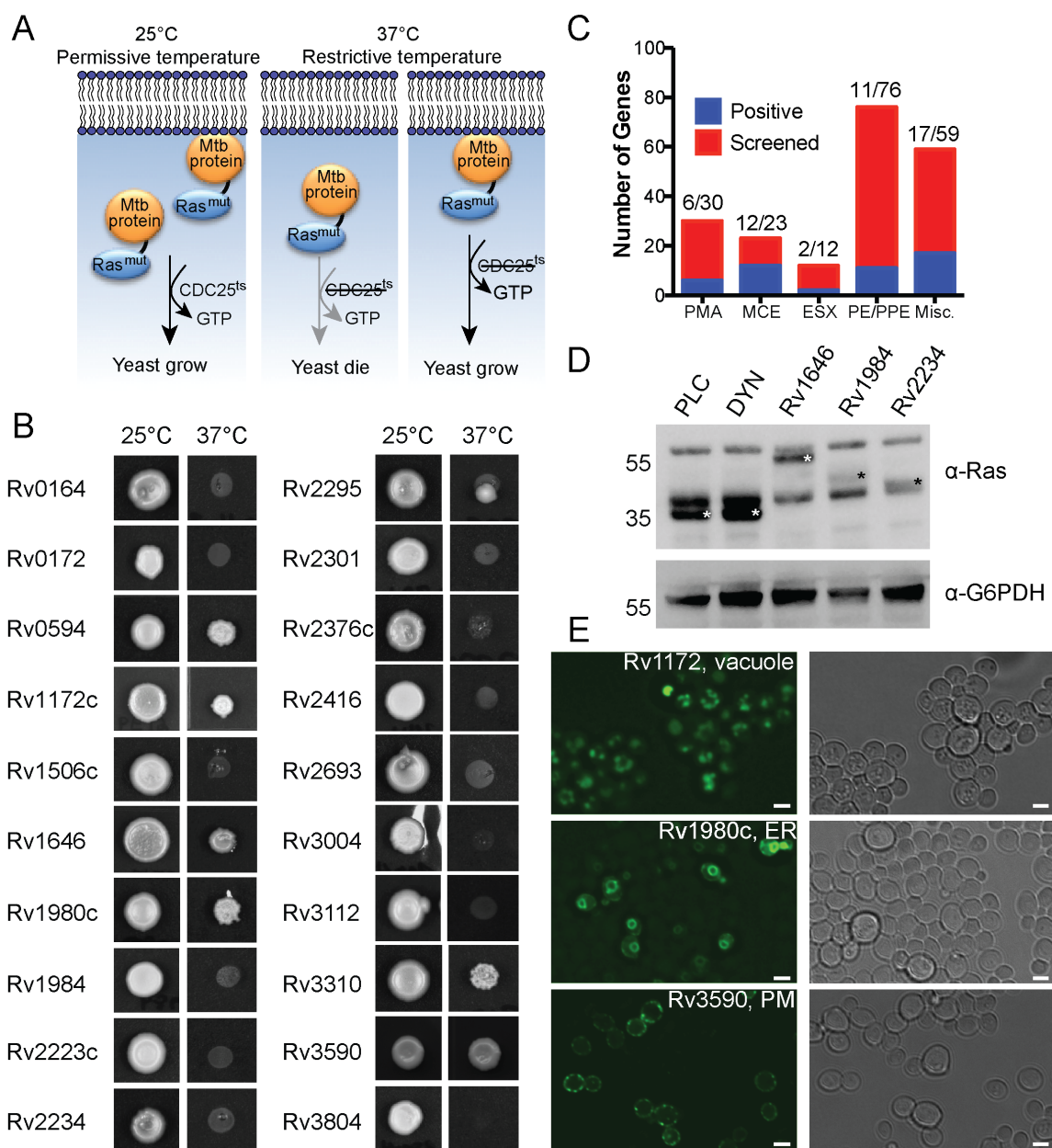


Figure 2. *M. tuberculosis* secreted proteins interact with yeast membranes. (A) Ras rescue assay schematic. (B) *S. cerevisiae* (*cdc25^{ts}*) transformed with Mtb protein fusions to Ras^{mut}, duplicate plated and incubated 48-72 h at the permissive (25°C) and restrictive (37°C) temperatures. Shown are representative images of 20 yeast strains from one experiment. (C) Summary results of Ras rescue screen. (D) Western blot of lysates from yeast transformed with the indicated fusion proteins and probed with anti-Ras or anti-G6PDH antibodies. Ras^{mut} fusion proteins are marked by white or black asterisks. PLC (phospholipase C) and DYN (dynamin) are fusions to Ras^{mut} known to be membrane associated (PLC) or cytoplasmic (DYN). Shown is one experiment of a total of three. (E)

Representative fluorescence microscopy of *S. cerevisiae* (INVSc1) transformed with GFP-MSP fusion proteins. Images are representative of three independent experiments. Scale bars are 3 μ m.

Subcellular localization of membrane-localizing MSPs

While many cellular processes are conserved in eukaryotes, humans represent the primary natural host for Mtb. Therefore, to confirm that MSPs that rescued *S. cerevisiae cdc25^{ts}* growth at 37°C also bound mammalian membranes and to determine their subcellular localization in human cells, I transiently transfected HeLa cells with vectors for constitutive expression of GFP-MSP fusion proteins and then used fluorescence microscopy with co-localization markers to identify the specific membrane to which each MSP localized (Figure 3A). I identified GFP-MSP fusion proteins that localized to a variety of subcellular compartments including the ER, Golgi, mitochondria and peroxisomes (Figures 3A and 3B). The largest proportion of the GFP-MSP fusion proteins expressed in human cells co-localized with the ER marker calreticulin (Figure 3B). In yeast, I observed a similar number of GFP-Mtb fusion proteins which localized to compact, punctate structures (data not shown). Although there was only moderate overlap in the subcellular localization identified between yeast and HeLa cells (Figure 3B), I was able to verify that the proteins identified by the Ras rescue assay are localized to membranous organelles in human cells.

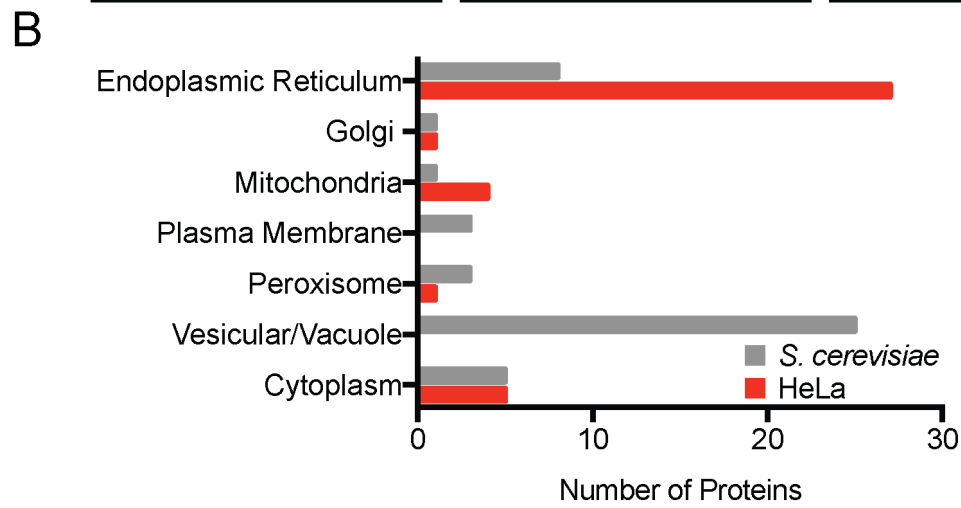
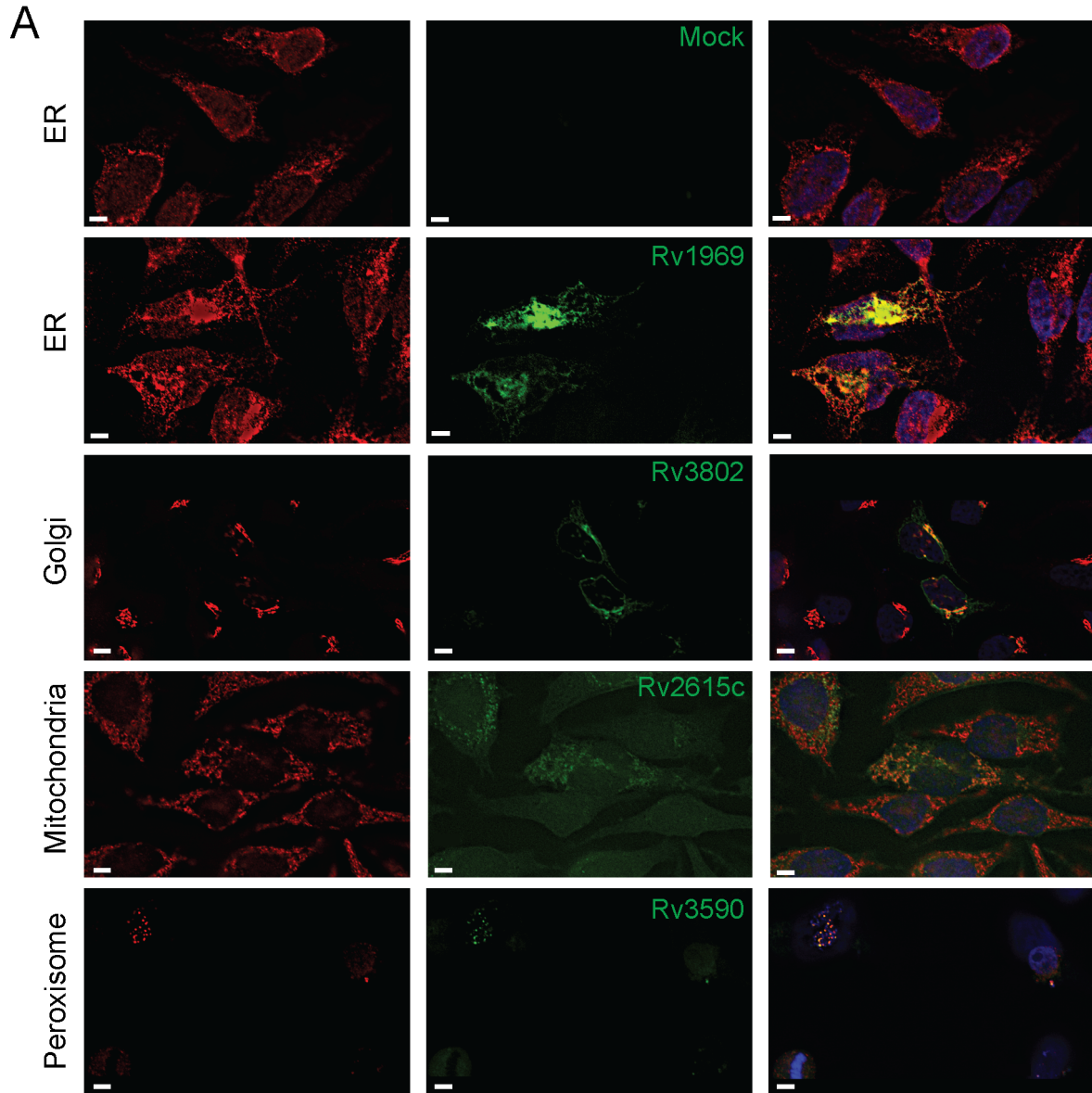
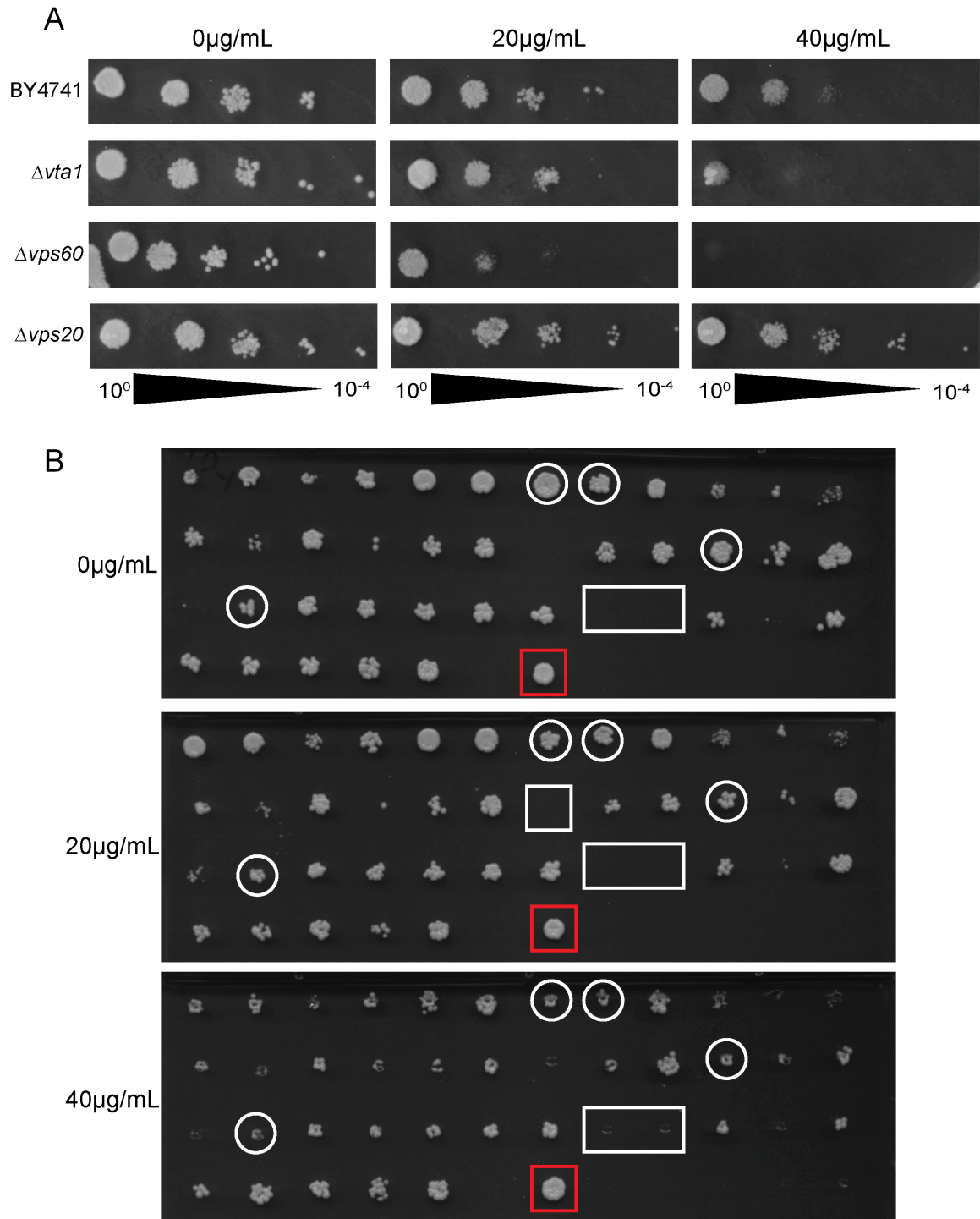


Figure 3. Host subcellular localization of membrane-binding MSP. (A) Fluorescent images of HeLa cells transfected with the indicated GFP-MSP fusion proteins (green) and stained with antibodies (red) to calreticulin (ER), GM-130 (Golgi), Tom20 (Mitochondria) or PMP70 (Peroxisomes). Images are representative of two independent experiments. Ten fields of about five cells each were observed for co-localization. Scale bars are 5 μ m. (B) Comparison of the organelle localization of MSP expressed in yeast and HeLa cells.

Mycobacterial secreted proteins do not affect yeast sensitivity to calcofluor white

Calcofluor white is a fluorescent dye that binds to chitin, a major polymer of yeast cell walls. Binding of calcofluor white to chitin prevents its assembly into macromolecular structures, ultimately disrupting the stability of the cell wall and yeast viability [114]. Thus, changes in chitin levels lead to concomitant changes in calcofluor white sensitivity [114, 115]. For example, deletions in proteins from the ESCRT complexes involved in multivesicular body formation and vacuole sorting lead to hyper-resistance ($\Delta vps20$) or hyper-sensitivity ($\Delta vta1$ and $\Delta vps60$) to calcofluor white depending on the stage of sorting they carry out (Figure 4A)[115]. To determine if MSP could alter yeast sensitivity to calcofluor white as an indicator of vesicular trafficking alterations, I compared the growth of yeast expressing GFP-MSP fusion proteins on agar plates in the presence or absence of calcofluor white. As shown in Figure 4B, all yeast, with a few exceptions (circles), were able to grow equally on both the control plate and plates containing 20 or 40 μ g/mL calcofluor white. Some yeast did not grow well on either condition (white boxes), likely due to poor growth under the high throughput screening conditions or inconstant application of cells to the agar plates (Figure 4B). Indeed, when I repeated these experiments manually spotting the yeast to reduce growth variability, I observed no differences in calcofluor white sensitivity and thus was unable to make any conclusions about the effects of MSP expression on yeast cell wall stability.



dilutions and incubated 48-72 hours at 30°C. (B) Wild type *S. cerevisiae* transformed with Mtb protein fusions to GFP under a galactose inducible promoter were diluted 1:10 then duplicate plated on induction plates with and without calcofluor white and incubated 48-72 hours at 30°C. Shown are representative images of 42 yeast strains from one experiment. The red box indicates untransformed wild type yeast. White boxes indicate yeast strains that did not grow under these conditions. White circles show examples of yeast strains that were sensitive to calcofluor white.

A subset of mycobacterial secreted proteins alters eukaryotic vesicular transport

To determine if Mtb proteins can broadly affect the host vesicular trafficking pathways in mammalian cells as an indicator of interaction with membranes, I took advantage of the reverse dimerization system [116]. In this system, a protein detectable by ELISA is sequestered in the ER by fusion to a conditional aggregation domain (CAD). Addition of a solubilization molecule that disrupts the CAD then frees the fusion protein for trafficking and release into the extracellular space. I used a fusion of human growth hormone (hGH) to the CAD domain of the ligand-reversible crosslinking protein, FKBP F36M. Thus, hGH can be quantified in cell supernatants by ELISA after addition of the small molecular, D/D Solubilizer (Figure 5A) [48, 116]. Another advantage of this system is that it permits determination of the impact of expressed proteins on vesicular trafficking events independent of the bacterial effect on host innate immune responses. I transfected HeLa cells expressing hGH-CAD with each MSP individually, a negative control protein (GFP), or an EHEC effector (EspG) that inhibits vesicular trafficking by promoting the tethering of vesicles to the Golgi apparatus [48, 117]. When I treated transfected cells with D/D Solubilizer, I observed increased, decreased and normal hGH release (Figure 5B and Appendix A). Using a cut-off of normalized hGH release below 0.25 or above 1.75, I identified 18 proteins that decreased hGH release and 11 proteins that increased hGH release as compared to the GFP control (Figure 5C and Appendix C). Next I compared the MSPs that altered host vesicular trafficking to those that bound eukaryotic membranes, and identified five proteins with overlapping activities: Rv0594, Rv1646, Rv1810, Rv1980c and Rv2075 (Figure 5D). During expression in HeLa cells, all but one protein localized to the ER and all five proteins reduced hGH release (Figure 5E).

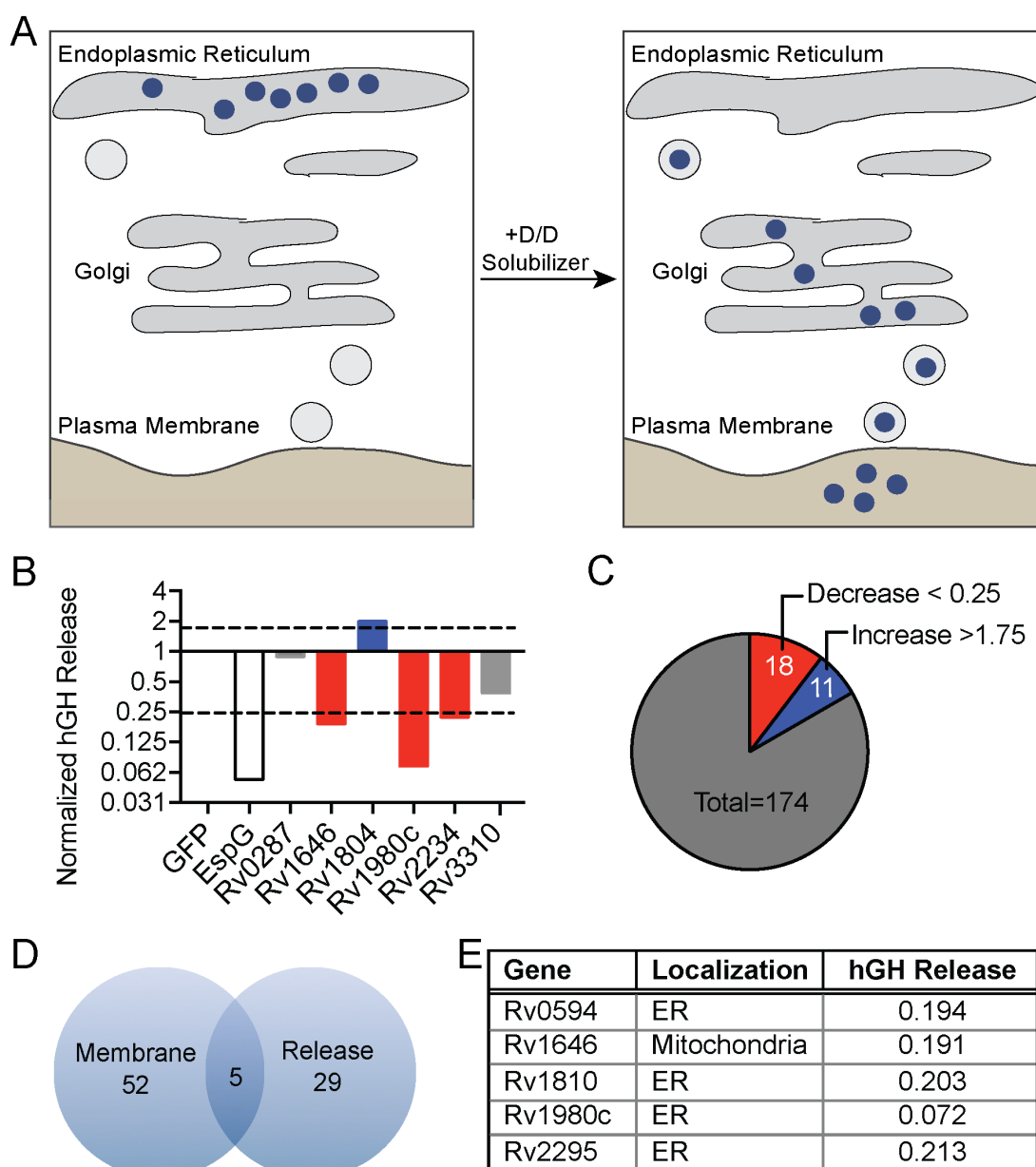


Figure 5. *M. tuberculosis* secreted proteins alter hGH secretion (A) Inducible secretion assay schematic. (B) Supernatant hGH ELISA from HeLa cells transfected overnight with hGH-CAD and either GFP or GFP-MSP fusion proteins prior to addition of drug to allow for hGH release. hGH release by GFP-MSP transfected cells was normalized to hGH release of cells transfected with GFP alone. hGH release was measured once for the entire group of GFP-MSP transfections. (C) Summary of results from inducible secretion screen. (D) Venn diagram of MSP that are membrane-localized, alter host secretion, or both. (E) Table summarizing the membrane localization and degree of hGH secretion in cells transfected with the five overlapping proteins from D.

Discussion

Numerous efforts have been undertaken to identify Mtb secreted proteins, from lipoproteins that are incorporated into the cell wall, to virulence factors that reach the extracellular environment such as ESAT-6 [77-79]. However, little is known about the function of this “exoproteome” as a whole. Here I took a systematic approach towards characterizing host-dependent interactions of a collated list of Mtb proteins. I created a library of 200 putative secreted proteins and then through a series of cell biological screens characterized these MSPs for their ability to bind eukaryotic membranes, their subcellular localization and their ability to modulate release of a model substrate.

I identified some MSPs that rescued yeast growth in the Ras rescue assay but localized to the cytoplasm when expressed as GFP fusions in HeLa cells. These proteins represent either false positives from the Ras rescue assay or proteins that do associate with lipids whose abundance is sufficient in yeast but not HeLa cells. In contrast, because I only confirmed subcellular localization of positive hits from the screen, I cannot predict the number of false negatives that were missed. While yeast represent a good model system with many conserved pathways to humans, it is likely that not all Mtb host molecular targets are present [118].

The vast majority of MSPs localized to the ER when expressed in HeLa cells. Whether this localization reflects the importance of modulating ER function for Mtb survival cannot be determined directly, as that would require significant resources to raise protein specific antibodies against individual proteins in order to determine the localization of each untagged, endogenous, secreted protein during infection. It is possible that some of the observed localizations represent false positives, as overexpression of Mtb proteins

with signal sequences results in aberrant ER localization in 293T cells [119]. Alternatively, because the microscopy and co-localization was performed in the absence of infection, ER localization could represent not false positives but false targeting of Mtb proteins due to low abundance of their protein or lipid targets under basal conditions.

Although I did not identify any MSP that affected calcofluor white sensitivity in yeast, this was likely due to the technical limitations of the experiment. Growing the yeast in 96-well plates to perform the assay under high-throughput conditions led to inconsistent yeast growth and possibly inconsistent expression of the GFP-MSP fusion proteins. Instead, I used an inducible secretion assay to indirectly assess the effects of MSP expression on host vesicular trafficking, as this was successful to characterize effectors from *E. coli* [48]. I identified 18 MSP that decreased hGH release. An obvious physiological effect of inhibiting secretion in host macrophages would be to prevent cytokine secretion. However, I also identified 11 proteins that increased hGH release. It may be that increased hGH release is a readout for gross rearrangements to vesicular trafficking routes or capacity by MSP.

Finally, five proteins were identified in both the Ras rescue assay and the hGH release assay. Interestingly, all decreased hGH release and all but one localized to the ER, emphasizing the importance of the ER in coordinating important cellular processes including protein secretion. Although all five proteins are of unknown function, several have published virulence qualities, such as Mce2F (Rv0594) which was isolated from Mtb -infected mice and Rv1810 which is required for virulence of Mtb in non-human primates which supports that the screens enriched for putative effector proteins.

CHAPTER FOUR Results

CHARACTERIZATION OF MPT64 MEMBRANE BINDING AND VIRULENCE FUNCTIONS

Introduction

In the previous chapter, I identified five proteins that localize to eukaryotic membranes and reduced hGH release. I chose to focus on the characterization of one of these proteins, Mpt64, because it is a secreted protein that is highly antigenic and can be used to diagnose human tuberculosis infection [120, 121]. Furthermore, mpt64 is a component of the region of difference 2 (RD2) locus, one of the genomic regions deleted during attenuation of the *M. bovis* BCG vaccine strain [122]. Loss of RD2 from Mtb attenuates its virulence, and complementation with a three gene cluster that includes mpt64 can partially restore virulence [123]. Interestingly, Mpt64 has been incorporated into subunit vaccines tested for their efficacy in animal models [124, 125] despite the fact that its function in Mtb pathogenesis remains unknown.

Mpt64 localized to the ER, an organelle that is at the nexus of multiple cellular processes including protein and lipid synthesis, cargo secretion and calcium signaling [126]. Coupled with its ability to decrease hGH release, these characteristics led me to hypothesize that Mpt64 is a candidate effector protein from Mtb. I endeavored to confirm this hypothesis by characterizing the mechanism of Mpt64 membrane interaction, the subcellular localization of Mpt64 during infection and the effect of Mpt64 on host cell

physiology. Finally, I sought to understand if loss of mpt64 from Mtb could explain the attenuation of the RD2 deletion strain. Thus, I used combined tools described in Chapter 3 such as the Ras rescue assay and fluorescence microscopy with new assays including yeast two hybrid, PIPs strips, and bacterial pathogenesis.

Results

Mpt64 does not interact with lysozyme from two species

Mpt64 is a 25kDa protein with a predicted signal peptidase 1 cleavage site between amino acids 23 and 24, such that the mature, secreted form of the protein starts at amino acid 24 [79, 80, 127]. While the solution structure of Mpt64 was previously solved [128], the structure does not align to a known catalytic domain but does contain a domain of unknown function (DUF3298). This domain is also present in the lysozyme-binding anti sigma factor RsiV [129]. Despite structural homology between Mpt64 and RsiV (Figure 6A) [130], there is little primary sequence homology. To determine if Mpt64 binds lysozyme, I purified recombinant Mpt64 from *E. coli* and tested binding to human or hen egg white lysozyme in an *in vitro* pull-down assay [129]. Using this assay I was unable to demonstrate lysozyme binding by Mpt64 as most lysozyme was lost in the wash fraction and there was no enrichment of lysozyme during elution of Mpt64 or the control protein, Cor (Figure 6B).

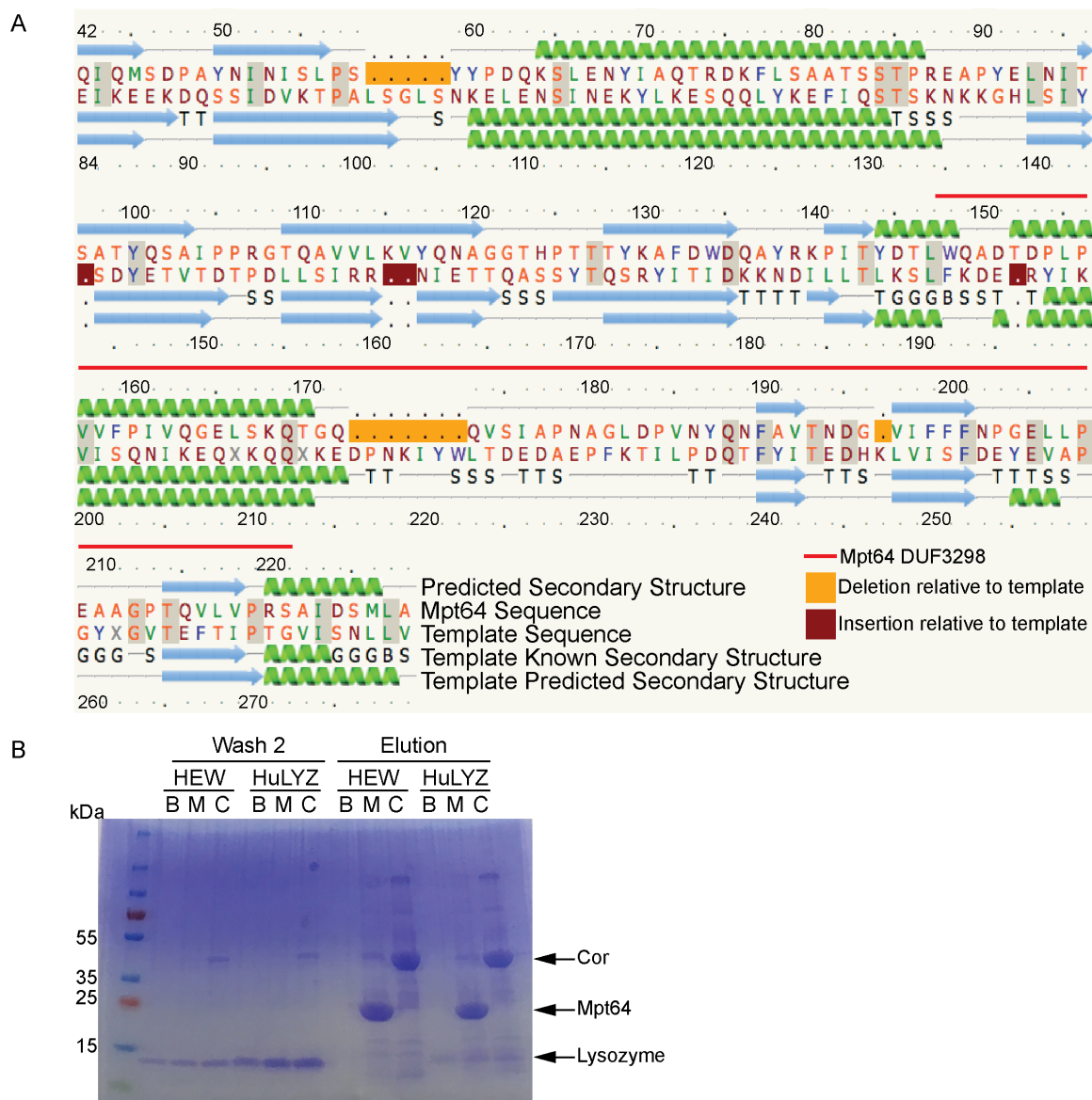


Figure 6. Recombinant Mpt64 does not interact with lysozyme. (A) Sequence and secondary structure alignment of Mpt64 and *B. subtilis* RsiV (template) performed by Phyre² software (<http://www.sbg.bio.ic.ac.uk/phyre2/>). The Mpt64 DUF3298 is indicated by a red line above the Mpt64 amino acid numbering. (B) Mpt64 (M) or an unrelated protein Cor (C) were immobilized on cobalt beads and hen egg white (HEW) or human lysozyme (HuLYZ) was incubated with these or beads alone (B) for five minutes. After washes, proteins were eluted with 300mM imidazole.

Mpt64 N-terminus is important for ER localization and inhibition of vesicular trafficking

I next used the solution structure to guide truncation analysis of Mpt64 in order to identify the membrane binding sequences of Mpt64 (Figure 7A and Figure 7B). *S. cerevisiae cdc25^{ts}* expressing a fusion of Ras^{mut} with either full length Mpt64, mature Mpt64 lacking its predicted signal peptide or the N-terminal half of Mpt64 also lacking the signal peptide (Mpt64_24-143) were able to grow at 37°C, whereas *S. cerevisiae cdc25^{ts}* expressing Ras^{mut} fused to the C-terminal half of Mpt64 (Mpt64_144-228) could not (Figure 78C). I detected expression of Ras^{mut} fusions of full length Mpt64 and mature Mpt64 by Western blot. In contrast, I could not detect Ras^{mut} fusions of Mpt64_24-143 or Mpt64_144-228 despite the fact that the Mpt64_24-143 fusion rescued yeast growth, suggesting that expression of Mpt64_24-143 below the limit of detection by Western blot was still sufficient to rescue yeast growth (Figure 7D). However, I could not determine whether the C-terminal domain plays a role in membrane binding because I was unable to demonstrate stable fusion protein expression in yeast.

Finally, I sought to determine if the N-terminal portion of Mpt64 was also sufficient to inhibit hGH release using the hGH-CAD assay. I co-transfected HeLa cells with plasmids for expression of hGH-CAD and Mpt64 truncation alleles and determined their ability to inhibit hGH release in the presence of drug. Similar to the Ras rescue assay, full length, mature and Mpt64_24-143 inhibited hGH release compared to the GFP control. In contrast, co-transfection of Mpt64_144-228 with hGH-CAD had no effect on its release (Figure 7E). These data suggest that the ability of Mpt64 to bind membranes and to inhibit host vesicular trafficking *in vitro* is dependent on the N-terminus of the protein.

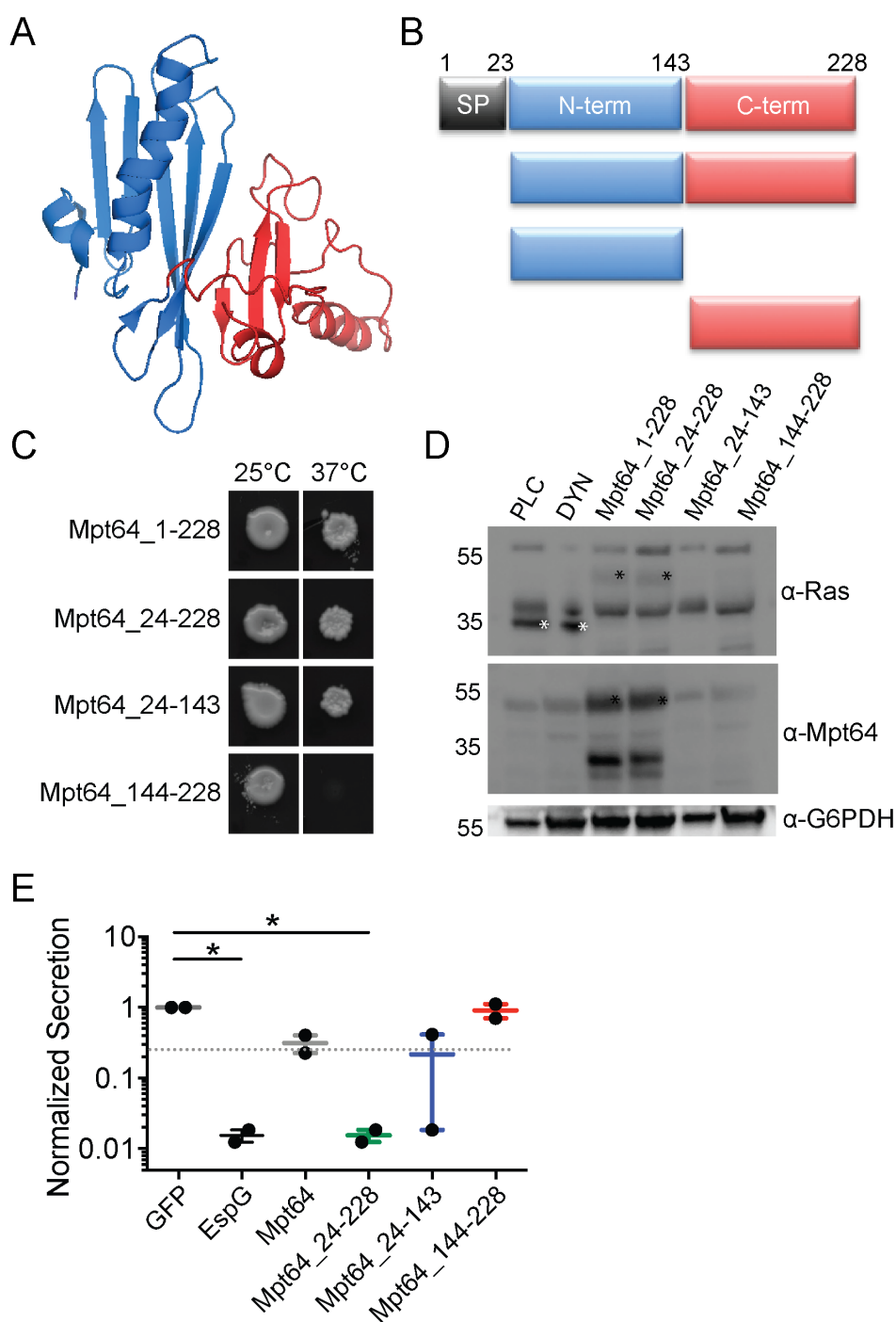


Figure 7. hGH release inhibition is dependent on membrane localization of Mpt64. (A) Solution structure of Mpt64. PDB 2hhi. (B) Schematic of Mpt64 truncations, colored to match solution structure in A. SP, signal peptide. (C) Full length Mpt64 or protein truncations expressed in the Ras rescue assay. Shown is one of two independent

experiments. (D) Western blot of lysates from *cdc25^{ts}* yeast expressing Ras^{mut} fusion proteins to Mpt64 or Mpt64 truncations. Blots were probed with rabbit anti-Ras, anti-Mpt64 or anti-G6PDH antibodies. Control protein bands are marked by a white asterisk and Mpt64 truncations are marked by a black asterisk. Image is representative of three experiments. (E) ELISA results of hGH in supernatants of cells co-expressing full length Mpt64, Mpt64 truncations or controls. Data are one representative experiment plotted as box and whiskers from two (Mpt64_24-143, Mpt64_144-228) or four (Mpt64, Mpt64_24-228) total experiments. * $p=0.02$ by ANOVA with Dunnett's multiple comparisons test.

Mpt64 ER localization depends on its N-terminus

As full-length Mpt64 localized to the ER in yeast and HeLa cells (Figures 2 and 5), I next tested the impact of Mpt64 truncations on ER localization. First, I determined the phenotypic localization of Mpt64 truncations expressed as GFP fusions in yeast using fluorescence microscopy. Mpt64₁₋₂₂₈ and Mpt64₂₄₋₂₂₈ localized in a ring indicative of the ER [131, 132](Figure 8A). In contrast Mpt64₁₄₄₋₂₂₈, which did not rescue yeast growth in the Ras Rescue assay (Figure 7C), was diffuse throughout the yeast cell (Figure 8A). Interestingly, Mpt64₂₄₋₁₄₃ localized to bright puncta within the cells (Figure 8A). To confirm the N-terminal dependence of Mpt64 localization, I transfected HeLa cells with GFP fusions to each Mpt64 truncation or GFP alone and assayed for co-localization with calreticulin through immunofluorescence microscopy. While full length Mpt64, mature Mpt64 and Mpt64₂₄₋₁₄₃ co-localized with calreticulin, GFP did not (Figure 8B). Mpt64₁₄₄₋₂₂₈ localized to a bright aggregate that did not co-localize with calreticulin, suggesting the C-terminus of Mpt64 is misfolded and/or unstable when expressed on its own. These results demonstrate that Mpt64 localizes to the ER during exogenous expression in both yeast and mammalian cells and the N-terminal 143 amino acids are sufficient to mediate subcellular localization of Mpt64 to the ER.

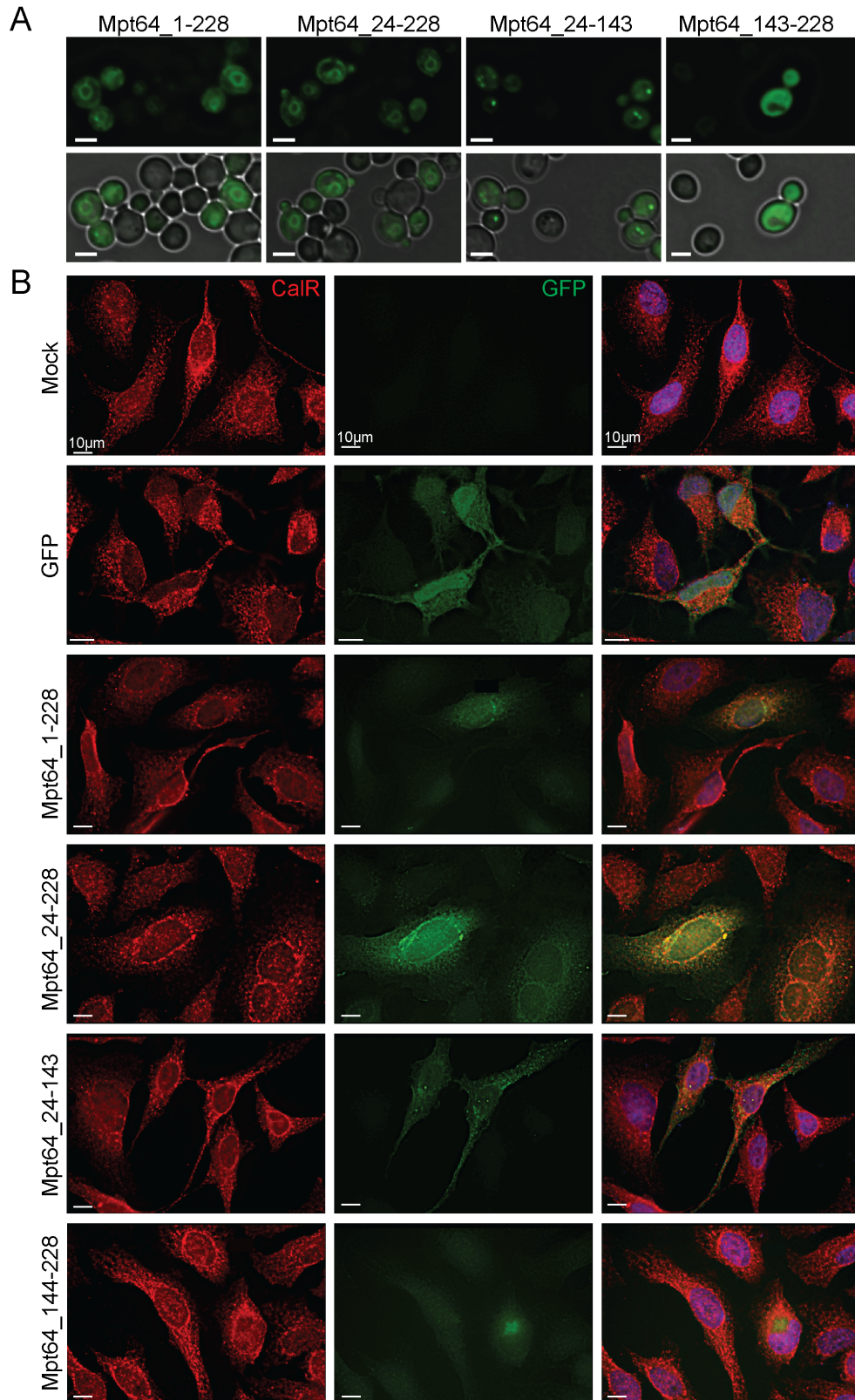


Figure 8. Mpt64 localizes to the endoplasmic reticulum during heterologous expression in yeast and HeLa cells. (A) Immunofluorescence (top panels) and bright field overlay (bottom panels) images of *S. cerevisiae* transformed with GFP fusion proteins to Mpt64 truncations. Images are representative of three independent experiments. Scale bars are 3 μm . (B) HeLa cells transfected overnight with GFP alone (green) or GFP-Mpt64 fusion proteins (green) and stained for ER localization with anti-calreticulin antibody (red). Nuclei are stained with DAPI (blue). Images are representative of two independent experiments. Ten fields of about five cells each were observed for co-localization. Scale bars are 10 μm .

Probing Mpt64 protein-protein interactions through yeast two hybrid

Because I had originally identified Mpt64 in a screen for membrane-binding and subsequently confirmed it localized to the ER, I wanted to determine if the Mpt64 subcellular localization of Mpt64 depends on a host protein-interacting partner. To that end, I performed a Y2H using mature Mpt64 (Mpt64 Δ SP) as bait against three separate cDNA prey libraries. After stringent selection, I sequenced the cDNA inserts of over 100 colonies. Independent of the prey library source (universal human, HeLa or universal mouse), three predominant proteins emerged as possible Mpt64-binding proteins. The three proteins were the sodium/potassium ATPase, beta chain 1 or 3 (ATPase β 1 or β 3) or phosphoglucomutase 1 (PGM1). To eliminate the possibility that these cDNAs were capable of auto-activation of the GAL4 promoter, I purified the plasmids directly from colonies that arose after selection and co-transformed them with control vectors into the yeast strain, Y2H Gold, which encodes several selectable genetic markers under the GAL4 promoter. While yeast transformed with both empty vectors or Mpt64 Δ SP—or its ortholog Rv3036c—co-transformed with an empty prey (EP) vector did not survive selection (Figure 9A, 1-3), the three cDNA prey vectors, ATPase β 1 ATPase β 3 and PGM1, did survive selection when co-transformed with the empty bait (EB) vectors and were able to convert x- α -gal causing the colonies to turn blue (Figure 9A, 4-6). This suggests that the interactions identified could be false positives.

To better understand if Mpt64 interacts directly with ATPase β 1, ATPase β 3 or PGM1, I cloned each gene into the prey vector pGADT7, transformed Y187 yeast with the resulting constructs or appropriate controls and performed a mating with bait yeast.

After mating, the yeast were spotted on DDO/X to select for both plasmids. The mated yeast were duplicate spotted on QDO/X/A to select for all possible markers under the GAL4 promoter. When I mated yeast with an empty vector in one or both strains the resulting colonies were able to grow on DDO/X but not on QDO/X/A (Figure 9B, left column). I also mated yeast containing proteins that are known to interact, p53 and TA, which survived selection on QDO/X/A and turned blue, as expected (Figure 9B, left column). I then mated yeast containing Mpt64 Δ SP bait with the EP vector or ATPase β 1, ATPase β 3 or PGM1 prey. I also performed the opposite mating with the EB vector and ATPase β 1, ATPase β 3 or PGM1 prey and assessed growth on DDO/X and QDO/X/A. I observed white colonies on DDO/X in the yeast mating between the EB and PGM1 prey, which did not survive on QDO/X/A (Figure 9B, right column). However, when Mpt64 Δ SP was mated with the EP vector or ATPase β 1 and ATPase β 3 were mated with an EB vector, the colonies on DDO/X were faintly blue. More concerning, the mating between EB and ATPase β 1 was able to grow very slightly on QDO/X/A media (Figure 9B, right column). Finally, the matings between Mpt64 Δ SP and ATPase β 1 or ATPase β 3 resulted in blue colonies that survived on QDO/X/A whereas the directed mating between Mpt64 Δ SP and PGM1 did not (Figure 9B, right column). These results suggest that Mpt64 Δ SP does not interact directly with PGM1 but may be able to interact with ATPase β 1 and ATPase β 3.

Due to possible autoactivation, I wanted to confirm the interaction of Mpt64 Δ SP with ATPase β 1 biochemically. To that end, I expressed recombinant 6xHIS-Mpt64 Δ SP or 6xHIS-MBP in *E. coli* and immobilized the proteins on cobalt beads. Next, I incubated the immobilized proteins with lysates from HEK293T or HeLa cells which both express the

sodium/potassium ATPase β 1 (Figure 9C, WCL). After washing away excess protein, I eluted the 6xHIS-tagged proteins from the beads with imidazole and separated the fractions on SDS-PAGE followed by Western blotting for ATPase β 1. I observed that most of the ATPase β 1 was in the fraction that did not bind to the beads (FT) and the fraction that did elute with the 6xHIS-tagged proteins was equal between 6xHIS-Mpt64 Δ SP and the control protein 6xHIS-MBP (Figure 9C). From this, I concluded that 6xHIS-Mpt64 Δ SP does not interact with native ATPase β 1 from HEK293T or HeLa cells, suggesting all results from the Y2H were false positives.

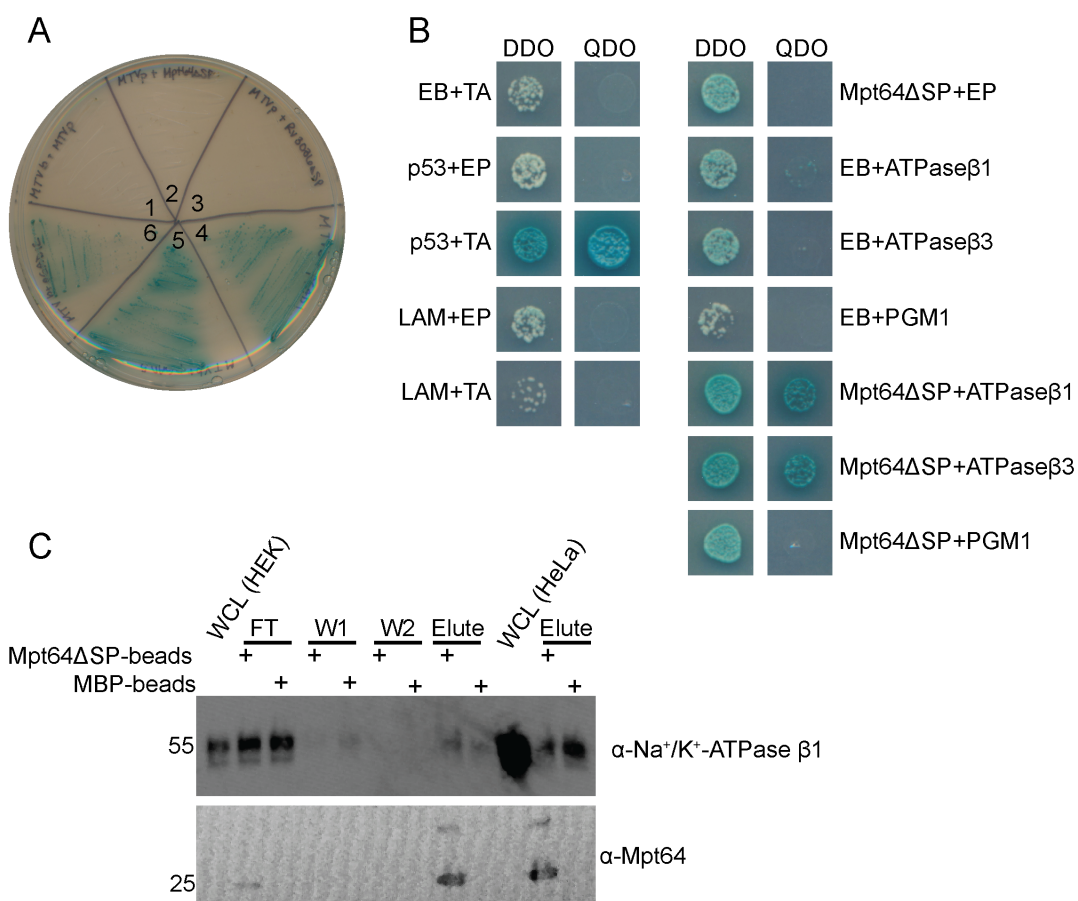


Figure 9. Mpt64 does not interact with the sodium/potassium ATPase beta chain. (A) Quadrant streaks of Y2H Gold yeast co-transformed with combinations of bait and prey vectors and plated on DDO/X/A. 1, EB+EP; 2, Mpt64ΔSP+EP; 3, Rv3036cΔSP+EP; 4, EB+ATPaseβ1; 5, EB+ATPaseβ3; 6, EB+PGM1. (B) Directed matings of Y2H Gold yeast carrying bait vectors with Y187 yeast carrying prey vectors and selected on DDO/X/A or QDO/X/A. Images are from one of two separate matings (C). Western blots detecting ATPaseβ1 or Mpt64 in whole cell lysates (WCL) or fractions of a pull-down experiment. Representative of two independent experiments. EB, empty bait vector; EP, empty prey vector; FT, flow through; W1, wash 1; W2, wash 2.

Mpt64 interacts with phosphatidylinositol phosphates in vitro

Because I was unable to identify a protein binding partner through Y2H, I next hypothesized that Mpt64 interacts with lipids to localize to the ER. To test if Mpt64 could interact with lipids directly, I expressed and purified recombinant Mpt64 and Mpt64 variants from *E. coli* (Appendix D) and tested their ability to bind unique lipid species *in vitro* using membranes spotted with lipids. Recombinant Mpt64₂₄₋₂₂₈ bound phosphatidylinositol 4-phosphate (PI4P), phosphatidylinositol 5-phosphate (PI5P), phosphatidylinositol 4,5-bisphosphate [PI(4,5)P₂] and phosphatidylinositol (3,4,5)-trisphosphate [PI(3,4,5)P₃] on PIP strips membranes (Figure 10A). Similarly, recombinant Mpt64₂₄₋₁₄₃, the N-terminal portion of the protein, also bound PI4P and PI5P with additional binding to PI3P, PI(3,4)P₂ and phosphatidylserine (Figure 10A). However, interaction with PI(4,5)P₂ and PI(3,4,5)P₃ was weak, suggesting that the C-terminal region of Mpt64 modifies its interactions with host phospholipids. I was unable to test PIP binding by Mpt64₁₄₄₋₂₂₈ because its expression in *E. coli* was weak and the protein was insoluble after purification using similar conditions for Mpt64₂₄₋₂₂₈ and Mpt64₂₄₋₁₄₃.

Mpt64 ER localization in yeast is dependent on PI3P and PI(3,5)P₂

Based on the results from the PIP strips (Figure 10A), and to further characterize the lipid binding of Mpt64 *in vivo*, I took advantage of yeast strains mutated in phosphatidylinositide (PI) kinases that either lack or have reduced levels of specific phosphatidylinositol phosphates (PIPs) (Figure 10B). Because PIPs are geographically restricted within cells and their position-specific phosphorylation patterns can function as

organelle-specific markers to recruit proteins to areas with unique membrane constituents [56, 133, 134], inactivation of yeast PI-kinases causes mislocalization of bacterial effectors that need such PIP interactions for appropriate membrane targeting [56] (Figure 10C). I inhibited expression of each yeast PI-kinase gene either by isogenic knockout of the non-essential PI-kinase gene (VPS34, FAB1, and LSB6) or by doxycycline-mediated (Dox) repression of TetO₇-promoter alleles of essential PI-kinase genes (PIK1, STT4, and MSS4). I optimized repression conditions for the TetO₇-promoter alleles by monitoring the distribution of the PI4P-specific binding protein Osh2, which shuttles between the plasma membrane and Golgi apparatus upon depletion of the essential PI4-kinases PIK1 and STT4, respectively (Figure 10D) [56, 135, 136]. Dox-mediated loss of PIK1 and STT4 expression led to Osh2 redistribution to the plasma membrane (PM) or Golgi, respectively, as previously reported [56]. As a further control for the isogenic deletion strains, I observed that deletion of LSB6 and VPS34 along with Dox-mediated loss of MSS4 and PIK1 caused relocalization of the *S. Typhimurium* effector SopA from the PM to internal puncta, consistent with its affinity for several PIP isoforms [56]. Using this assay, Mpt64 relocalized from the ER to the PM and internal puncta in the absence of VPS34 and FAB1 (Figure 10D). As these strains lack PI3P and PI(3,5)P₂, and because the VPS34 strain lacks both PIPs while the FAB1 strain lacks only PI(3,5)P₂, I conclude that recruitment of Mpt64 to the ER in yeast is likely dependent on PI(3,5)P₂. Though the PIP strips (Figure 10A) showed strong binding to PI4P, I would propose that the failure to relocalize in yeast lacking various PI-kinases that produce PI4P (i.e. LSB6, PIK1 and STT4) is due to their redundancy. Taken together, the data indicate that Mpt64 interacts with PIPs *in vitro* and *in vivo* to facilitate its localization to the ER.

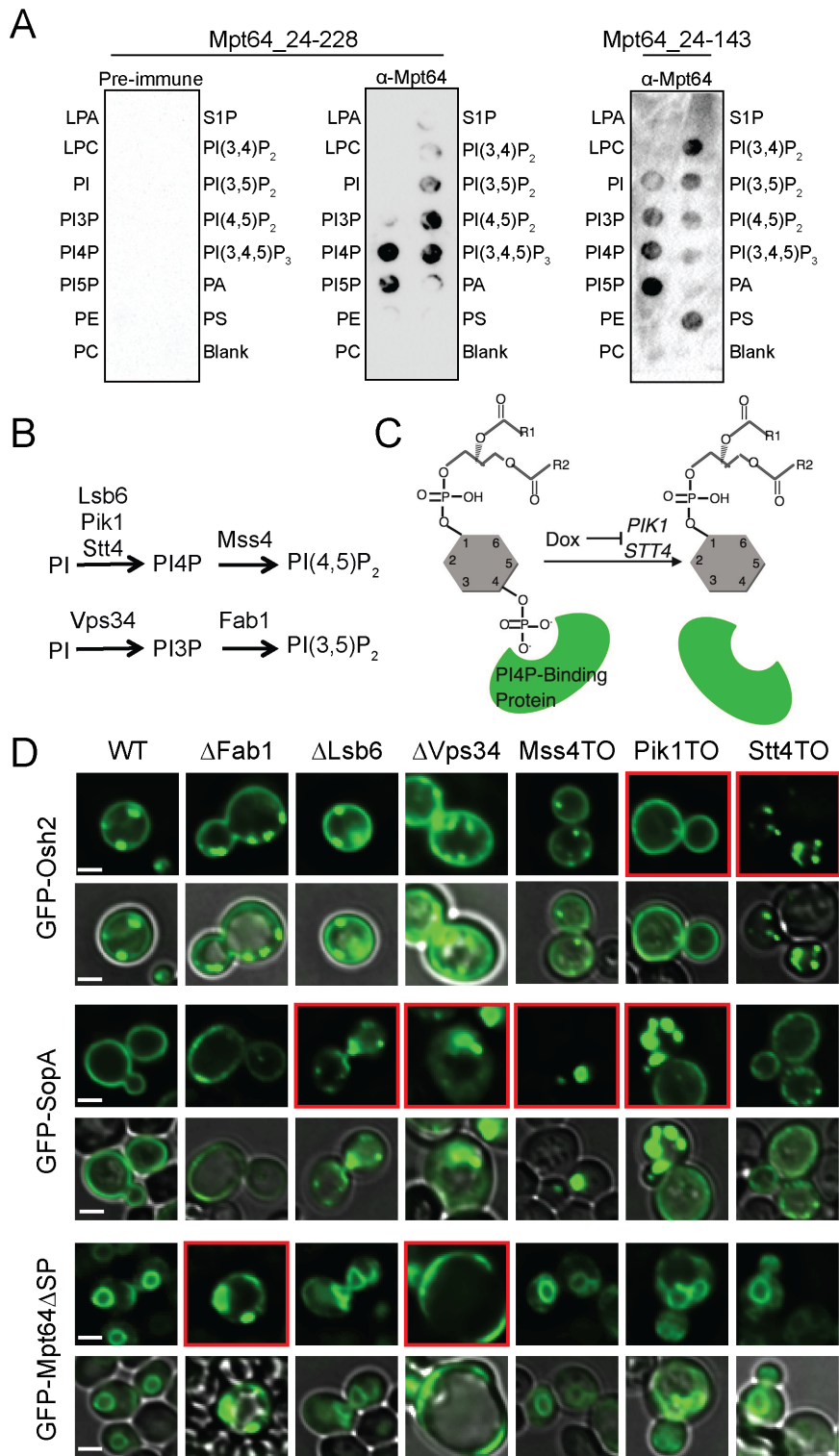


Figure 10. Mpt64 binds phosphatidylinositol phosphates to mediate its ER localization (A) PIPs strips membranes incubated with recombinant Mpt64₂₄₋₂₂₈ or Mpt64₂₄₋₁₄₃. Binding of Mpt64 to lipids was detected by incubation with α -Mpt64 or pre-immune serum. Abbreviations indicate specific lipids as follows: LPA, lysophosphatidic acid; LPC, lysophosphatidylcholine; PI, phosphatidylinositol; PI3P, phosphatidylinositol-3-phosphate; PI4P, phosphatidylinositol-4-phosphate; PI5P, phosphatidylinositol-5-phosphate; PE, phosphatidylethanolamine; PC, phosphatidylcholine; S1P, sphingosine 1-phosphate; PI(3,4)P₂, phosphatidylinositol-3,4-bisphosphate; PI(3,5)P₂, phosphatidylinositol-3,5-bisphosphate; PI(4,5)P₂, phosphatidylinositol-4,5-bisphosphate; PI(3,4,5)P₃, phosphatidylinositol-3,4,5-trisphosphate; PA, phosphatidic acid; PS, phosphatidylserine. Images are representative of two (Mpt64₂₄₋₁₄₃) or four (Mpt64₂₄₋₂₂₈) independent experiments. (B) PIP synthesis is regulated by six PI-kinases in yeast by the indicated pathways. (C) Design of the PI kinase experiment. Representative results for Osh2, a PI4P binding protein. Doxycycline repression of a PI kinase (PIK1 and STT4 are shown) depletes the PIP, causing loss of localization of proteins that have a membrane localization governed by PI4P (i.e. Osh2). (D) Localization of GFP-Osh2 (a known PI4P binding protein), GFP-SopA (a promiscuous PIP binding protein) or GFP-Mpt64 in wild-type *S. cerevisiae* cells and the six PI kinase yeast strains. Images are representative of two (FAB1, LSB6, VPS34) or three (MSS4, PIK1, STT4) independent experiments.

Secreted Mpt64 localizes to the ER during infection

Although I observed Mpt64 localization to the ER in yeast (Figure 2E and Figure 8A) and HeLa cells (Figure 8B), I wanted to determine if endogenous, untagged Mpt64 localizes to the ER during an Mtb infection of macrophages. To that end, I infected mouse RAW267.4 macrophages with mCherry-labeled Mtb at a MOI of 20:1 and fixed cells at various time points after infection. I used a rabbit polyclonal antibody raised against recombinant, mature Mpt64 protein to track Mpt64 secretion from Mtb into macrophages using immunofluorescence microscopy. Of note, this antibody was generated without complete Freund's adjuvant in order to avoid any cross-reactivity against Mtb antigens generated by the use of this adjuvant. As little as four hours after infection, endogenous Mpt64 was detected in both the cytoplasm and ER of host cells (Figure 11A, upper panels). When I infected macrophages with Mtb Δ eccD1, a strain that is deficient in ESX-1 secretion [66, 137], and does not result in communication between the phagosome and cytoplasm [30, 59, 60, 138-140], Mpt64 appeared to be secreted but trapped adjacent to the bacteria (Figure 11A, lower panels), suggesting that it could not escape the phagosome. Importantly, Mpt64 was detected in the culture filtrate prepared from Mtb Δ eccD1 (Appendix E). Thus, although Mpt64 is likely secreted from Mtb by the canonical Sec-dependent pathway, its access to the macrophage cytoplasm and other targets in the cell was dependent on the Type VII secretion system.

In order to better understand the role of Mpt64 in Mtb virulence, I used mycobacteriophage [83, 141, 142] to introduce the hygromycin resistance cassette into the *mpt64* gene to create an in-frame deletion (Figure 11B). I confirmed disruption of *mpt64* by PCR (Appendix E) and loss of Mpt64 by the absence of protein on Western blot

(Figure 11C). To confirm that there are no pleiotropic effects of this mutant in downstream experiments, I complemented *MtbΔmpt64* with either full length *mpt64* (*MtbΔmpt64::mpt64*) or *mpt64* lacking its signal peptide (*MtbΔmpt64::mpt64-NS*) under the control of the constitutive mycobacterial strong promoter [143]. Both complemented strains expressed Mpt64 but only full-length Mpt64 (*MtbΔmpt64::mpt64*) could be detected in the supernatant of cultures, confirming that deletion of the signal peptide inhibits Mpt64 secretion from *Mtb* (Figure 11C). Furthermore, the *MtbΔmpt64::mpt64* strain had modestly higher expression of Mpt64 compared to wild-type *Mtb* by western blot, consistent with the use of a strong constitutive promoter for complementation. All four strains grew equally under axenic growth conditions (Appendix E), and we confirmed that both *Mtb* and *MtbΔmpt64* produced phthiocerol dimycocerosate by mass spectrometry (Appendix E).

To test if secreted Mpt64 localizes to the ER during infection, I assessed its colocalization with calreticulin in RAW267.4 cells using confocal immunofluorescence microscopy. When I infected RAW267.4 macrophages, the Mpt64 signal in *Mtb* infected macrophages co-localized with calreticulin, confirming the subcellular localization of Mpt64 secreted during infection (Figures 11D and 11E and Appendix F). However, this co-localization was lost in cells infected with *MtbΔmpt64::mpt64-NS* bacteria (Figures 11D and 11F and Appendix F). As a control for antibody specificity, no Mpt64 was detected in macrophages infected with *MtbΔmpt64* mutant bacteria (Figure 11D and Appendix F). From these data, I can confirm that the signal peptide of Mpt64 is sufficient for the protein's secretion *in vivo* and is required (with concerted action of the Type VII secretion system) for Mpt64 to localize to the ER during infection.

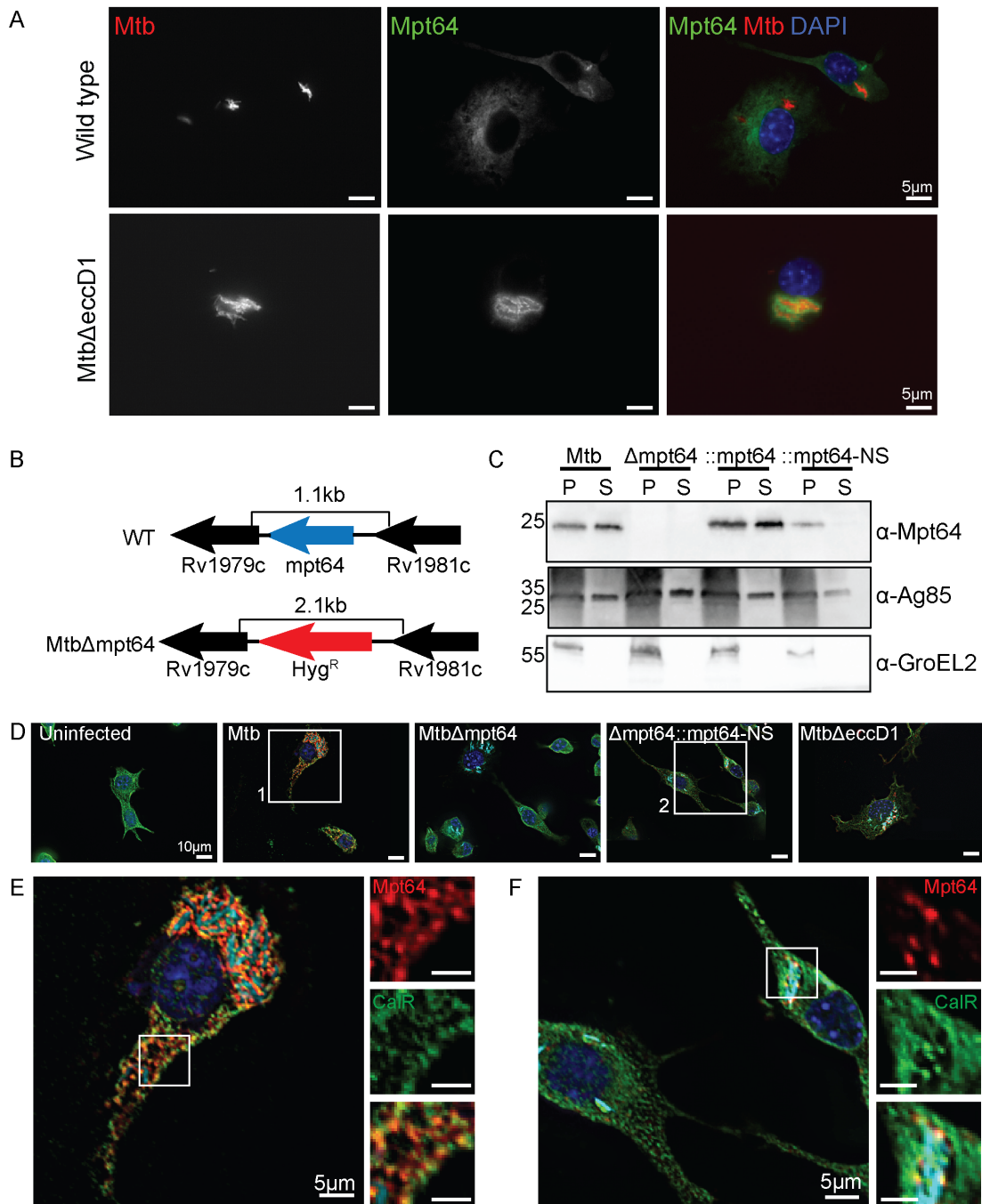


Figure 11. Mpt64 ER localization is ESX1-dependant during *M. tuberculosis* infection of macrophages. (A) RAW267.4 murine macrophages were infected with mCherry-expressing (red) WT (upper panels) or *Mtb* Δ eccD1 (lower panels) for 4 hours at a MOI 20:1. Cells were fixed and stained for Mpt64 (green) and nuclei (blue). Scale bars are 5 μ m. (B) Schematic detailing in-frame deletion of *mpt64* by insertion of a hygromycin

resistance gene. (C) Representative Western blot from one of three experiments detecting expression of Mpt64, Ag85 and GroEL2 in either the lysate of the cell pellet (P) or culture supernatant (S) of four Mtb strains. (D) RAW267.4 macrophages were infected with the indicated strains of mCherry-expressing (cyan) Mtb for 4 hours at a MOI 20:1. Cells were fixed and stained for Mpt64 (red), calreticulin (green) and nuclei (blue). Images in (E) and (F) correspond to box 1 and box 2, respectively. Scale bars are 10 μ m. (E) Enlarged image from box 1 in (D) of an Mtb-infected macrophage stained for Mpt64, calreticulin and DAPI. Insets show an area of Mpt64-calreticulin co-localization. Scale bars are 5 μ m. (F) Enlarged image from box 2 in (D) of macrophages infected with Mtb Δ Mpt64::Mpt64-NS and stained for Mpt64, calreticulin and DAPI. Insets show Mpt64 localization in relation to bacteria. Scale bars are 5 μ m. Images in A and D-F are representative of one of three experiments. Ten fields of about five cells each were observed for co-localization.

Mpt64 does not inhibit cytokine secretion during macrophage infection

Secretion of cytokines is an important macrophage response to Mtb infection [144, 145]. Since I confirmed that Mpt64 is secreted into host macrophages, and Mpt64 could inhibit the release of hGH in HeLa cells, I hypothesized that Mpt64 could function to inhibit cytokine secretion during infection. To test this hypothesis, I infected RAW267.4 for 24 hours or primary human macrophages for 6 hours and measured cytokines in the supernatant of cells using multiplexed ELISAs. I quantified murine TNF- α , GM-CSF and IL-6 in the supernatants of RAW267.4 cells (Figure 12A) and human TNF- α , MIP-1 β (also called CCL4) and IL-8 in the supernatants of primary macrophages (Figure 12B). If Mpt64 inhibited cytokine secretion, I would expect more cytokines released by cells infected with the Mpt64 deletion strain. However, I measured lower levels of cytokines from cells infected with Mtb Δ mpt64, regardless of the cell type or cytokine measured (Figures 12A and 12B). In all cases the differences in cytokines measured between wild type and Mtb Δ mpt64-infected cells was not statistically significant. From these data I concluded that Mpt64 does not affect cytokine secretion during infection. Interestingly, I observed that cytokine secretion increased in cells infected with Mtb Δ mpt64::mpt64 compared to wild type. Again, this difference was not statistically significant, but it may be indicative of the immunogenic properties of Mpt64 as the complemented strain produces slightly more Mpt64 than wild type (Figure 11C).

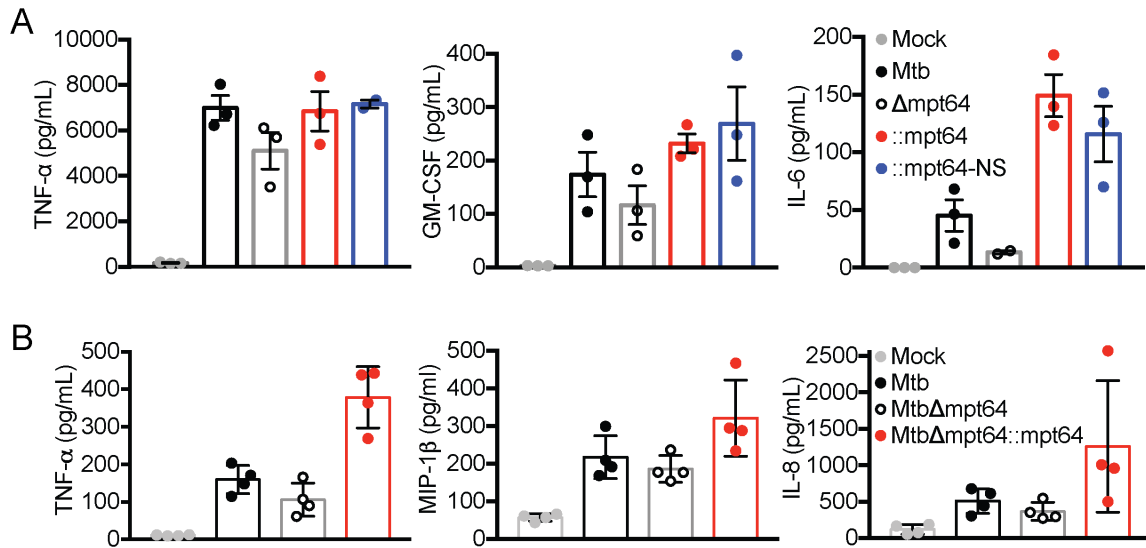


Figure 12. Mpt64 does not inhibit cytokine secretion in macrophages (A) Cytokines measured from supernatants of RAW267.4 cells infected with the indicated strains at MOI 5:1 for 24 hours. One representative of two independent experiments. (B) Cytokines measured from supernatants of primary human macrophages infected with the indicated strains at MOI 5:1 for 6 hours. One experiment of 4 biological replicates.

Mpt64 inhibits the unfolded protein response

ER stress and the UPR have recently been associated with Mtb infection and pathogenesis [146-148]. Because I found that Mpt64 localizes to the ER during infection, I hypothesized that it might regulate the UPR. To test if Mpt64 was sufficient on its own to impact the UPR, I stably transduced murine RAW267.4 cells with empty lentivirus or a lentivirus with Mpt64 under the control of a CMV promoter and induced the UPR by treating with thapsigargin, a known UPR activator [149]. In the presence of thapsigargin, I detected robust accumulation of the UPR-activated transcription factor CCAAT-enhancer-binding protein homologous protein (CHOP), a protein whose expression is low under non-stressed conditions but high in the setting of ER stress [149](Figure 13A). Expression of Mpt64 resulted in a 75% reduction in CHOP compared to control cells, indicating that Mpt64 alone could inhibit the UPR (Figure 13B).

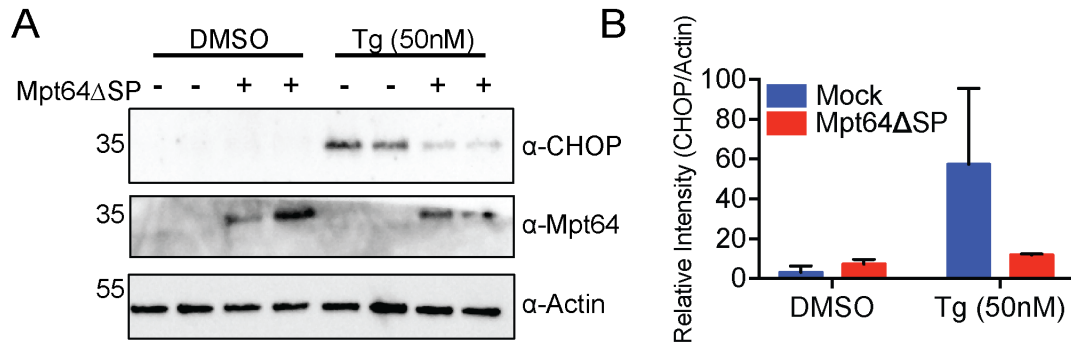


Figure 13. Mpt64 inhibits the unfolded protein response (A) RAW267.4 cells stably transduced with empty lentivirus or lentivirus expressing Mpt64 Δ SP under control of the CMV promoter were treated with DMSO or thapsigargin (50 nM) for 4 hours and CHOP protein accumulation detected by Western blot. (B) Quantitative densitometry analysis of the Western blot in (A). One experiment representative of >3 experiments.

Mpt64 contributes to the Mtb modulation of the unfolded protein response during infection

To further test if Mpt64 could impact the UPR in the setting of Mtb infection, I infected mouse RAW267.4 macrophages with wild type Mtb or Mtb Δ mpt64 and assayed for accumulation of the protein CHOP by Western blot (Figure 14A). After 4 hours, infection of RAW267.4 cells by either Mtb strain alone was insufficient to induce the UPR to levels of uninfected cells treated with thapsigargin (Figure 14A and 14B) consistent with previous data [146, 147]. To better understand the role of Mpt64 in modulating the UPR during infection, I repeated the infection of RAW267.4 cells with Mtb or Mtb Δ mpt64 but added thapsigargin during the 4 hour incubation. In this case, CHOP protein accumulated in all cells treated with thapsigargin compared to DMSO (Figure 14C), but there was no significant difference in relative protein levels between cells infected with Mtb or Mtb Δ mpt64 (Figure 14D). Therefore, I infected RAW267.4 cells with Mtb, Mtb Δ mpt64, Mtb Δ mpt64::mpt64 and Mtb Δ mpt64::mpt64-NS in the presence of thapsigargin and measured expression levels of CHOP, the ER chaperone immunoglobulin heavy-chain-binding protein (BiP; also known as GRP78) and the spliced variant of the transcription factor X-box binding protein 1 (Xbp-1) by quantitative PCR as transcription of these genes is increased after ER stress [149]. As expected, stimulation of either uninfected or infected cells with thapsigargin resulted in transcriptional upregulation of CHOP, BiP and spliced Xbp-1 (Figure 14E). RAW267.4 cells infected with Mtb Δ mpt64 trended toward increased expression of CHOP and sXbp-1 compared to cells infected with Mtb, but these changes were not statistically significant.

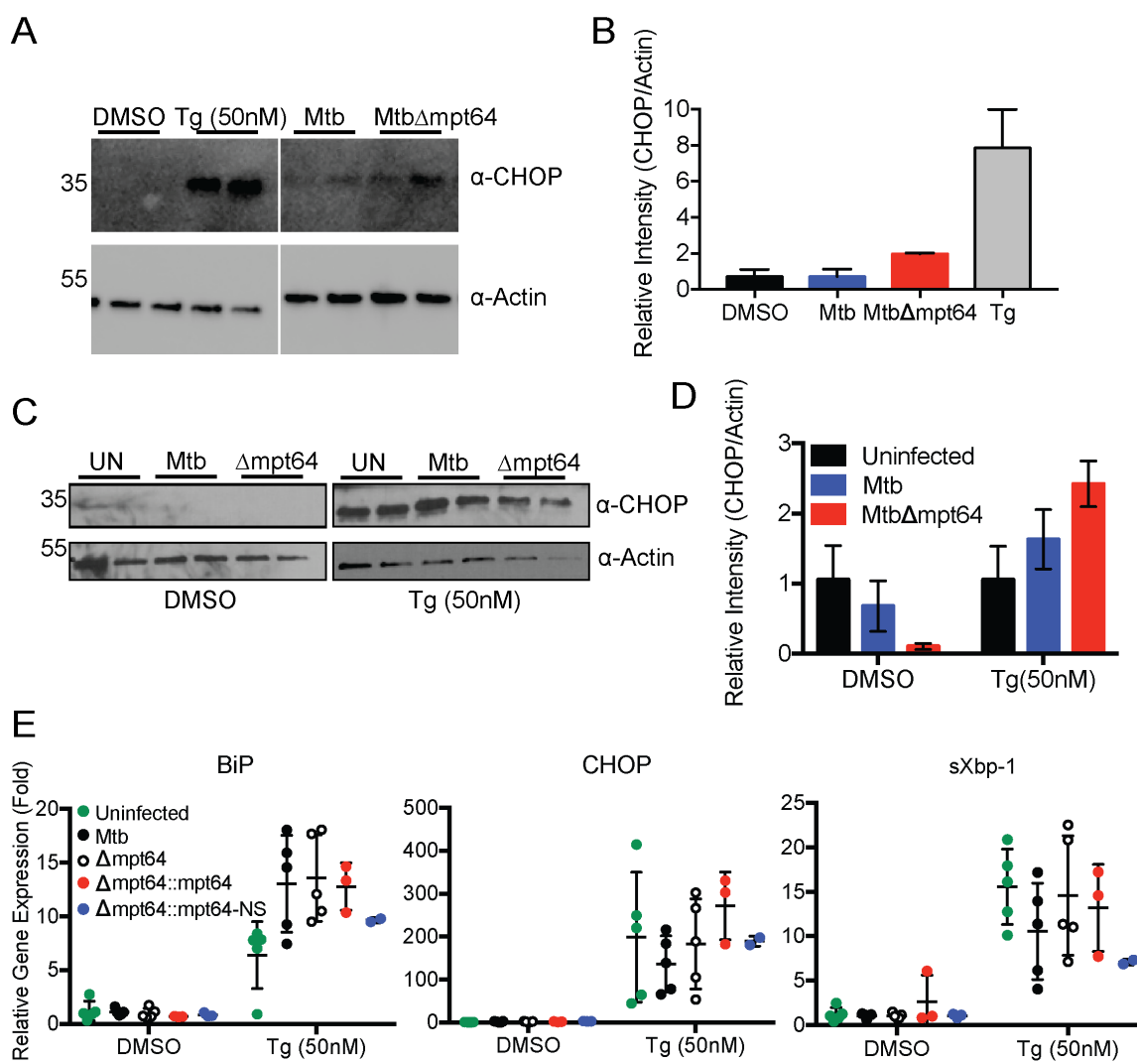


Figure 14. Mpt64 contributes to the Mtb modulation of the unfolded protein response during infection (A) RAW267.4 cells were infected with Mtb, Mtb Δ mpt64 at a MOI 1:1 or uninfected cells were treated with DMSO or thapsigargin (50 nM) for 4 hours and CHOP protein accumulation was detected by Western blot. (B) Quantitative densitometry analysis of the Western blots in (A). One experiment representative of 2 experiments. (C) RAW267.4 cells were infected with Mtb, Mtb Δ mpt64 at a MOI 10:1 or left uninfected in the presence of DMSO or thapsigargin (50 nM) for 4 hours and CHOP protein accumulation was detected by Western blot. (D) Quantitative densitometry analysis of the Western blots in (C). Relative gene expression of BiP, CHOP and sXbp-1 from RAW267.4 cells infected as in (C).

Mpt64 contributes to early Mtb growth after aerosol infection of mice.

Because Mpt64 is part of the Mtb RD2 locus that partially accounts for the attenuation of Mtb [123], and my data indicating that Mpt64 may function as a secreted effector that modulates the UPR, I investigated the role of Mpt64 in Mtb virulence in a murine model of infection. I infected BALB/c mice via aerosol with a low bacterial inoculum (~50-100 CFU Mtb) and collected lungs at various time points to determine CFU and histopathology. I compared the infections of four strains: wild type Mtb, Mtb Δ mpt64, Mtb Δ mpt64::mpt64 and Mtb Δ mpt64::mpt64-NS (described in Figure 11). While all mice received equal numbers of bacteria between the four strains at day 0, there were one-third fewer Mtb isolated from lungs of mice infected with the Mtb Δ mpt64 mutant compared to wild type at 21 days (mean CFU wild type Mtb 2.7×10^6 vs Mtb Δ mpt64 1.7×10^6 , $p=0.07$) and 42 days (mean CFU wild type Mtb 5.0×10^5 vs Mtb Δ mpt64 3.4×10^5) post infection. Though these effect sizes were modest and consistent for both time points, they did not meet statistical significance at an alpha of $P < 0.05$. By 42 days post-infection I observed statistically significant decrease in the CFU isolated from lungs of mice infected with the Mtb Δ mpt64::mpt64-NS strain (mean CFU wild type Mtb 5.0×10^5 vs Mtb Δ mpt64::mpt64-NS 1.8×10^5 , $p=0.001$) (Figure 15A). At these time points, I also observed a reduction in the area of inflammation in hematoxylin and eosin (H&E) stained lungs of mice infected with Mtb Δ mpt64::mpt64-NS compared to wild type. (Figures 15B and 15D). Despite modest reductions in CFU in the lungs of mice infected with mutant bacteria, there was no impact on mouse survival (Figure 15C).

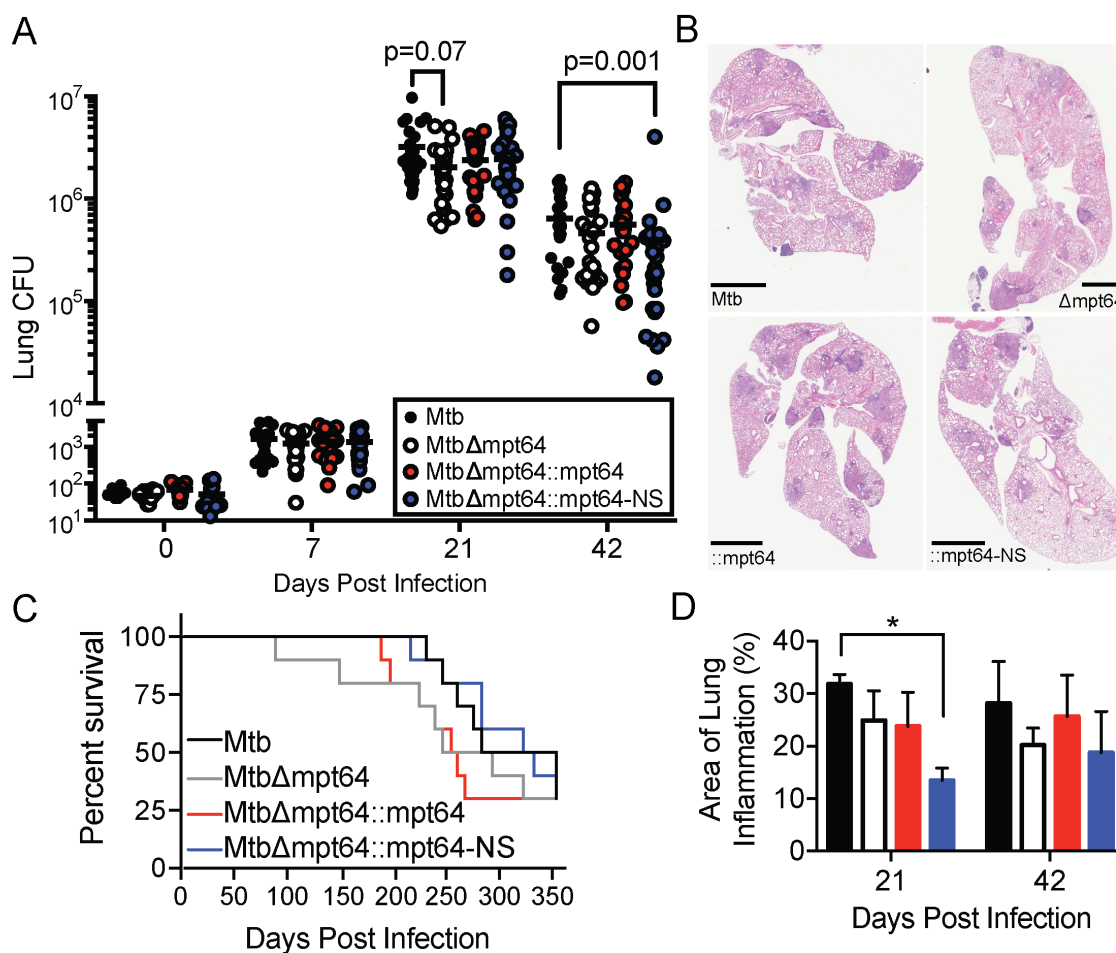


Figure 15. Mpt64 contributes to early Mtb growth after aerosol infection of mice (A) Bacterial burden in lungs of mice 0, 7, 21 and 42 days after aerosol infection with indicated Mtb strains. Results are a combination of three independent experiments, n=25 mice total per group. Horizontal bar indicates the geometric mean. p values are determined by nonparametric Kruskal-Wallis analysis. (B) Representative images of H&E stained lungs at 42 days post-infection with the indicated strains of Mtb. Scale bars, 2mm. (C) Ten mice per group were monitored for survival. There were no significant differences in survival rates between groups by Kaplan–Meier analysis. (D) Quantitation of lung inflammation of mice infected with indicated Mtb strains. Measurement was determined using ImageJ software (NIH). Bars are colored as in (A). Results are the mean \pm SEM for three animals per group. * $p < 0.02$ by Kruskal-Wallis test.

Mpt64 localized to the ER in primary human macrophages but is dispensable for Mtb survival

Finally, I assessed whether the localization of Mpt64 in human cells is similar to that in murine macrophages. To that end, I infected primary human monocyte-derived macrophages with mCherry-expressing WT Mtb or Mtb Δ eccD1 and stained for Mpt64. Consistent with our data in RAW267.4 cells (Figure 11A) Mpt64 localization to extra-phagosomal sites in primary human macrophages was dependent on the Type VII Secretion System (Figure 16A). I then infected primary human macrophages with WT Mtb, Mtb Δ mpt64, Mtb Δ mpt64::mpt64 or Mtb Δ mpt64::mpt64-NS and determined the co-localization of Mpt64 with calreticulin by fluorescence microscopy (Figure 16B and Appendix G). At 4 hours post infection, I detected co-localization of Mpt64 with calreticulin in cells infected with WT Mtb and Mtb Δ mpt64::mpt64 but not in cells infected with Mtb Δ mpt64 or Mtb Δ mpt64::mpt64-NS (Figure 16B).

To better understand the contribution of Mpt64 in the context of human Mtb infection, I determined the growth of wild type Mtb, Mtb Δ mpt64, Mtb Δ mpt64::mpt64, Mtb Δ mpt64::mpt64-NS, and Mtb Δ eccD1 as a control for attenuation in primary monocyte-derived human macrophages during acute infection. I recovered CFU from cells directly after infection (Day 0) and one and three days post infection (Figure 16C). I observed significant donor-to-donor variability both in the ability to restrict intracellular Mtb replication (compare the growth of WT Mtb between representative donor 1 and donor 2) and the relative growth of Mtb Δ mpt64, Mtb Δ mpt64::mpt64, Mtb Δ mpt64::mpt64-NS in various donors. Thus, while in some donors the CFU at day 3 post-infection of strains lacking mpt64 was modestly but not statistically significantly lower compared to WT Mtb

(i.e. donor 1), in other donors there was no impact on the presence or absence of mpt64 (i.e. donor 2). Thus, in this acute primary human macrophage infection model, the presence of Mpt64 appeared to be dispensable for Mtb survival.

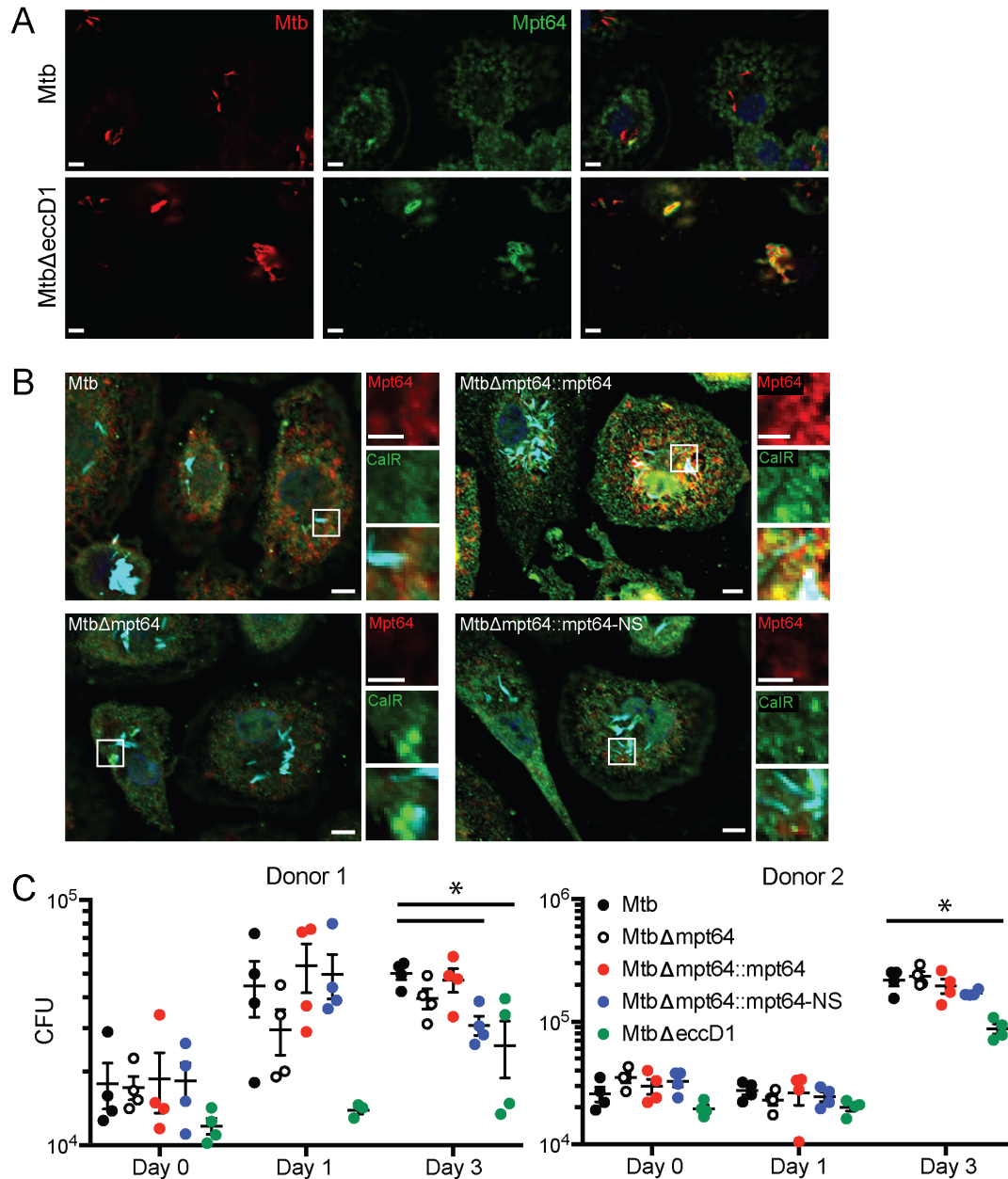


Figure 16. Mpt64 localization and impact on survival in primary human macrophages (A) Primary human monocyte-derived macrophages were infected with mCherry-expressing (red) Mtb or MtbΔeccD1 for 4 hours at a MOI 10:1. Cells were fixed and stained for Mpt64 (green). Scale bars are 5μm. (B) Primary human monocyte-derived macrophages were infected with the indicated strains of mCherry-expressing Mtb for 4 hours at a MOI 10:1. Cells were fixed and stained for Mpt64 (red) and calreticulin (green). Nuclei are stained blue. Scale bars are 5 μm. Images in A and B are representative of three independent experiments. Ten fields of about five cells each were observed for co-localization. (C)

CFU recovered from primary human macrophages from two independent donors infected with Mtb, Mtb Δ mpt64, Mtb Δ mpt64::mpt64, Mtb Δ mpt64::mpt64-NS or Mtb Δ ecccD1 at indicated time points. Each point represents a biologic replicate at each time point per strain and the bars indicate the mean with standard error. Two donors of 4 are shown. * $p=0.02$ by Kruskal-Wallis test with Dunn's correction for multiple comparisons.

Discussion

The ability of Mpt64 to localize to the ER could occur through a host protein interaction or through direct lipid binding. Although I identified ATPase β 1 and ATPase β 3 as interacting partners of Mpt64 Δ SP through Y2H, I also observed false activation of the Y2H reporters which made it difficult to interpret the results. Indeed, I was unable to confirm the interaction of Mpt64 Δ SP with ATPase β 1 through biochemical studies. While Y2H has been used to identify protein binding partners between Mtb proteins [138, 150], it may not be as robust in identifying host-interacting proteins. Also, the technical limitations of standard Y2H, such as the requirement of both proteins to interact in the nucleus may not be ideal for studies with membrane-localized proteins like Mpt64 [151]. A more direct method, such as immunoprecipitation followed by mass spectrometry (IP-MS) may uncover protein-protein interactions since it can be performed within eukaryotic cells and with cross-linking to preserve transient interactions. However, my data using PIPs strips and PI kinase loss of function yeast suggests that Mpt64 could directly interact with charged lipids. Since changes in PIP levels in the loss of function yeast can also affect localization and activity of host proteins, I cannot rule out that Mpt64 has a host protein interacting partner.

Although an enzymatic activity for Mpt64 could not be deduced from its structure, I was able to demonstrate that the N-terminus of Mpt64 was sufficient to mediate membrane binding, interaction with PIPs and inhibition of vesicular trafficking. Mature Mpt64 was also able to inhibit the UPR in the setting of thapsigargin-induced ER stress

in macrophages. Since ER stress has been observed *in vivo* during Mtb infection, and ER stress is known to activate autophagy and apoptosis [152], the ability of Mpt64 to downregulate the UPR may allow Mtb to fine-tune the host response in order to provide a long-term replicative niche. Indeed, Mpt64 staining of human tuberculosis granulomas is negatively correlated with apoptosis markers [153], which is in agreement with my data in that decreased UPR would also lead to a decrease in apoptosis.

GFP-Mpt64 localized to the ER in both yeast and mammalian cells. Additionally, endogenous Mpt64 localized to the ER during Mtb infection of macrophages, suggesting that the observed localization of Mpt64 is not an artifact of heterologous over-expression. Mpt64 did not co-localize with the ER after infection with a Mtb Type VII secretion system mutant underscoring the importance of the phagosome disrupting properties of the ESX-1 system in establishing communication with the host cell [96]. This ESX-1 dependent mechanism of cytoplasmic access is similar to the route taken by the autotransporter-like protein tuberculosis necrotizing toxin (TNT) [154, 155]. Thus, my data strengthen the argument that the Type VII secretion system facilitates access of non-ESX-1 substrates beyond the phagosome and into the host cell.

While I was able to measure decreased hGH from HeLa cells overexpressing Mpt64 and decreased UPR from macrophages overexpressing Mpt64, I did not observe similar phenotypic effects in macrophages infected with Mtb or the mpt64 deletion strain. Neither the subtle changes in cytokine secretion nor UPR marker activation were significantly different between Mtb and Mtb Δ mpt64. Although I was able to detect changes in CHOP protein accumulation when Mpt64 was overexpressed, Western blotting may

not be sensitive enough to detect changes in the complex system of an infection where levels of Mpt64 in the host are expected to be lower. Furthermore, it may be that cultured, naive macrophages are a poor substitute for the environment Mtb normally experiences during infection of the human host. I did not collect serum or lung homogenates to measure cytokines during the murine infections. Perhaps subtle changes in cytokine profiles would be revealed from such an experiment. Furthermore, it is possible that one or more of the other Mtb secreted proteins I identified, including the 27 proteins that also localized to the ER are able to perform a redundant function to that of Mpt64 during macrophage infections. In a similar vein, whereas *L. pneumophila* encodes over 300 effectors, individual *L. pneumophila* effector deletion mutants are not defective for growth in cells or mice [156, 157]. Indeed, a *L. pneumophila* strain in which 11 effectors that function to inhibit protein translation are deleted is still able to inhibit host protein translation, though a mutant in the Type IV secretion machine itself cannot [158], indicating remarkable redundancy in effector activity. Thus, future work disrupting multiple Mtb MSPs simultaneously will help address this issue.

CHAPTER FIVE Conclusions and Recommendations

DISCUSSION OF RESULTS

Identification and screening of mycobacterial secreted proteins

The cohort of 200 MSPs I generated was large but not necessarily exhaustive (Appendix A). This is likely a result of the criteria to which I constrained the library. As a result, I may have excluded ORFs with no protein characterization. For example, the 76 PE/PPE genes I included represent less than half (45%) of the total number of PE/PPE genes in the Mtb genome [69] because many are not identified in secreted fractions by conventional mass spectrometry sequencing analysis due to an absence of trypsin sites [159]. However, the direct approach allowed me to curate the library to include proteins likely to interact with membranes and have important roles in Mtb virulence. In the end, I identified 5 proteins of unknown function that have intriguing properties as potential Mtb effectors.

Recently, similar studies used unbiased approaches to identify secreted proteins with virulence functions. For example, Penn *et al.* first identified secreted proteins by mass spectrometry, then purified each individually in the presence of a macrophage lysate to create a human-Mtb protein-protein interactome [119]. In doing so they identified a novel function of LpqN. In addition, a recent technology called EXIT identified 593 Mtb proteins secreted during intravenous infection of mice including 38 proteins that are significantly enriched only during *in vivo* infection as compared to growth on 7H10 agar, suggesting a virulence function for these proteins [98]. Of the 200 MSPs I characterized, 51 overlap with those identified by EXIT and of the 51 overlapping proteins, 25 are

membrane associated in our study. These studies emphasize that host membranes and membrane proteins can be targets of Mtb secreted proteins. Integrating my dataset with others like the ones described above may reveal novel Mtb protein interactions or functions.

I found 52 Mtb proteins that associated with eukaryotic membranes, representing nearly 25% of the total screened. When the membrane association of type III and type IV effectors from several Gram negative pathogens was explored, about 30% of effectors screened also associated with eukaryotic membranes [56]. While my data are in agreement with this value, pathogens that replicate intracellularly in vacuoles had even higher numbers of membrane-associated effectors [56]. This suggests that there may be additional secreted virulence proteins from Mtb that associate with the host membranes than my screen identified. Indeed, while I corroborated previously known membrane-interacting proteins such as the SecA2-secreted PI3P phosphatase SapM [20, 21], the Rac1-binding protein Ndk [160] and the cholesterol-binding Mce4A [161], I failed to identify others such as LipY which hydrolyzes extracellular lipids [162] and the ESX1 substrate ESAT-6, whose ability to directly interact with the phagosomal membrane [163, 164] has recently been questioned [96, 165].

When I assessed the subcellular localization of MSP in HeLa cells, I observed that most localized to the ER. However, I was unable to identify the localization of some membrane-binding MSPs either due to low transfection efficiency or failure to co-localize with the organelle-specific markers tested. The latter possibility suggests MSPs could potentially localize to distinct microdomains of the organelles we tested [166] to harder to define membrane species such as those along the endosomal pathways or to the

transient membrane contact sites between organelles used to transfer lipids and proteins in a fusion independent process [36]. Moreover, I was able to identify a number of proteins that localized to other non-ER organelles such as the mitochondria and Golgi. This variety of localizations suggests that Mtb secretes proteins to target organelle-distinct processes across the cell. Indeed, since both autophagy [167, 168] and apoptosis [169] have critical roles in the outcome of Mtb infection, engagement by Mtb of high-value targets such as the ER, Golgi and mitochondria - organelles vital to cellular regulation of vesicular trafficking, autophagy and apoptosis - with its entire secreted effector armament such as the membrane-binding MSPs identified here likely allows Mtb to tightly control the host response to facilitate successful infection.

Characterization of Mpt64 membrane binding and virulence functions

The differential accumulation of individual PIP species in organelle membranes that facilitates appropriate localization of host proteins can be hijacked by bacterial effector proteins for their localization and activity [55, 170]. Similarly, Mpt64 bound several PIPs *in vitro* with the most prominent interactions being with the monophosphatidylinositols PI3P, PI4P and PI5P. Furthermore, the ER localization of Mpt64 in yeast changed when the PIP kinases generating PI3P and PI(3,5)P were deleted, suggesting that its function *in vivo* is connected to its ability to interact with membrane PIPs. While PI3P is mainly detected in endosomes and autophagosomes [171], PI3P has also been identified at specialized ER sites called omegasomes where a dynamic exchange of PI3P-positive vesicles and ER occurs, allowing for assembly of autophagy proteins and expansion of autophagosome membranes, leading to initiation of autophagosome formation [172]. The

major pools of PI4P are at the PM and the Golgi [173], but it has an established role in mediating protein trafficking from ER exit sites [174, 175] and can be transferred from the PM or Golgi to the ER at membrane contact sites to regulate PI4P levels [36]. Less is known about PI5P as its basal level is only about 1% of PI4P [176]. However, PI5P is increased during bacterial infection and other stresses, and can be found throughout the cell, including the ER [176] and on lipid droplets that arise from the ER [177]. Similarly PI(3,5)P₂ is in low abundance but levels are elevated by stress such as hyperosmotic shock in yeast [178]. Conserved functions of PI(3,5)P₂ from yeast to mammals include regulation of autophagy and retrograde trafficking, activation of some ion channels, and cargo sorting into multivesicular bodies [178]. Although the relative contribution of binding to individual PIPs to the activity of Mpt64 remains unknown, the subcellular localization of Mpt64 at the ER may result from its interaction with the monophosphatidylinositols PI3P, PI4P and PI5P in addition to PI(3,5)P₂. Interaction with organelle and activity-specific PIPs could allow Mpt64 to interfere with ER to Golgi trafficking to prevent release of the model substrate hGH and also to inhibit the UPR. Further experiments to confirm the direct interaction of Mpt64 with PIPs and to understand the specificity of Mpt64 for specific PIPs *in vivo* may give better insight to its molecular mechanism.

Disruption of the RD2 locus in Mtb H37Rv leads to decreased bacterial burdens in the lungs and spleen of aerosol-infected mice at 3 weeks after infection [123]. As Mpt64 is within the RD2 locus, I hypothesized that the single, in-frame deletion of Mpt64 might explain the attenuation phenotype of the RD2 mutant. Though I did not perform a head-to-head comparison of an Mtb Δ RD2 strain versus my Mtb Δ mpt64 strain on the Erdman genetic background, I did observe modestly decreased bacterial burdens of Mtb Δ mpt64

compared to WT Mtb in the lungs of mice at 3 weeks post-infection. Although this decrease was not statistically significant and was not associated with a survival defect, it suggests that Mpt64 may contribute to the virulence of the RD2 region. Other genes located in the RD2 locus that were not complemented in the RD2 survival study [123] such as *pe_pgrs35* (Rv1983) and *cfp21* (Rv1984) may also contribute alongside *mpt64* to the virulence defect observed in RD2 deletions.

When I infected mice with *Mtb* Δ *mpt64::mpt64-NS*, a strain of Mtb that still expresses Mpt64 but cannot secrete it into the host cell, I recovered fewer CFU compared to WT from the lungs of *Mtb* Δ *mpt64::mpt64-NS* infected mice. I hypothesize that this strain suffers from two detrimental consequences. First, blocking Mpt64 secretion prevents it from exerting its function in the host. Second, non-secreted Mpt64 can still be cross-presented to the adaptive immune system [179], thus leading to a cell mediated immune response against Mpt64. This observation is consistent with data that both human patients with active tuberculosis and their PPD positive contacts have T-cell responses to Mpt64 [180] and T-cell reactive Mpt64 epitopes have been mapped [181]. Furthermore, Mpt64 staining is observed in granulomas of infected individuals [153, 182]. Thus, Mpt64 is highly immunogenic during human infection with Mtb and suggests an evolutionary tradeoff between the effector function of Mpt64 and its antigenicity. When I explored the importance of Mpt64 in human disease, I observed that Mpt64 secreted from wild type bacteria localized to the ER of infected human monocyte-derived macrophages, though a mutant in *mpt64* did not have a consistent defect in survival within macrophages. Future work on other mycobacterial, secreted, ER-binding proteins may ultimately reveal functional redundancy with Mpt64 important for the virulence of Mtb.

DISCUSSION OF CONTINUING EXPERIMENTS

Characterization of MSPs through novel screening

High resolution subcellular localization

While fluorescence microscopy was useful to gather basic localization information about the MSP, including using known resident organelle proteins to confirm colocalization, the resolution of light microscopy is limited. Correlative light and electron microscopy (CLEM) is a powerful tool that combines brightfield, fluorescence and electron microscopy of the same sample, providing levels of detail unattainable from the individual procedures alone [183]. Thus, localization of proteins of interest such as MSP that have unassigned localizations, can be assessed by the combination of fluorescence and electron microscopy in microinjected or transfected cells [183, 184]. The addition of immunogold labeling to electron microscopy procedures can confirm definitively the localization of proteins of interest. Furthermore, perturbations to organelle structure would be observable by electron microscopy. Having high resolution information about the localization of other MSP from my study could help design future experiments with the goal of determining their function in pathogenesis.

Using model organisms to uncover MSP interaction with conserved pathways

My study used the model organism *S. cerevisiae* for several phenotypic experiments including to identify membrane-binding and mis-localization after PI kinase loss of

function. Similarly, yeast were used for the calcofluor white assay and Y2H. Though the results from the latter two assays were less promising, all four experiments highlight the usefulness of yeast as a screening tool. Genetic conservation, genetic tools, the quick doubling time of yeast and the variety of selectable markers allow for robust screening methods [118]. Thus, the yeast tools used to characterize Mpt64 like Y2H and PI kinase loss of function can be broadly applied to any other MSP of interest rather easily. Moreover, new yeast screens could be optimized to dissect the interaction of MSP with conserved cellular pathways such as using the membrane specific dye FM 4-64 to probe endosome transport and vacuole function [185] or the already well-established tools to study autophagy activation [186, 187].

Organelle-specific assays to assess MSP function

As I suggested above, the subcellular localization of MSP could be used to direct organelle-specific experiments. For example, preliminary experiments by colleagues in the lab have focused on the four MSP that localized to the mitochondria by characterizing perturbations in mitochondrial homeostasis and DNA release. The latter result could add to the growing appreciation for the purpose of IFN-I activation during Mtb infection [188].

Unbiased approaches to uncover the function of Mpt64

The molecular function or activity of Mpt64 remains elusive. The identification of a host-protein interacting partner may give insight to how Mpt64 inhibits the UPR and release of a model substrate in cultured cells. Since I can produce soluble recombinant protein, it

would be possible to reproduce the methods recently used to identify host interacting partners of Mtb secreted proteins [119]. Alternatively, expressing Mpt64 in a mammalian cell would allow direct immunoprecipitation of Mpt64 with interacting partners.

Transcriptional analysis of infected cells was successful in identifying that ESX-1 is required for Mtb activation of the cytosolic surveillance pathway [59]. RNA sequencing of infected cells in response to Mtb Δ mpt64 compared to wild type Mtb or the Mtb Δ mpt64 complementation strains could uncover a pathway affected by Mpt64 during macrophage infection.

APPENDIX A

Characterization of Mycobacterial Secreted Proteins

Table 2. Characterization of mycobacterial secreted proteins. Proteins are listed in order of their corresponding gene open reading frame (ORF). The ability of the proteins to rescue yeast growth at 37°C is listed as Yes or No. The normalized hGH release is reported. ND, not determined.

ORF	Name	Description	Ras Rescue	hGH Release
Rv0096	PPE1	PPE family protein	No	1.179
Rv0109	PE_PGRS1	PE-PGRS family protein	No	0.465
Rv0129	FbpC	Secreted antigen 85C	No	1.895
Rv0151	PE1	PE family protein	No	0.044
Rv0153c	ptbB	Phosphotyrosine protein phosphatase	No	1.206
Rv0159	PE3	PE family protein	No	1.706
Rv0160c	PE4	PE family protein	No	0.127
Rv0164	TB18.5	T-cell antigen	No	1.662
Rv0170	Mce1B	Mce-family protein	Yes	0.663
Rv0171	Mce1C	Mce-family protein	No	0.368
Rv0172	Mce1D	Mce-family protein	No	ND
Rv0175	Rv0175	Probable conserved MCE-related protein	Yes	0.408
Rv0176	Rv0176	Probable conserved MCE-related protein	No	ND
Rv0177	Rv0177	Probable conserved MCE-related protein	Yes	0.896
Rv0178	Rv0178	Probable conserved MCE-related protein	Yes	0.485
Rv0183	Rv0183	Exported monoacylglycerol lipase	No	0.734
Rv0199	Rv0199	MCE1-related protein	No	0.384
Rv0201c	Rv0201c	conserved hypothetical	Yes	ND
Rv0249c	Rv0249c	Succinate dehydrogenase membrane anchor su	Yes	0.296
Rv0256c	PPE2	PPE family protein	Yes	1.016
Rv0282	eccA3	ESX-3 AAA ATPase	No	0.408
Rv0283	eccB3	ESX-3 secretion-associated protein	Yes	0.44
Rv0285	PE5	PE family protein	No	0.054
Rv0287	EsxG	ESAT-6 like protein	No	0.893
Rv0288	EsxH	Low molecular weight protein antigen 7	No	0.578
Rv0289	espG3	ESX-3 secretion-associated protein	No	0.456
Rv0290	eccD3	ESX-3 secretion-associated protein	Yes	0.315
Rv0291	mycP3	subtilisin-like protease mycosin	No	0.599
Rv0292	EccE3	ESX-3 secretion-associated protein	No	0.769
Rv0325	Rv0325		No	0.45
Rv0335	PE6	PE family protein	No	0.066
Rv0387c	Rv0387c		No	ND
Rv0453	PPE11	PPE family protein	No	1.428

ORF	Name	Description	Ras Rescue	hGH Release
Rv0470c	pcaA	cyclopropane mycolic acid synthase	No	0.45
Rv0481c	Rv0481c	conserved hypothetical	No	0.652
Rv0589	Mce2A	Mce-family protein	Yes	0.889
Rv0590	Mce2B	Mce-family protein	Yes	0.376
Rv0590A	Rv0590A	Mce associated protein	No	0.599
Rv0591	Mce2C	Mce-family protein	No	0.83
Rv0592	Mce2D	Mce-family protein	No	1.09
Rv0594	Mce2F	Mce-family protein	Yes	0.194
Rv0754	PE_PGRS11	PE-PGRS family protein	No	0.561
Rv0774c	Rv0774c	an iron stress-inducible esterase	No	0.368
Rv0787	Rv0787	conserved hypothetical, secreted	Yes	1.022
Rv0878	PPE13	PPE family protein	No	0.798
Rv0888	SpmT	Sphingomyelinase	No	0.779
Rv0915	PPE14	PPE family protein	No	0.665
Rv0916	PE7	PE family protein	No	ND
Rv0928	pstS3	phosphate-binding lipoprotein	No	ND
Rv0986	Rv0986	ABC transporter	No	0.841
Rv1037c	EsxI	ESAT-6 like protein	No	0.74
Rv1039	PPE15	mycobacterial perilipin-1 (MPER1)	No	ND
Rv1040	PE8	PE family protein	No	ND
Rv1088	PE9	PE family protein	No	0.044
Rv1089	PE10	PE family protein	No	0.052
Rv1093	glyA1	serine hydroxymethyltransferase	No	1.003
Rv1168c	PPE17	PPE family protein	No	0.603
Rv1172c	PE12	PE family protein	Yes	0.271
Rv1174c	TB8.4	Low molecular weight T-cell antigen	No	0.683
Rv1196	PPE18	PPE family protein	Yes	0.875
Rv1197	EsxK	ESAT-6 like protein	Yes	0.982
Rv1214c	PE14	PE family protein	No	0.436
Rv1357c	Rv1357c	c-di-GMP phosphodiesterase	No	0.738
Rv1426c	LipO	esterase	No	0.923
Rv1430	PE16	esterase	No	0.277
Rv1503c	Rv1503c	predicted TDP-4-oxo-6-deoxy-D-glucose transan	No	1.137
Rv1504c	Rv1504c	Conserved hypothetical protein	No	1.08
Rv1505c	Rv1505c	putative acyltransferase	No	1.835
Rv1506c	Rv1506c	putative methyltransferase	No	1.18
Rv1646	PE17	PE family protein	Yes	0.191
Rv1729c	Rv1729c	Possible S-adenosylmethionine-dependent meth	No	1.196
Rv1768	PE_PGRS31	PE-PGRS family protein	Yes	1.136
Rv1787	PPE25	PPE family protein	Yes	0.774

ORF	Name	Description	Ras Rescue	hGH Release
Rv1789	PPE26	PPE family protein	No	0.844
Rv1790	PPE27	PPE family protein	No	0.922
Rv1791	PE19	PE family protein	No	0.569
Rv1793	EsxN	ESAT-6 like protein	No	1.619
Rv1800	PPE28	PPE family protein	No	1.817
Rv1801	PPE29	PPE family protein	No	1.988
Rv1804c	Rv1804c	conserved hypothetical	No	1.99
Rv1806	PE20	PE family protein	No	0.471
Rv1807	PPE31	PPE family protein	Yes	ND
Rv1809	PPE33	PPE family protein	No	ND
Rv1810	Rv1810	conserved hypothetical	Yes	0.203
Rv1815	Rv1815	conserved hypothetical, secreted	No	0.226
Rv1886	fbpB	Secreted antigen 85B	No	ND
Rv1887	Rv1887	conserved hypothetical, secreted	No	0.339
Rv1891	Rv1891	conserved hypothetical, secreted	No	0.562
Rv1926c	Mpt63	Immunogenic protein Mpt63	Yes	0.47
Rv1966	Mce3A	Mce-family protein	Yes	0.8098
Rv1967	Mce3B	Mce-family protein	No	0.558
Rv1968	Mce3C	Mce-family protein	Yes	ND
Rv1969	Mce3D	Mce-family protein	Yes	0.27
Rv1980c	Mpt64	Immunogenic protein Mpt64	Yes	0.072
Rv1983	PE_PGRS35	PE-PGRS family protein	No	0.79
Rv1984c	Cfp21	Probable cutinase with esterase and lipolytic acti	No	ND
Rv2075c	Rv2075c	conserved hypothetical protein	Yes	0.28
Rv2099c	PE21	PE family protein	No	1.274
Rv2107	PE22	PE family protein	No	0.271
Rv2108	PPE36	PPE family protein, heme binding	No	ND
Rv2140c	TB18.6	conserved protein	No	0.223
Rv2190c	Rv2190c	possibly involved in cell wall maintenance and c	Yes	0.414
Rv2206	Rv2206		Yes	0.465
Rv2223c	CaeB	Proable exported carboxylesterase	No	0.229
Rv2232	ptkA	Protein tyrosine kinase	No	0.217
Rv2234	ptpA	Tyr phosphatase	No	0.223
Rv2295	Rv2295	Conserved hypothetical protein, cysteine-rich pro	Yes	0.214
Rv2301	Cut2	Probable cutinase	No	0.284

ORF	Name	Description	Ras Rescue	hGH Release
Rv2328	PE23	PE family protein	No	0.804
Rv2340c	PE_PGRS39	PE-PGRS family protein	No	0.321
Rv2346c	esxO	ESAT-6 like protein	No	0.556
Rv2349c	PlcC	Probable phospholipase C 3	No	0.707
Rv2350c	PlcB	Membrane-associated phospholipase C 2	No	0.228
Rv2351c	PlcA	Membrane-associated phospholipase C 1	No	1.195
Rv2352c	PPE38	PPE family protein	No	1.755
Rv2353c	PPE39	PPE family protein	Yes	ND
Rv2356c	PPE40	PPE family protein	No	0.681
Rv2371	PE_PGRS40	PE-PGRS family protein	No	0.359
Rv2376	CFP2	Low molecular weight antigen	No	0.235
Rv2401	Rv2401	conserved hypothetical protein	No	0.3134
Rv2408	PE24	PE family protein	No	1.136
Rv2416c	EIS	aminoglycoside acetyltransferase	No	1.084
Rv2430c	PPE41	PPE family protein	No	2.989
Rv2431c	PE25	PE family protein	No	0.365
Rv2445c	ndkA	secreted nucleoside diphosphate kinase	Yes	0.416
Rv2469c	Rv2469c	conserved hypothetical protein	No	1.044
Rv2519	PE26	PE family protein	No	0.73
Rv2548	vapC19	possible toxin	Yes	0.5
Rv2608	PPE42	PPE family protein	No	1.559
Rv2615c	PE_PGRS45	PE-PGRS family protein	Yes	0.799
Rv2693c	Rv2693c	Probable conserved integral membrane alanine	No	0.334
Rv2768c	PPE43	PPE family protein	No	3.67
Rv2770c	PPE44	PPE family protein	No	2.061
Rv2875	Mpt70	Major secreted immunogenic protein	No	0.833
Rv2878c	Mpt53	Soluble secreted antigen, possible dsb	Yes	0.526
Rv2892c	PPE45	PPE family protein	No	0.844
Rv2930	fadD26	DIM biosynthesis	Yes	0.395
Rv2941	fadD28	DIM biosynthesis	No	0.535
Rv3004	CFP6	Low molecular weight protein antigen 6	No	0.982
Rv3022A	PE29	PE family protein	No	0.635
Rv3022c	PPE48	PPE family protein	No	0.933
Rv3036c	TB22.2	nonlipolytic hydrolase	Yes	1.596
Rv3097c	PE_PGRS63	lipY triacylglycerol lipase	No	0.851
Rv3110	moaB1	Probable pterin-4-alpha-carbinolamine dehydrat	No	0.711
Rv3111	moaC1	Involved in the biosynthesis of molybdopterin	Yes	0.614
Rv3112	moaD1	Involved in molybdenum cofactor biosynthesis	No	0.886

ORF	Name	Description	Ras Rescue	hGH Release
Rv3125c	PPE49	PPE family protein	Yes	1.112
Rv3135	PPE50	PPE family protein	No	1.402
Rv3136	PPE51	PPE family protein	No	1.168
Rv3206c	moeB1	molybdopterin synthase sulphurylase	No	0.623
Rv3310	SapM	acid phosphatase	Yes	0.386
Rv3377c	Rv3377c	Required for production of diterpenoid isotubercolin	No	0.816
Rv3378c	Rv3378c	Diterpene synthase, produces isotubercolinol	No	0.331
Rv3425	PPE57	PPE family protein	No	1.894
Rv3426	PPE58	PPE family protein	No	1.458
Rv3429	PPE59	PPE family protein	No	2.307
Rv3477	PE31	PE family protein	No	0.513
Rv3483c	Rv3483c		No	ND
Rv3491	Rv3491		Yes	0.519
Rv3493c	Rv3493c	Mce4 associated protein	Yes	0.321
Rv3496c	Mce4D	Mce-family protein	No	0.658
Rv3497c	Mce4C	Mce-family protein	No	ND
Rv3498c	Mce4B	Mce-family protein	Yes	0.541
Rv3499c	Mce4A	Mce-family protein	Yes	1.21
Rv3527	Rv3527		No	0.571
Rv3532	PPE61	PPE family protein	No	ND
Rv3533c	PPE62	PPE family protein	Yes	ND
Rv3539	PPE63	PPE family protein	No	0.978
Rv3558	PPE64	PPE family protein	No	ND
Rv3587	Rv3587		Yes	0.368
Rv3590c	PE_PGRS58	PE-PGRS family protein	Yes	0.29
Rv3621c	PPE65	PPE family protein	No	1.134
Rv3653	PE_PGRS61	PE-PGRS family protein	No	0.308
Rv3668	Rv3668	serine protease	Yes	0.259
Rv3705c	Rv3705c		No	0.373
Rv3707c	Rv3707c	conserved hypothetical protein	No	0.259
Rv3738c	PPE66	PPE family protein	Yes	1.123
Rv3739	PPE67	PPE family protein	No	0.765
Rv3746	PE34	PE family protein	No	0.655
Rv3802c	Culp6	cell wall lipase	Yes	0.646
Rv3804	fbpA	mycolyl transferase, antigen 85A	No	ND
Rv3810	pirG		No	0.401

ORF	Name	Description	Ras Rescue	hGH Release
Rv3811	csp		No	0.448
Rv3812	PE_PGRS62	PE-PGRS family protein	Yes	0.344
Rv3864	EspE	ESX-1 secretion-associated protein	Yes	0.853
Rv3865	EspF	ESX-1 secretion-associated protein	Yes	0.316
Rv3871	eccCb1	ESX conserved component	No	0.378
Rv3872	PE35	PE family protein	No	0.561
Rv3873	PPE68	PPE family protein	No	0.293
Rv3874	CFP-10	10 kDa culture filtrate antigen EsxB	No	0.425
Rv3875	ESAT-6	6 kDa early secretory antigenic target	No	1.288
Rv3881c	EspB	Secreted ESX-1 substrate protein B	No	0.274
Rv3887c	eccD2	ESX conserved component	No	0.547
Rv3892c	PPE69	PPE family protein	No	1.246
Rv3899c	Rv3899c	Conserved hypothetical protein	Yes	0.533

APPENDIX B

Summary of Hits from the Ras rescue assay

Table 3. Mtb proteins that rescued yeast growth in Ras Rescue Assay. Proteins are listed in order of their corresponding gene open reading frame (ORF).

ORF	Name	Description
Rv0170	Mce1B	Mce-family protein
Rv0175	Rv0175	Probable conserved MCE-related protein
Rv0177	Rv0177	Probable conserved MCE-related protein
Rv0178	Rv0178	Probable conserved MCE-related protein
Rv0201c	Rv0201c	conserved hypothetical
Rv0249c	Rv0249c	Succinate dehydrogenase membrane anchor subunit
Rv0283	eccB3	ESX-3 secretion-associated protein
Rv0290	eccD3	ESX-3 secretion-associated protein
Rv0589	Mce2A	Mce-family protein
Rv0590	Mce2B	Mce-family protein
Rv0594	Mce2F	Mce-family protein
Rv0787	Rv0787	conserved hypothetical, secreted
Rv1172c	PE12	PE family protein
Rv1196	PPE18	PPE family protein
Rv1197	EsxK	ESAT-6 like protein
Rv1646	PE17	PE family protein
Rv1768	PE_PGRS31	PE-PGRS family protein
Rv1787	PPE25	PPE family protein
Rv1807	PPE31	PPE family protein
Rv1810	Rv1810	conserved hypothetical
Rv1926c	Mpt63	Immunogenic protein Mpt63
Rv1966	Mce3A	Mce-family protein
Rv1968	Mce3C	Mce-family protein
Rv1969	Mce3D	Mce-family protein
Rv1980c	Mpt64	Immunogenic protein Mpt64
Rv2075c	Rv2075c	conserved hypothetical protein
Rv2190c	Rv2190c	possibly involved in cell wall maintenance and composition
Rv2206	Rv2206	
Rv2295	Rv2295	Conserved hypothetical protein, cysteine-rich protein
Rv2353c	PPE39	PPE family protein
Rv2445c	ndkA	secreted nucleoside diphosphate kinase

Rv2548	vapC19	possible toxin
Rv2615c	PE_PGRS45	PE-PGRS family protein
Rv2878c	Mpt53	Soluble secreted antigen, possible dsb
Rv2930	fadD26	DIM biosynthesis
Rv3036c	TB22.2	nonlipolytic hydrolase
Rv3111	moaC1	Involved in the biosynthesis of molybdopterin
Rv3125c	PPE49	PPE family protein
Rv3310	SapM	acid phosphatase
Rv3491	Rv3491	
Rv3493c	Rv3493c	Mce4 associated protein
Rv3498c	Mce4B	Mce-family protein
Rv3499c	Mce4A	Mce-family protein
Rv3533c	PPE62	PPE family protein
Rv3587	Rv3587	
Rv3590c	PE_PGRS58	PE-PGRS family protein
Rv3668	Rv3668	serine protease
Rv3738c	PPE66	PPE family protein
Rv3802c	Culp6	cell wall lipase
Rv3812	PE_PGRS62	PE-PGRS family protein
Rv3864	EspE	ESX-1 secretion-associated protein
Rv3899c	Rv3899c	Conserved hypothetical protein

APPENDIX C

Summary of Hits from the hGH Release Assay

Table 4. Mtb proteins that exceeded cut-offs in hGH release assay. Proteins are listed in order of their corresponding gene open reading frame (ORF). The normalized hGH released from cells expressing each protein is listed in the final column. Red text indicates proteins that were identified in both the Ras rescue assay and the hGH release assay.

ORF	Name	Description	hGH Release
Rv0129	FbpC	Secreted antigen 85C	1.895
Rv0151	PE1	PE family protein	0.044
Rv0160c	PE4	PE family protein	0.127
Rv0285	PE5	PE family protein	0.054
Rv0335	PE6	PE family protein	0.066
Rv0594	Mce2F	Mce-family protein	0.194
Rv1088	PE9	PE family protein	0.044
Rv1089	PE10	PE family protein	0.052
Rv1505c	Rv1505c	putative acyltransferase	1.835
Rv1646	PE17	PE family protein	0.191
Rv1800	PPE28	PPE family protein	1.817
Rv1801	PPE29	PPE family protein	1.988
Rv1804c	Rv1804c	conserved hypothetical	1.99
Rv1810	Rv1810	conserved hypothetical	0.203
Rv1815	Rv1815	conserved hypothetical, secreted	0.226
Rv1980c	Mpt64	Immunogenic protein Mpt64	0.072
Rv2140c	TB18.6	conserved protein	0.223
Rv2223c	CaeB	Probable exported carboxylesterase	0.229
Rv2232	ptkA	Protein tyrosine kinase	0.217
Rv2234	ptpA	Tyr phosphatase	0.223
Rv2295	Rv2295	Conserved hypothetical protein, cysteine-rich protein	0.214
Rv2350c	PlcB	Membrane-associated phospholipase C 2	0.228
Rv2352c	PPE38	PPE family protein	1.755
Rv2376	CFP2	Low molecular weight antigen	0.235
Rv2430c	PPE41	PPE family protein	2.989
Rv2768c	PPE43	PPE family protein	3.67
Rv2770c	PPE44	PPE family protein	2.061
Rv3425	PPE57	PPE family protein	1.894

Rv3429	PPE59	PPE family protein	2.307
--------	-------	--------------------	-------

APPENDIX D Purification of Recombinant Mpt64

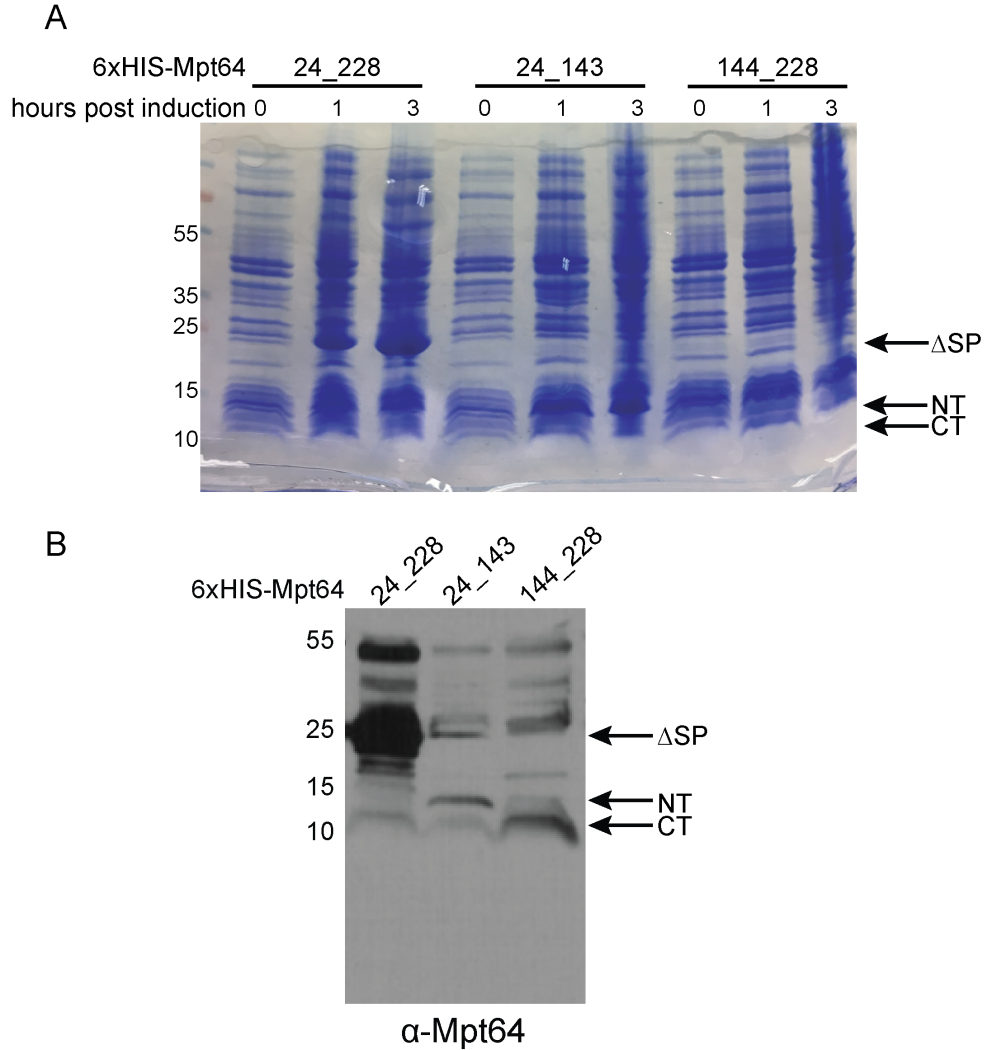


Figure 17. Expression and purification of recombinant Mpt64 truncations. (A) Detection of recombinant Mpt64 protein expression by PAGE followed by Coomassie Brilliant Blue stain. (B) Detection of recombinant Mpt64 protein expression in *E. coli* whole cell lysates by Western blot. Mpt64₂₄₋₂₂₈ (Δ SP), Mpt64₂₄₋₁₄₃ (NT), Mpt64₁₄₄₋₂₂₈ (CT) were detected by anti-Mpt64.

APPENDIX E

Characterization of Mpt64 Deletion Mutant

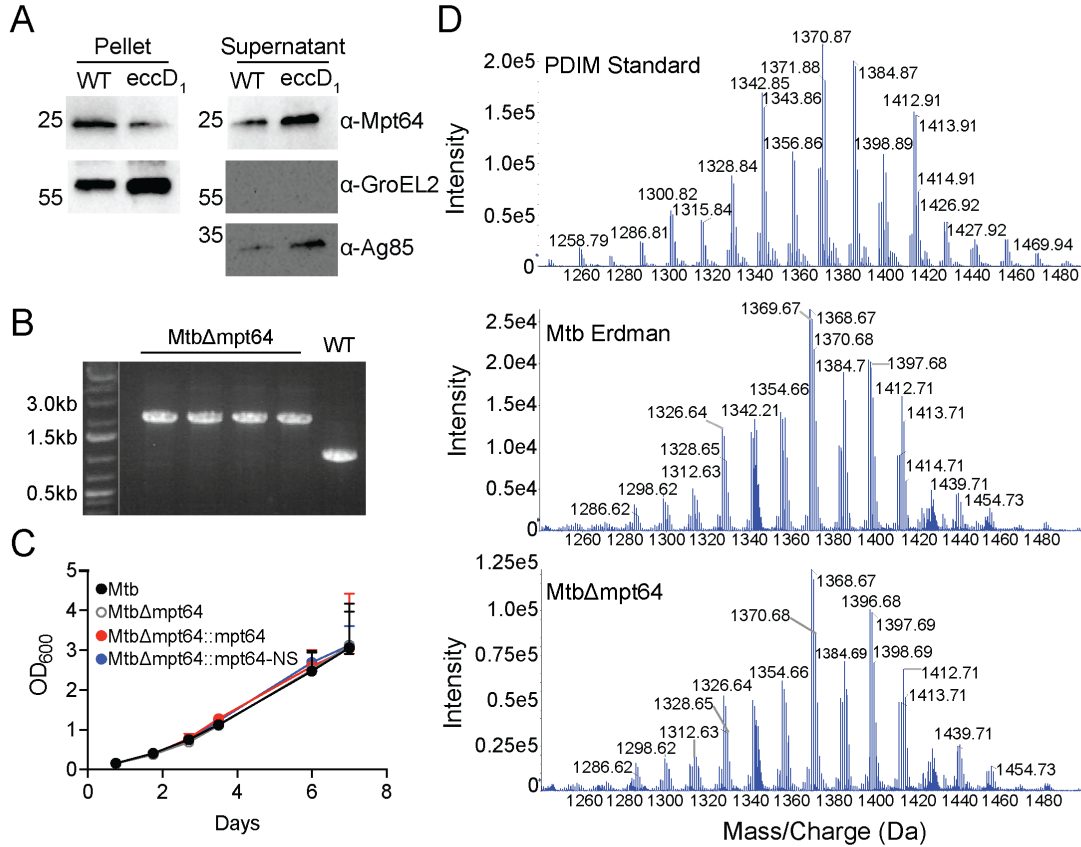


Figure 18. Construction and phenotypic analysis of MtbΔmpt64. (A) Western blot detecting expression of Mpt64, Ag85 and GroEL2 in either the lysate of the cell pellet (P) or culture supernatant (S) of wild type Mtb or MtbΔeccD1. (B) Detection of hygromycin resistance cassette insertion in place of *mpt64*. Genomic DNA from wild type Mtb or MtbΔmpt64 was amplified by polymerase chain reaction and products were analyzed by agarose gel electrophoresis. (C) Growth of Mtb, MtbΔmpt64, MtbΔmpt64::mpt64 and MtbΔmpt64::mpt64-NS in 7H9 measured by optical density at 600nm. (D) PDIM standard or apolar lipid extracts from Mtb or MtbΔmpt64 were analyzed on an AbSciex TripleTOF 5600/5600+ mass spectrometer.

APPENDIX F
Localization of Mpt64 in Murine Macrophages

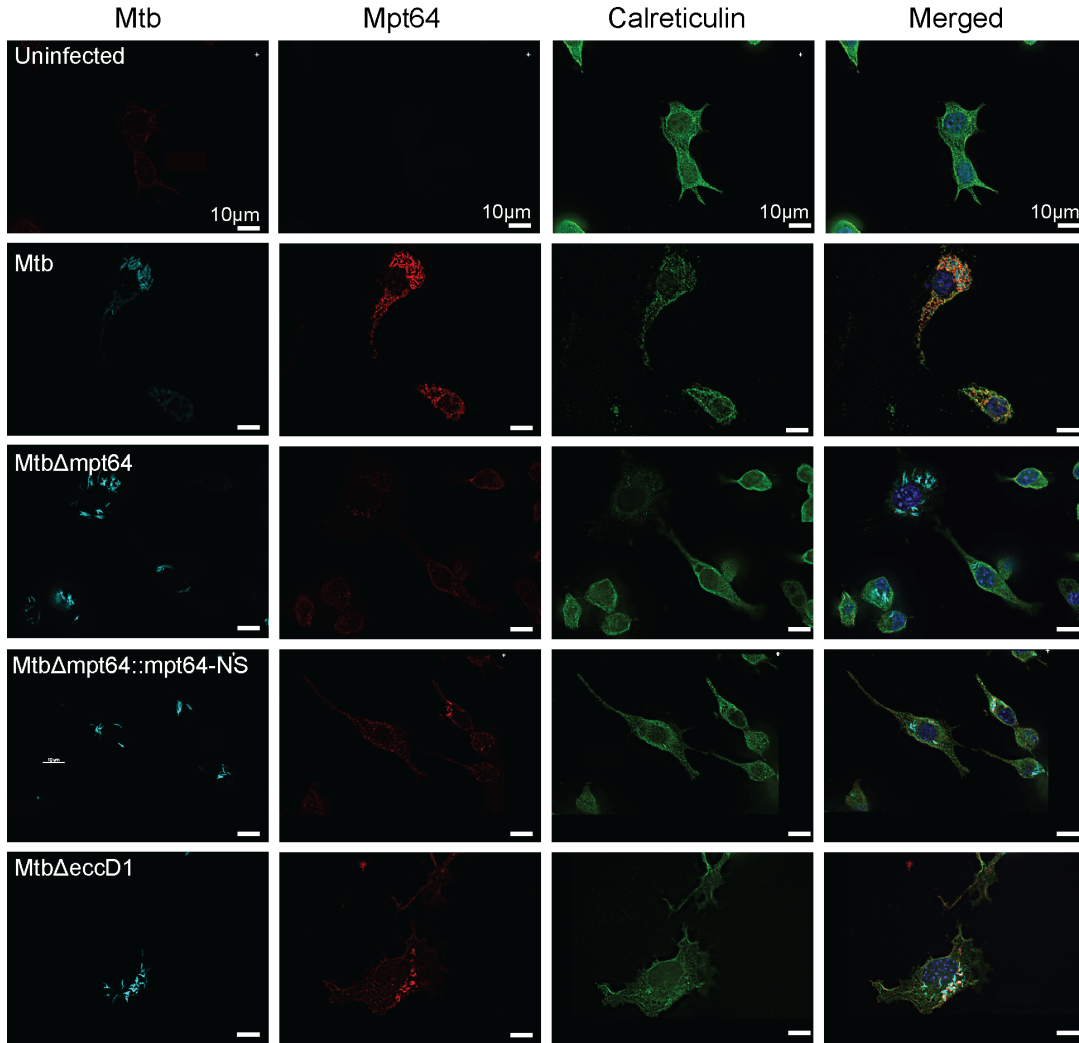


Figure 19. Secreted Mpt64 co-localizes with calreticulin in murine macrophages. RAW267.4 murine macrophages were infected with the indicated strains of mCherry expressing Mtb (cyan) for four hours and subsequently stained for Mpt64 (red) and calreticulin (green). Nuclei are stained in blue. Scale bars are 10 μ m.

APPENDIX G
Localization of Mpt64 in Primary Human Macrophages

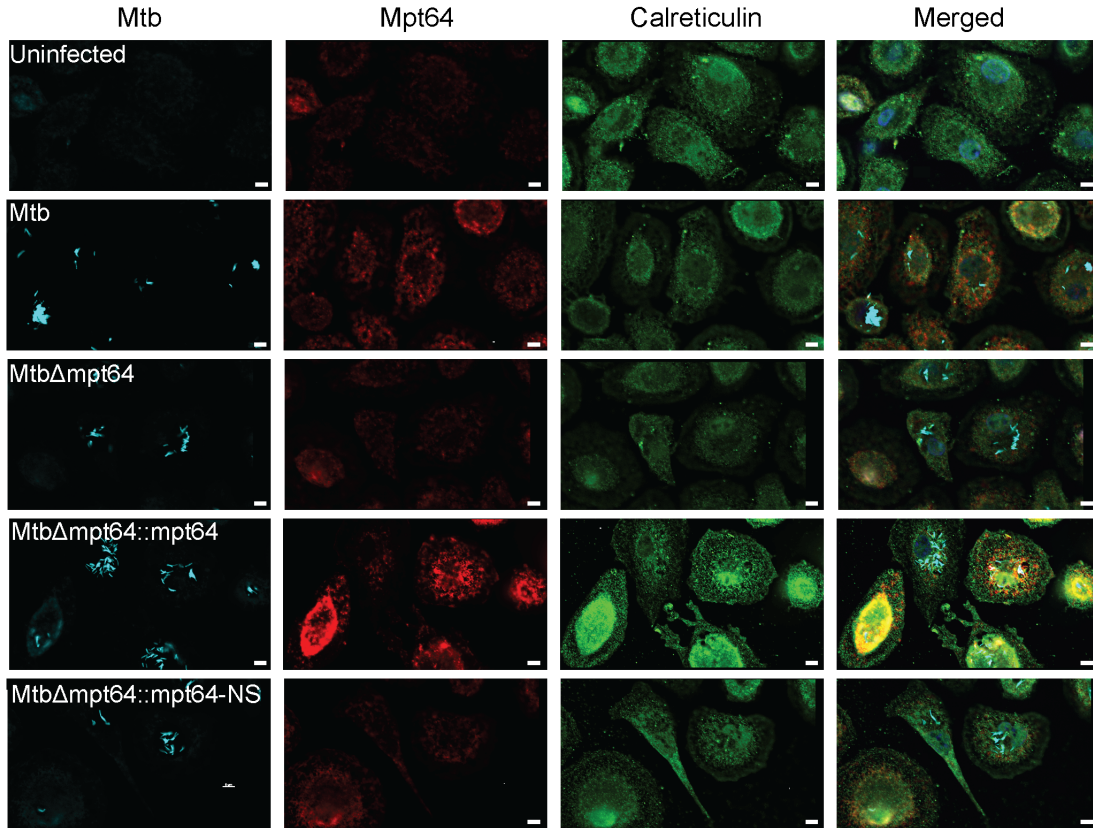


Figure 20. Secreted Mpt64 co-localizes with calreticulin in human macrophages. Primary human macrophages were infected with the indicated strains of mCherry expressing Mtb (cyan) or left uninfected for four hours prior to fixation and staining for Mpt64 (red) and calreticulin (green). Scale bars are 5 μ m.

BIBLIOGRAPHY

1. Global Tuberculosis Report. World Health Organization. 2016; http://www.who.int/tb/publications/global_report/en/.
2. Colditz GA, Brewer TF, Berkey CS, Wilson ME, Burdick E, Fineberg HV, et al. Efficacy of BCG vaccine in the prevention of tuberculosis. Meta-analysis of the published literature. JAMA. 1994;271(9):698-702. Epub 1994/03/02. PubMed PMID: 8309034.
3. Fennelly KP, Jones-Lopez EC. Quantity and Quality of Inhaled Dose Predicts Immunopathology in Tuberculosis. Front Immunol. 2015;6:313. Epub 2015/07/16. doi: 10.3389/fimmu.2015.00313. PubMed PMID: 26175730; PubMed Central PMCID: PMC4484340.
4. Russell DG, Barry CE, 3rd, Flynn JL. Tuberculosis: what we don't know can, and does, hurt us. Science. 2010;328(5980):852-6. Epub 2010/05/15. doi: 10.1126/science.1184784. PubMed PMID: 20466922; PubMed Central PMCID: PMC2872107.
5. Stamm CE, Collins AC, Shiloh MU. Sensing of Mycobacterium tuberculosis and consequences to both host and bacillus. Immunol Rev. 2015;264(1):204-19. Epub 2015/02/24. doi: 10.1111/imr.12263. PubMed PMID: 25703561; PubMed Central PMCID: PMC4339209.
6. Huynh KK, Joshi SA, Brown EJ. A delicate dance: host response to mycobacteria. Curr Opin Immunol. 2011;23(4):464-72. Epub 2011/07/06. doi: 10.1016/j.coi.2011.06.002. PubMed PMID: 21726990.
7. Flannagan RS, Cosio G, Grinstein S. Antimicrobial mechanisms of phagocytes and bacterial evasion strategies. Nat Rev Microbiol. 2009;7(5):355-66. Epub 2009/04/17. doi: 10.1038/nrmicro2128. PubMed PMID: 19369951.
8. Weiss G, Schaible UE. Macrophage defense mechanisms against intracellular bacteria. Immunol Rev. 2015;264(1):182-203. Epub 2015/02/24. doi: 10.1111/imr.12266. PubMed PMID: 25703560; PubMed Central PMCID: PMC4368383.
9. Bradfute SB, Castillo EF, Arko-Mensah J, Chauhan S, Jiang S, Mandell M, et al. Autophagy as an immune effector against tuberculosis. Current opinion in microbiology. 2013;16(3):355-65. doi: 10.1016/j.mib.2013.05.003. PubMed PMID: 23790398; PubMed Central PMCID: PMC3742717.
10. Davis AS, Vergne I, Master SS, Kyei GB, Chua J, Deretic V. Mechanism of inducible nitric oxide synthase exclusion from mycobacterial phagosomes. PLoS Pathog.

- 2007;3(12):e186. Epub 2007/12/12. doi: 10.1371/journal.ppat.0030186. PubMed PMID: 18069890; PubMed Central PMCID: PMCPMC2134953.
11. Vandal OH, Pierini LM, Schnappinger D, Nathan CF, Ehrt S. A membrane protein preserves intrabacterial pH in intraphagosomal *Mycobacterium tuberculosis*. *Nat Med*. 2008;14(8):849-54. Epub 2008/07/22. doi: 10.1038/nm.1795. PubMed PMID: 18641659; PubMed Central PMCID: PMCPMC2538620.
 12. Ehrt S, Schnappinger D. Mycobacterial survival strategies in the phagosome: defence against host stresses. *Cell Microbiol*. 2009;11(8):1170-8. Epub 2009/05/15. doi: 10.1111/j.1462-5822.2009.01335.x. PubMed PMID: 19438516; PubMed Central PMCID: PMCPMC3170014.
 13. Vergne I, Chua J, Singh SB, Deretic V. Cell biology of mycobacterium tuberculosis phagosome. *Annu Rev Cell Dev Biol*. 2004;20:367-94. Epub 2004/10/12. doi: 10.1146/annurev.cellbio.20.010403.114015. PubMed PMID: 15473845.
 14. Sturgill-Koszycki S, Schlesinger PH, Chakraborty P, Haddix PL, Collins HL, Fok AK, et al. Lack of acidification in *Mycobacterium* phagosomes produced by exclusion of the vesicular proton-ATPase. *Science*. 1994;263(5147):678-81. Epub 1994/02/04. PubMed PMID: 8303277.
 15. Via LE, Deretic D, Ulmer RJ, Hibler NS, Huber LA, Deretic V. Arrest of mycobacterial phagosome maturation is caused by a block in vesicle fusion between stages controlled by rab5 and rab7. *J Biol Chem*. 1997;272(20):13326-31. Epub 1997/05/16. PubMed PMID: 9148954.
 16. Pethe K, Swenson DL, Alonso S, Anderson J, Wang C, Russell DG. Isolation of *Mycobacterium tuberculosis* mutants defective in the arrest of phagosome maturation. *Proc Natl Acad Sci U S A*. 2004;101(37):13642-7. doi: 10.1073/pnas.0401657101. PubMed PMID: 15340136; PubMed Central PMCID: PMCPMC518761.
 17. Stewart GR, Patel J, Robertson BD, Rae A, Young DB. Mycobacterial mutants with defective control of phagosomal acidification. *PLoS Pathog*. 2005;1(3):269-78. Epub 2005/12/03. doi: 10.1371/journal.ppat.0010033. PubMed PMID: 16322769; PubMed Central PMCID: PMCPMC1291353.
 18. MacGurn JA, Cox JS. A genetic screen for *Mycobacterium tuberculosis* mutants defective for phagosome maturation arrest identifies components of the ESX-1 secretion system. *Infect Immun*. 2007;75(6):2668-78. Epub 2007/03/14. doi: 10.1128/IAI.01872-06. PubMed PMID: 17353284; PubMed Central PMCID: PMCPMC1932882.
 19. Saleh MT, Belisle JT. Secretion of an acid phosphatase (SapM) by *Mycobacterium tuberculosis* that is similar to eukaryotic acid phosphatases. *J Bacteriol*.

- 2000;182(23):6850-3. Epub 2000/11/14. PubMed PMID: 11073936; PubMed Central PMCID: PMCPMC111434.
20. Vergne I, Chua J, Lee HH, Lucas M, Belisle J, Deretic V. Mechanism of phagolysosome biogenesis block by viable *Mycobacterium tuberculosis*. *Proc Natl Acad Sci U S A*. 2005;102(11):4033-8. Epub 2005/03/09. doi: 10.1073/pnas.0409716102. PubMed PMID: 15753315; PubMed Central PMCID: PMCPMC554822.
21. Zulauf KE, Sullivan JT, Braunstein M. The SecA2 pathway of *Mycobacterium tuberculosis* exports effectors that work in concert to arrest phagosome and autophagosome maturation. *PLoS Pathog*. 2018;14(4):e1007011. Epub 2018/05/01. doi: 10.1371/journal.ppat.1007011. PubMed PMID: 29709019.
22. Sassetti CM, Rubin EJ. Genetic requirements for mycobacterial survival during infection. *Proc Natl Acad Sci U S A*. 2003;100(22):12989-94. doi: 10.1073/pnas.2134250100. PubMed PMID: 14569030; PubMed Central PMCID: PMC240732.
23. Costa TR, Felisberto-Rodrigues C, Meir A, Prevost MS, Redzej A, Trokter M, et al. Secretion systems in Gram-negative bacteria: structural and mechanistic insights. *Nat Rev Microbiol*. 2015;13(6):343-59. Epub 2015/05/16. doi: 10.1038/nrmicro3456. PubMed PMID: 25978706.
24. Galan JE, Collmer A. Type III secretion machines: bacterial devices for protein delivery into host cells. *Science*. 1999;284(5418):1322-8. Epub 1999/05/21. PubMed PMID: 10334981.
25. Deng W, Marshall NC, Rowland JL, McCoy JM, Worrall LJ, Santos AS, et al. Assembly, structure, function and regulation of type III secretion systems. *Nat Rev Microbiol*. 2017;15(6):323-37. Epub 2017/04/11. doi: 10.1038/nrmicro.2017.20. PubMed PMID: 28392566.
26. Alvarez-Martinez CE, Christie PJ. Biological diversity of prokaryotic type IV secretion systems. *Microbiol Mol Biol Rev*. 2009;73(4):775-808. Epub 2009/12/01. doi: 10.1128/MMBR.00023-09. PubMed PMID: 19946141; PubMed Central PMCID: PMCPMC2786583.
27. Ho BT, Dong TG, Mekalanos JJ. A view to a kill: the bacterial type VI secretion system. *Cell Host Microbe*. 2014;15(1):9-21. Epub 2013/12/18. doi: 10.1016/j.chom.2013.11.008. PubMed PMID: 24332978; PubMed Central PMCID: PMCPMC3936019.
28. Isaac DT, Isberg R. Master manipulators: an update on *Legionella pneumophila* Icm/Dot translocated substrates and their host targets. *Future Microbiol*.

- 2014;9(3):343-59. Epub 2014/04/26. doi: 10.2217/fmb.13.162. PubMed PMID: 24762308; PubMed Central PMCID: PMC4148032.
29. Backert S, Meyer TF. Type IV secretion systems and their effectors in bacterial pathogenesis. *Curr Opin Microbiol.* 2006;9(2):207-17. Epub 2006/03/15. doi: 10.1016/j.mib.2006.02.008. PubMed PMID: 16529981.
30. Stanley SA, Raghavan S, Hwang WW, Cox JS. Acute infection and macrophage subversion by *Mycobacterium tuberculosis* require a specialized secretion system. *Proc Natl Acad Sci U S A.* 2003;100(22):13001-6. Epub 2003/10/15. doi: 10.1073/pnas.2235593100. PubMed PMID: 14557536; PubMed Central PMCID: PMC240734.
31. Groschel MI, Sayes F, Simeone R, Majlessi L, Brosch R. ESX secretion systems: mycobacterial evolution to counter host immunity. *Nat Rev Microbiol.* 2016;14(11):677-91. Epub 2016/09/27. doi: 10.1038/nrmicro.2016.131. PubMed PMID: 27665717.
32. Bosserman RE, Champion PA. Esx Systems and the Mycobacterial Cell Envelope: What's the Connection? *J Bacteriol.* 2017;199(17). Epub 2017/05/04. doi: 10.1128/JB.00131-17. PubMed PMID: 28461452; PubMed Central PMCID: PMC5553030.
33. Alix E, Mukherjee S, Roy CR. Subversion of membrane transport pathways by vacuolar pathogens. *J Cell Biol.* 2011;195(6):943-52. Epub 2011/11/30. doi: 10.1083/jcb.201105019. PubMed PMID: 22123831; PubMed Central PMCID: PMC3241728.
34. Alto NM, Orth K. Subversion of cell signaling by pathogens. *Cold Spring Harb Perspect Biol.* 2012;4(9):a006114. Epub 2012/09/07. doi: 10.1101/cshperspect.a006114. PubMed PMID: 22952390; PubMed Central PMCID: PMC3428769.
35. Ham H, Sreelatha A, Orth K. Manipulation of host membranes by bacterial effectors. *Nat Rev Microbiol.* 2011;9(9):635-46. Epub 2011/07/19. doi: 10.1038/nrmicro2602. PubMed PMID: 21765451.
36. Dickson EJ, Hille B. Understanding phosphoinositides: rare, dynamic, and essential membrane phospholipids. *Biochem J.* 2019;476(1):1-23. Epub 2019/01/09. doi: 10.1042/BCJ20180022. PubMed PMID: 30617162; PubMed Central PMCID: PMC6342281.
37. Gaspar AH, Machner MP. VipD is a Rab5-activated phospholipase A1 that protects *Legionella pneumophila* from endosomal fusion. *Proc Natl Acad Sci U S A.* 2014;111(12):4560-5. Epub 2014/03/13. doi: 10.1073/pnas.1316376111. PubMed PMID: 24616501; PubMed Central PMCID: PMC3970493.

38. Toulabi L, Wu X, Cheng Y, Mao Y. Identification and structural characterization of a Legionella phosphoinositide phosphatase. *J Biol Chem*. 2013;288(34):24518-27. Epub 2013/07/12. doi: 10.1074/jbc.M113.474239. PubMed PMID: 23843460; PubMed Central PMCID: PMC3750150.
39. Ledvina HE, Kelly KA, Eshraghi A, Plemel RL, Peterson SB, Lee B, et al. A Phosphatidylinositol 3-Kinase Effector Alters Phagosomal Maturation to Promote Intracellular Growth of Francisella. *Cell Host Microbe*. 2018;24(2):285-95 e8. Epub 2018/07/31. doi: 10.1016/j.chom.2018.07.003. PubMed PMID: 30057173; PubMed Central PMCID: PMC6394229.
40. Ustun S, Konig P, Guttman DS, Bornke F. HopZ4 from *Pseudomonas syringae*, a member of the HopZ type III effector family from the YopJ superfamily, inhibits the proteasome in plants. *Mol Plant Microbe Interact*. 2014;27(7):611-23. Epub 2014/03/15. doi: 10.1094/MPMI-12-13-0363-R. PubMed PMID: 24625030.
41. Gendrin C, Contreras-Martel C, Bouillot S, Elsen S, Lemaire D, Skoufias DA, et al. Structural basis of cytotoxicity mediated by the type III secretion toxin ExoU from *Pseudomonas aeruginosa*. *PLoS Pathog*. 2012;8(4):e1002637. Epub 2012/04/13. doi: 10.1371/journal.ppat.1002637. PubMed PMID: 22496657; PubMed Central PMCID: PMC3320612.
42. Niebuhr K, Giuriato S, Pedron T, Philpott DJ, Gaits F, Sable J, et al. Conversion of PtdIns(4,5)P(2) into PtdIns(5)P by the *S. flexneri* effector IpgD reorganizes host cell morphology. *EMBO J*. 2002;21(19):5069-78. Epub 2002/10/03. PubMed PMID: 12356723; PubMed Central PMCID: PMC129044.
43. Boucrot E, Beuzon CR, Holden DW, Gorvel JP, Meresse S. *Salmonella typhimurium* SifA effector protein requires its membrane-anchoring C-terminal hexapeptide for its biological function. *J Biol Chem*. 2003;278(16):14196-202. Epub 2003/02/08. doi: 10.1074/jbc.M207901200. PubMed PMID: 12574170.
44. Zhao W, Moest T, Zhao Y, Guilhon AA, Buffat C, Gorvel JP, et al. The *Salmonella* effector protein SifA plays a dual role in virulence. *Sci Rep*. 2015;5:12979. Epub 2015/08/14. doi: 10.1038/srep12979. PubMed PMID: 26268777; PubMed Central PMCID: PMC4534788.
45. Murata T, Delprato A, Ingmundson A, Toomre DK, Lambright DG, Roy CR. The *Legionella pneumophila* effector protein DrrA is a Rab1 guanine nucleotide-exchange factor. *Nat Cell Biol*. 2006;8(9):971-7. Epub 2006/08/15. doi: 10.1038/ncb1463. PubMed PMID: 16906144.
46. Mounier J, Boncompain G, Senerovic L, Lagache T, Chretien F, Perez F, et al. *Shigella* effector IpaB-induced cholesterol relocation disrupts the Golgi complex and recycling network to inhibit host cell secretion. *Cell Host Microbe*.

- 2012;12(3):381-9. Epub 2012/09/18. doi: 10.1016/j.chom.2012.07.010. PubMed PMID: 22980334.
47. Burnaevskiy N, Fox TG, Plymire DA, Ertelt JM, Weigele BA, Selyunin AS, et al. Proteolytic elimination of N-myristoyl modifications by the Shigella virulence factor IpaJ. *Nature*. 2013;496(7443):106-9. Epub 2013/03/29. doi: 10.1038/nature12004. PubMed PMID: 23535599; PubMed Central PMCID: PMC3722872.
48. Selyunin AS, Sutton SE, Weigele BA, Reddick LE, Orchard RC, Bresson SM, et al. The assembly of a GTPase-kinase signalling complex by a bacterial catalytic scaffold. *Nature*. 2011;469(7328):107-11. Epub 2010/12/21. doi: 10.1038/nature09593. PubMed PMID: 21170023; PubMed Central PMCID: PMC3675890.
49. Kim J, Thanabalasuriar A, Chaworth-Musters T, Fromme JC, Frey EA, Lario PI, et al. The bacterial virulence factor NleA inhibits cellular protein secretion by disrupting mammalian COPII function. *Cell Host Microbe*. 2007;2(3):160-71. Epub 2007/11/17. doi: 10.1016/j.chom.2007.07.010. PubMed PMID: 18005731.
50. Kenny B, Jepson M. Targeting of an enteropathogenic Escherichia coli (EPEC) effector protein to host mitochondria. *Cell Microbiol*. 2000;2(6):579-90. Epub 2001/02/24. PubMed PMID: 11207610.
51. Salcedo SP, Holden DW. Bacterial interactions with the eukaryotic secretory pathway. *Curr Opin Microbiol*. 2005;8(1):92-8. Epub 2005/02/08. doi:10.1016/j.mib.2004.12.007. PubMed PMID: 15694862.
52. Salcedo SP, Holden DW. SseG, a virulence protein that targets Salmonella to the Golgi network. *EMBO J*. 2003;22(19):5003-14. Epub 2003/10/01. doi: 10.1093/emboj/cdg517. PubMed PMID: 14517239; PubMed Central PMCID: PMC204495.
53. Wesolowski J, Paumet F. Taking control: reorganization of the host cytoskeleton by Chlamydia. *F1000Res*. 2017;6:2058. Epub 2017/12/12. doi: 10.12688/f1000research.12316.1. PubMed PMID: 29225789; PubMed Central PMCID: PMC5710305.
54. Ragaz C, Pietsch H, Urwyler S, Tiaden A, Weber SS, Hilbi H. The Legionella pneumophila phosphatidylinositol-4 phosphate-binding type IV substrate SidC recruits endoplasmic reticulum vesicles to a replication-permissive vacuole. *Cell Microbiol*. 2008;10(12):2416-33. Epub 2008/08/05. doi: 10.1111/j.1462-5822.2008.01219.x. PubMed PMID: 18673369.
55. Pizarro-Cerda J, Charbit A, Enninga J, Lafont F, Cossart P. Manipulation of host membranes by the bacterial pathogens Listeria, Francisella, Shigella and

- Yersinia*. *Semin Cell Dev Biol*. 2016;60:155-67. Epub 2016/07/28. doi: 10.1016/j.semcdb.2016.07.019. PubMed PMID: 27448494.
56. Weigle BA, Orchard RC, Jimenez A, Cox GW, Alto NM. A systematic exploration of the interactions between bacterial effector proteins and host cell membranes. *Nat Commun*. 2017;8(1):532. Epub 2017/09/16. doi: 10.1038/s41467-017-00700-7. PubMed PMID: 28912547; PubMed Central PMCID: PMC5599653.
57. Ligon LS, Hayden JD, Braunstein M. The ins and outs of *Mycobacterium tuberculosis* protein export. *Tuberculosis (Edinb)*. 2012;92(2):121-32. Epub 2011/12/24. doi: 10.1016/j.tube.2011.11.005. PubMed PMID: 22192870; PubMed Central PMCID: PMC3288827.
58. Feltcher ME, Sullivan JT, Braunstein M. Protein export systems of *Mycobacterium tuberculosis*: novel targets for drug development? *Future Microbiol*. 2010;5(10):1581-97. Epub 2010/11/16. doi: 10.2217/fmb.10.112. PubMed PMID: 21073315; PubMed Central PMCID: PMC3034451.
59. Manzanillo PS, Shiloh MU, Portnoy DA, Cox JS. *Mycobacterium tuberculosis* activates the DNA-dependent cytosolic surveillance pathway within macrophages. *Cell host & microbe*. 2012;11(5):469-80. doi: 10.1016/j.chom.2012.03.007. PubMed PMID: 22607800; PubMed Central PMCID: PMC3662372.
60. Stanley SA, Johndrow JE, Manzanillo P, Cox JS. The Type I IFN response to infection with *Mycobacterium tuberculosis* requires ESX-1-mediated secretion and contributes to pathogenesis. *Journal of immunology (Baltimore, Md : 1950)*. 2007;178(5):3143-52. PubMed PMID: 17312162.
61. Siegrist MS, Unnikrishnan M, McConnell MJ, Borowsky M, Cheng TY, Siddiqi N, et al. *Mycobacterial* Esx-3 is required for mycobactin-mediated iron acquisition. *Proc Natl Acad Sci U S A*. 2009;106(44):18792-7. Epub 2009/10/23. doi: 10.1073/pnas.0900589106. PubMed PMID: 19846780; PubMed Central PMCID: PMC2774023.
62. Tufariello JM, Chapman JR, Kerantzas CA, Wong KW, Vilcheze C, Jones CM, et al. Separable roles for *Mycobacterium tuberculosis* ESX-3 effectors in iron acquisition and virulence. *Proc Natl Acad Sci U S A*. 2016;113(3):E348-57. Epub 2016/01/06. doi: 10.1073/pnas.1523321113. PubMed PMID: 26729876; PubMed Central PMCID: PMC4725510.
63. Mehra A, Zahra A, Thompson V, Sirisaengtaksin N, Wells A, Porto M, et al. *Mycobacterium tuberculosis* type VII secreted effector EsxH targets host ESCRT to impair trafficking. *PLoS Pathog*. 2013;9(10):e1003734. Epub 2013/11/10. doi: 10.1371/journal.ppat.1003734. PubMed PMID: 24204276; PubMed Central PMCID: PMC3814348.

64. Portal-Celhay C, Tufariello JM, Srivastava S, Zahra A, Klevorn T, Grace PS, et al. Mycobacterium tuberculosis EsxH inhibits ESCRT-dependent CD4+ T-cell activation. *Nat Microbiol.* 2016;2:16232. Epub 2016/12/06. doi: 10.1038/nmicrobiol.2016.232. PubMed PMID: 27918526; PubMed Central PMCID: PMC5453184.
65. Abdallah AM, Verboom T, Weerdenburg EM, Gey van Pittius NC, Mahasha PW, Jimenez C, et al. PPE and PE_PGRS proteins of Mycobacterium marinum are transported via the type VII secretion system ESX-5. *Mol Microbiol.* 2009;73(3):329-40. Epub 2009/07/16. doi: 10.1111/j.1365-2958.2009.06783.x. PubMed PMID: 19602152.
66. Houben EN, Bestebroer J, Ummels R, Wilson L, Piersma SR, Jimenez CR, et al. Composition of the type VII secretion system membrane complex. *Mol Microbiol.* 2012;86(2):472-84. Epub 2012/08/29. doi: 10.1111/j.1365-2958.2012.08206.x. PubMed PMID: 22925462.
67. Bottai D, Di Luca M, Majlessi L, Frigui W, Simeone R, Sayes F, et al. Disruption of the ESX-5 system of Mycobacterium tuberculosis causes loss of PPE protein secretion, reduction of cell wall integrity and strong attenuation. *Mol Microbiol.* 2012;83(6):1195-209. Epub 2012/02/22. doi: 10.1111/j.1365-2958.2012.08001.x. PubMed PMID: 22340629.
68. Ates LS, van der Woude AD, Bestebroer J, van Stempvoort G, Musters RJ, Garcia-Vallejo JJ, et al. The ESX-5 System of Pathogenic Mycobacteria Is Involved In Capsule Integrity and Virulence through Its Substrate PPE10. *PLoS Pathog.* 2016;12(6):e1005696. Epub 2016/06/10. doi: 10.1371/journal.ppat.1005696. PubMed PMID: 27280885; PubMed Central PMCID: PMC4900558.
69. Brennan MJ. The Enigmatic PE/PPE Multigene Family of Mycobacteria and Tuberculosis Vaccination. *Infect Immun.* 2017;85(6). Epub 2017/03/30. doi: 10.1128/IAI.00969-16. PubMed PMID: 28348055; PubMed Central PMCID: PMC5442627.
70. Sampson SL. Mycobacterial PE/PPE proteins at the host-pathogen interface. *Clin Dev Immunol.* 2011;2011:497203. Epub 2011/02/15. doi: 10.1155/2011/497203. PubMed PMID: 21318182; PubMed Central PMCID: PMC3034920.
71. Bhat KH, Ahmed A, Kumar S, Sharma P, Mukhopadhyay S. Role of PPE18 protein in intracellular survival and pathogenicity of Mycobacterium tuberculosis in mice. *PLoS One.* 2012;7(12):e52601. Epub 2013/01/10. doi: 10.1371/journal.pone.0052601. PubMed PMID: 23300718; PubMed Central PMCID: PMC3532481.
72. Iantomasi R, Sali M, Cascioferro A, Palucci I, Zumbo A, Soldini S, et al. PE_PGRS30 is required for the full virulence of Mycobacterium tuberculosis. *Cell Microbiol.*

- 2012;14(3):356-67. Epub 2011/11/05. doi: 10.1111/j.1462-5822.2011.01721.x. PubMed PMID: 22050772.
73. Kurtz S, McKinnon KP, Runge MS, Ting JP, Braunstein M. The SecA2 secretion factor of *Mycobacterium tuberculosis* promotes growth in macrophages and inhibits the host immune response. *Infect Immun*. 2006;74(12):6855-64. Epub 2006/10/13. doi: 10.1128/IAI.01022-06. PubMed PMID: 17030572; PubMed Central PMCID: PMC1698048.
74. Feltcher ME, Gunawardena HP, Zulauf KE, Malik S, Griffin JE, Sassetti CM, et al. Label-free Quantitative Proteomics Reveals a Role for the *Mycobacterium tuberculosis* SecA2 Pathway in Exporting Solute Binding Proteins and Mce Transporters to the Cell Wall. *Mol Cell Proteomics*. 2015;14(6):1501-16. Epub 2015/03/31. doi: 10.1074/mcp.M114.044685. PubMed PMID: 25813378; PubMed Central PMCID: PMC1698048.
75. Walburger A, Koul A, Ferrari G, Nguyen L, Prescianotto-Baschong C, Huygen K, et al. Protein kinase G from pathogenic mycobacteria promotes survival within macrophages. *Science*. 2004;304(5678):1800-4. Epub 2004/05/25. doi: 10.1126/science.1099384. PubMed PMID: 15155913.
76. Jimenez A, Chen D, Alto NM. How Bacteria Subvert Animal Cell Structure and Function. *Annu Rev Cell Dev Biol*. 2016;32:373-97. Epub 2016/05/06. doi: 10.1146/annurev-cellbio-100814-125227. PubMed PMID: 27146312; PubMed Central PMCID: PMC1698048.
77. Rosenkrands I, Weldingh K, Jacobsen S, Hansen CV, Florio W, Gianetri I, et al. Mapping and identification of *Mycobacterium tuberculosis* proteins by two-dimensional gel electrophoresis, microsequencing and immunodetection. *Electrophoresis*. 2000;21(5):935-48. Epub 2000/04/18. doi: 10.1002/(SICI)1522-2683(20000301)21:5<935::AID-ELPS935>3.0.CO;2-P. PubMed PMID: 10768780.
78. Mattow J, Schaible UE, Schmidt F, Hagens K, Siejak F, Brestrich G, et al. Comparative proteome analysis of culture supernatant proteins from virulent *Mycobacterium tuberculosis* H37Rv and attenuated *M. bovis* BCG Copenhagen. *Electrophoresis*. 2003;24(19-20):3405-20. Epub 2003/11/05. doi: 10.1002/elps.200305601. PubMed PMID: 14595687.
79. Malen H, Berven FS, Fladmark KE, Wiker HG. Comprehensive analysis of exported proteins from *Mycobacterium tuberculosis* H37Rv. *Proteomics*. 2007;7(10):1702-18. Epub 2007/04/20. doi: 10.1002/pmic.200600853. PubMed PMID: 17443846.
80. de Souza GA, Leversen NA, Malen H, Wiker HG. Bacterial proteins with cleaved or uncleaved signal peptides of the general secretory pathway. *J Proteomics*.

- 2011;75(2):502-10. Epub 2011/09/17. doi: 10.1016/j.jprot.2011.08.016. PubMed PMID: 21920479.
81. Kelkar DS, Kumar D, Kumar P, Balakrishnan L, Muthusamy B, Yadav AK, et al. Proteogenomic analysis of *Mycobacterium tuberculosis* by high resolution mass spectrometry. *Mol Cell Proteomics*. 2011;10(12):M111 011627. Epub 2011/10/05. doi: 10.1074/mcp.M111.011445. PubMed PMID: 21969609; PubMed Central PMCID: PMC3275902.
82. Aronheim A, Zandi E, Hennemann H, Elledge SJ, Karin M. Isolation of an AP-1 repressor by a novel method for detecting protein-protein interactions. *Mol Cell Biol*. 1997;17(6):3094-102. Epub 1997/06/01. PubMed PMID: 9154808; PubMed Central PMCID: PMC232162.
83. Glickman MS, Cahill SM, Jacobs WR, Jr. The *Mycobacterium tuberculosis* *cmaA2* gene encodes a mycolic acid trans-cyclopropane synthetase. *J Biol Chem*. 2001;276(3):2228-33. Epub 2000/11/28. doi: 10.1074/jbc.C000652200. PubMed PMID: 11092877.
84. Collins AC, Cai H, Li T, Franco LH, Li XD, Nair VR, et al. Cyclic GMP-AMP Synthase Is an Innate Immune DNA Sensor for *Mycobacterium tuberculosis*. *Cell Host Microbe*. 2015;17(6):820-8. Epub 2015/06/07. doi: 10.1016/j.chom.2015.05.005. PubMed PMID: 26048137; PubMed Central PMCID: PMC4499468.
85. Sunshine H, Iruela-Arispe ML. Membrane lipids and cell signaling. *Curr Opin Lipidol*. 2017;28(5):408-13. Epub 2017/07/12. doi: 10.1097/MOL.0000000000000443. PubMed PMID: 28692598; PubMed Central PMCID: PMC5776726.
86. Bae YS, Lee HY, Jung YS, Lee M, Suh PG. Phospholipase Cgamma in Toll-like receptor-mediated inflammation and innate immunity. *Adv Biol Regul*. 2017;63:92-7. Epub 2016/10/07. doi: 10.1016/j.jbior.2016.09.006. PubMed PMID: 27707630.
87. Bonifacino JS, Glick BS. The mechanisms of vesicle budding and fusion. *Cell*. 2004;116(2):153-66. Epub 2004/01/28. PubMed PMID: 14744428.
88. Lippincott-Schwartz J, Phair RD. Lipids and cholesterol as regulators of traffic in the endomembrane system. *Annu Rev Biophys*. 2010;39:559-78. Epub 2010/03/03. doi: 10.1146/annurev.biophys.093008.131357. PubMed PMID: 20192772; PubMed Central PMCID: PMC3366628.
89. Martens S, Nakamura S, Yoshimori T. Phospholipids in Autophagosome Formation and Fusion. *J Mol Biol*. 2016. Epub 2016/12/17. doi: 10.1016/j.jmb.2016.10.029. PubMed PMID: 27984040.

90. Sullivan JT, Young EF, McCann JR, Braunstein M. The Mycobacterium tuberculosis SecA2 system subverts phagosome maturation to promote growth in macrophages. *Infect Immun*. 2012;80(3):996-1006. Epub 2012/01/05. doi: 10.1128/IAI.05987-11. PubMed PMID: 22215736; PubMed Central PMCID: PMC3294638.
91. Bach H, Papavinasasundaram KG, Wong D, Hmama Z, Av-Gay Y. Mycobacterium tuberculosis virulence is mediated by PtpA dephosphorylation of human vacuolar protein sorting 33B. *Cell Host Microbe*. 2008;3(5):316-22. Epub 2008/05/14. doi: 10.1016/j.chom.2008.03.008. PubMed PMID: 18474358.
92. Parveen N, Varman R, Nair S, Das G, Ghosh S, Mukhopadhyay S. Endocytosis of Mycobacterium tuberculosis heat shock protein 60 is required to induce interleukin-10 production in macrophages. *Journal of Biological Chemistry*. 2013;288(34):24956-71. doi: 10.1074/jbc.M113.461004. PubMed PMID: 23846686; PubMed Central PMCID: PMC3750191.
93. Nair S, Ramaswamy PA, Ghosh S, Joshi DC, Pathak N, Siddiqui I, et al. The PPE18 of Mycobacterium tuberculosis interacts with TLR2 and activates IL-10 induction in macrophage. *The Journal of Immunology*. 2009;183(10):6269-81. doi: 10.4049/jimmunol.0901367. PubMed PMID: 19880448.
94. Pathak SK, Basu S, Basu KK, Banerjee A, Pathak S, Bhattacharyya A, et al. Direct extracellular interaction between the early secreted antigen ESAT-6 of Mycobacterium tuberculosis and TLR2 inhibits TLR signaling in macrophages. *Nature immunology*. 2007;8(6):610-8. doi: 10.1038/ni1468. PubMed PMID: 17486091.
95. Desvaux M, Hebraud M, Talon R, Henderson IR. Secretion and subcellular localizations of bacterial proteins: a semantic awareness issue. *Trends Microbiol*. 2009;17(4):139-45. Epub 2009/03/21. doi: 10.1016/j.tim.2009.01.004. PubMed PMID: 19299134.
96. Conrad WH, Osman MM, Shanahan JK, Chu F, Takaki KK, Cameron J, et al. Mycobacterial ESX-1 secretion system mediates host cell lysis through bacterium contact-dependent gross membrane disruptions. *Proc Natl Acad Sci U S A*. 2017;114(6):1371-6. Epub 2017/01/26. doi: 10.1073/pnas.1620133114. PubMed PMID: 28119503; PubMed Central PMCID: PMC5307465.
97. Lou Y, Rybniker J, Sala C, Cole ST. EspC forms a filamentous structure in the cell envelope of Mycobacterium tuberculosis and impacts ESX-1 secretion. *Mol Microbiol*. 2017;103(1):26-38. Epub 2016/11/20. doi: 10.1111/mmi.13575. PubMed PMID: 27859904.
98. Perkowski EF, Zulauf KE, Weerakoon D, Hayden JD, Ioerger TR, Oreper D, et al. The EXIT Strategy: an Approach for Identifying Bacterial Proteins Exported

- during Host Infection. *MBio*. 2017;8(2). Epub 2017/04/27. doi: 10.1128/mBio.00333-17. PubMed PMID: 28442606; PubMed Central PMCID: PMC5405230.
99. Jungblut PR, Schaible UE, Mollenkopf HJ, Zimny-Arndt U, Raupach B, Mattow J, et al. Comparative proteome analysis of *Mycobacterium tuberculosis* and *Mycobacterium bovis* BCG strains: towards functional genomics of microbial pathogens. *Mol Microbiol*. 1999;33(6):1103-17. Epub 1999/10/06. PubMed PMID: 10510226.
100. Rosenkrands I, King A, Weldingh K, Moniatte M, Moertz E, Andersen P. Towards the proteome of *Mycobacterium tuberculosis*. *Electrophoresis*. 2000;21(17):3740-56. Epub 2001/03/29. doi: 10.1002/1522-2683(200011)21:17<3740::AID-ELPS3740>3.0.CO;2-3. PubMed PMID: 11271494.
101. Marjanovic O, Miyata T, Goodridge A, Kendall LV, Riley LW. Mce2 operon mutant strain of *Mycobacterium tuberculosis* is attenuated in C57BL/6 mice. *Tuberculosis (Edinb)*. 2010;90(1):50-6. Epub 2009/12/08. doi: 10.1016/j.tube.2009.10.004. PubMed PMID: 19963438; PubMed Central PMCID: PMC3228843.
102. Gioffre A, Infante E, Aguilar D, Santangelo MP, Klepp L, Amadio A, et al. Mutation in mce operons attenuates *Mycobacterium tuberculosis* virulence. *Microbes Infect*. 2005;7(3):325-34. Epub 2005/04/05. doi: 10.1016/j.micinf.2004.11.007. PubMed PMID: 15804490.
103. Saini NK, Sharma M, Chandolia A, Pasricha R, Brahmachari V, Bose M. Characterization of Mce4A protein of *Mycobacterium tuberculosis*: role in invasion and survival. *BMC Microbiol*. 2008;8:200. Epub 2008/11/21. doi: 10.1186/1471-2180-8-200. PubMed PMID: 19019220; PubMed Central PMCID: PMC2596156.
104. Brodin P, Poquet Y, Levillain F, Peguillet I, Larrouy-Maumus G, Gilleron M, et al. High content phenotypic cell-based visual screen identifies *Mycobacterium tuberculosis* acyltrehalose-containing glycolipids involved in phagosome remodeling. *PLoS Pathog*. 2010;6(9):e1001100. Epub 2010/09/17. doi: 10.1371/journal.ppat.1001100. PubMed PMID: 20844580; PubMed Central PMCID: PMC2936551.
105. Shah S, Briken V. Modular Organization of the ESX-5 Secretion System in *Mycobacterium tuberculosis*. *Front Cell Infect Microbiol*. 2016;6:49. Epub 2016/05/21. doi: 10.3389/fcimb.2016.00049. PubMed PMID: 27200304; PubMed Central PMCID: PMC4852179.

106. Sasseti CM, Boyd DH, Rubin EJ. Genes required for mycobacterial growth defined by high density mutagenesis. *Mol Microbiol.* 2003;48(1):77-84. Epub 2003/03/27. PubMed PMID: 12657046.
107. Rengarajan J, Bloom BR, Rubin EJ. Genome-wide requirements for *Mycobacterium tuberculosis* adaptation and survival in macrophages. *Proc Natl Acad Sci U S A.* 2005;102(23):8327-32. Epub 2005/06/02. doi: 10.1073/pnas.0503272102. PubMed PMID: 15928073; PubMed Central PMCID: PMC1142121.
108. McCann JR, McDonough JA, Sullivan JT, Feltcher ME, Braunstein M. Genome-wide identification of *Mycobacterium tuberculosis* exported proteins with roles in intracellular growth. *J Bacteriol.* 2011;193(4):854-61. Epub 2010/12/15. doi: 10.1128/JB.01271-10. PubMed PMID: 21148733; PubMed Central PMCID: PMC3028674.
109. Rosas-Magallanes V, Stadthagen-Gomez G, Rauzier J, Barreiro LB, Tailleux L, Boudou F, et al. Signature-tagged transposon mutagenesis identifies novel *Mycobacterium tuberculosis* genes involved in the parasitism of human macrophages. *Infect Immun.* 2007;75(1):504-7. Epub 2006/10/13. doi: 10.1128/IAI.00058-06. PubMed PMID: 17030567; PubMed Central PMCID: PMC1828433.
110. Isakoff SJ, Cardozo T, Andreev J, Li Z, Ferguson KM, Abagyan R, et al. Identification and analysis of PH domain-containing targets of phosphatidylinositol 3-kinase using a novel in vivo assay in yeast. *EMBO J.* 1998;17(18):5374-87. Epub 1998/09/16. doi: 10.1093/emboj/17.18.5374. PubMed PMID: 9736615; PubMed Central PMCID: PMC1170863.
111. Cowley SC, Babakaiff R, Av-Gay Y. Expression and localization of the *Mycobacterium tuberculosis* protein tyrosine phosphatase PtpA. *Res Microbiol.* 2002;153(4):233-41. Epub 2002/06/18. PubMed PMID: 12066895.
112. Chiu VK, Bivona T, Hach A, Sajous JB, Silletti J, Wiener H, et al. Ras signalling on the endoplasmic reticulum and the Golgi. *Nat Cell Biol.* 2002;4(5):343-50. Epub 2002/05/04. doi: 10.1038/ncb783. PubMed PMID: 11988737.
113. Yu JW, Mendrola JM, Audhya A, Singh S, Keleti D, DeWald DB, et al. Genome-wide analysis of membrane targeting by *S. cerevisiae* pleckstrin homology domains. *Mol Cell.* 2004;13(5):677-88. Epub 2004/03/17. PubMed PMID: 15023338.
114. Lussier M, White AM, Sheraton J, di Paolo T, Treadwell J, Southard SB, et al. Large scale identification of genes involved in cell surface biosynthesis and architecture in *Saccharomyces cerevisiae*. *Genetics.* 1997;147(2):435-50. Epub 1997/10/23. PubMed PMID: 9335584; PubMed Central PMCID: PMC1208169.

115. Shiflett SL, Ward DM, Huynh D, Vaughn MB, Simmons JC, Kaplan J. Characterization of Vta1p, a class E Vps protein in *Saccharomyces cerevisiae*. *J Biol Chem*. 2004;279(12):10982-90. Epub 2004/01/01. doi: 10.1074/jbc.M312669200. PubMed PMID: 14701806.
116. Rivera VM, Wang X, Wardwell S, Courage NL, Volchuk A, Keenan T, et al. Regulation of protein secretion through controlled aggregation in the endoplasmic reticulum. *Science*. 2000;287(5454):826-30. Epub 2000/02/05. PubMed PMID: 10657290.
117. Selyunin AS, Reddick LE, Weigele BA, Alto NM. Selective protection of an ARF1-GTP signaling axis by a bacterial scaffold induces bidirectional trafficking arrest. *Cell Rep*. 2014;6(5):878-91. Epub 2014/03/04. doi: 10.1016/j.celrep.2014.01.040. PubMed PMID: 24582959; PubMed Central PMCID: PMC4017587.
118. Popa C, Coll NS, Valls M, Sessa G. Yeast as a Heterologous Model System to Uncover Type III Effector Function. *PLoS Pathog*. 2016;12(2):e1005360. Epub 2016/02/26. doi: 10.1371/journal.ppat.1005360. PubMed PMID: 26914889; PubMed Central PMCID: PMC4767418.
119. Penn BH, Netter Z, Johnson JR, Von Dollen J, Jang GM, Johnson T, et al. An Mtb-Human Protein-Protein Interaction Map Identifies a Switch between Host Antiviral and Antibacterial Responses. *Mol Cell*. 2018;71(4):637-48 e5. doi: 10.1016/j.molcel.2018.07.010. PubMed PMID: 30118682; PubMed Central PMCID: PMC6329589.
120. Shenoy VP, Mukhopadhyay C. Rapid Immunochromatographic Test for the Identification and Discrimination of Mycobacterium tuberculosis Complex Isolates from Non-tuberculous Mycobacteria. *J Clin Diagn Res*. 2014;8(4):DC13-5. Epub 2014/06/25. doi: 10.7860/JCDR/2014/7098.4253. PubMed PMID: 24959442; PubMed Central PMCID: PMC4064930.
121. Arora J, Kumar G, Verma AK, Bhalla M, Sarin R, Myneedu VP. Utility of MPT64 Antigen Detection for Rapid Confirmation of Mycobacterium tuberculosis Complex. *J Glob Infect Dis*. 2015;7(2):66-9. Epub 2015/06/13. doi: 10.4103/0974-777X.154443. PubMed PMID: 26069425; PubMed Central PMCID: PMC4448327.
122. Behr MA, Wilson MA, Gill WP, Salamon H, Schoolnik GK, Rane S, et al. Comparative genomics of BCG vaccines by whole-genome DNA microarray. *Science*. 1999;284(5419):1520-3. Epub 1999/05/29. PubMed PMID: 10348738.
123. Kozak RA, Alexander DC, Liao R, Sherman DR, Behr MA. Region of difference 2 contributes to virulence of Mycobacterium tuberculosis. *Infect Immun*. 2011;79(1):59-66. Epub 2010/10/27. doi: 10.1128/IAI.00824-10. PubMed PMID: 20974821; PubMed Central PMCID: PMC3019914.

124. Sibley L, Reljic R, Radford DS, Huang JM, Hong HA, Cranenburgh RM, et al. Recombinant *Bacillus subtilis* spores expressing MPT64 evaluated as a vaccine against tuberculosis in the murine model. *FEMS Microbiol Lett*. 2014;358(2):170-9. Epub 2014/07/06. doi: 10.1111/1574-6968.12525. PubMed PMID: 24990572.
125. Chen H, Liu X, Ma X, Wang Q, Yang G, Niu H, et al. A New Rabbit-Skin Model to Evaluate Protective Efficacy of Tuberculosis Vaccines. *Front Microbiol*. 2017;8:842. Epub 2017/06/02. doi: 10.3389/fmicb.2017.00842. PubMed PMID: 28567030; PubMed Central PMCID: PMC5434645.
126. English AR, Voeltz GK. Endoplasmic reticulum structure and interconnections with other organelles. *Cold Spring Harb Perspect Biol*. 2013;5(4):a013227. Epub 2013/04/03. doi: 10.1101/cshperspect.a013227. PubMed PMID: 23545422; PubMed Central PMCID: PMC3683900.
127. Sonnenberg MG, Belisle JT. Definition of *Mycobacterium tuberculosis* culture filtrate proteins by two-dimensional polyacrylamide gel electrophoresis, N-terminal amino acid sequencing, and electrospray mass spectrometry. *Infect Immun*. 1997;65(11):4515-24. Epub 1997/11/14. PubMed PMID: 9353028; PubMed Central PMCID: PMC175649.
128. Wang Z, Potter BM, Gray AM, Sacksteder KA, Geisbrecht BV, Laity JH. The solution structure of antigen MPT64 from *Mycobacterium tuberculosis* defines a new family of beta-grasp proteins. *J Mol Biol*. 2007;366(2):375-81. Epub 2006/12/19. doi: 10.1016/j.jmb.2006.11.039. PubMed PMID: 17174329.
129. Hastie JL, Williams KB, Bohr LL, Houtman JC, Gakhar L, Ellermeier CD. The Anti-sigma Factor RsiV Is a Bacterial Receptor for Lysozyme: Co-crystal Structure Determination and Demonstration That Binding of Lysozyme to RsiV Is Required for sigmaV Activation. *PLoS Genet*. 2016;12(9):e1006287. Epub 2016/09/08. doi: 10.1371/journal.pgen.1006287. PubMed PMID: 27602573; PubMed Central PMCID: PMC5014341.
130. Kelley LA, Mezulis S, Yates CM, Wass MN, Sternberg MJ. The Phyre2 web portal for protein modeling, prediction and analysis. *Nat Protoc*. 2015;10(6):845-58. Epub 2015/05/08. doi: 10.1038/nprot.2015.053. PubMed PMID: 25950237; PubMed Central PMCID: PMC5298202.
131. Breker M, Gymrek M, Schuldiner M. A novel single-cell screening platform reveals proteome plasticity during yeast stress responses. *J Cell Biol*. 2013;200(6):839-50. Epub 2013/03/20. doi: 10.1083/jcb.201301120. PubMed PMID: 23509072; PubMed Central PMCID: PMC3601363.
132. Huh WK, Falvo JV, Gerke LC, Carroll AS, Howson RW, Weissman JS, et al. Global analysis of protein localization in budding yeast. *Nature*. 2003;425(6959):686-91. Epub 2003/10/17. doi: 10.1038/nature02026. PubMed PMID: 14562095.

133. Strahl T, Thorner J. Synthesis and function of membrane phosphoinositides in budding yeast, *Saccharomyces cerevisiae*. *Biochim Biophys Acta*. 2007;1771(3):353-404. doi: 10.1016/j.bbali.2007.01.015. PubMed PMID: 17382260; PubMed Central PMCID: PMC1868553.
134. Di Paolo G, De Camilli P. Phosphoinositides in cell regulation and membrane dynamics. *Nature*. 2006;443(7112):651-7. doi: 10.1038/nature05185. PubMed PMID: 17035995.
135. Levine TP, Munro S. Dual targeting of Osh1p, a yeast homologue of oxysterol-binding protein, to both the Golgi and the nucleus-vacuole junction. *Mol Biol Cell*. 2001;12(6):1633-44. doi: 10.1091/mbc.12.6.1633. PubMed PMID: 11408574; PubMed Central PMCID: PMC37330.
136. Roy A, Levine TP. Multiple pools of phosphatidylinositol 4-phosphate detected using the pleckstrin homology domain of Osh2p. *J Biol Chem*. 2004;279(43):44683-9. doi: 10.1074/jbc.M401583200. PubMed PMID: 15271978.
137. Abdallah AM, Gey van Pittius NC, Champion PA, Cox J, Luirink J, Vandenbroucke-Grauls CM, et al. Type VII secretion--mycobacteria show the way. *Nat Rev Microbiol*. 2007;5(11):883-91. Epub 2007/10/09. doi: 10.1038/nrmicro1773. PubMed PMID: 17922044.
138. Champion PA, Stanley SA, Champion MM, Brown EJ, Cox JS. C-terminal signal sequence promotes virulence factor secretion in *Mycobacterium tuberculosis*. *Science*. 2006;313(5793):1632-6. Epub 2006/09/16. doi: 10.1126/science.1131167. PubMed PMID: 16973880.
139. Hsu T, Hingley-Wilson SM, Chen B, Chen M, Dai AZ, Morin PM, et al. The primary mechanism of attenuation of bacillus Calmette-Guerin is a loss of secreted lytic function required for invasion of lung interstitial tissue. *Proc Natl Acad Sci U S A*. 2003;100(21):12420-5. doi: 10.1073/pnas.1635213100. PubMed PMID: 14557547; PubMed Central PMCID: PMC218773.
140. van der Wel N, Hava D, Houben D, Fluittsma D, van Zon M, Pierson J, et al. *M. tuberculosis* and *M. leprae* translocate from the phagolysosome to the cytosol in myeloid cells. *Cell*. 2007;129(7):1287-98. Epub 2007/07/03. doi: 10.1016/j.cell.2007.05.059. PubMed PMID: 17604718.
141. Bardarov S, Kriakov J, Carriere C, Yu S, Vaamonde C, McAdam RA, et al. Conditionally replicating mycobacteriophages: a system for transposon delivery to *Mycobacterium tuberculosis*. *Proc Natl Acad Sci U S A*. 1997;94(20):10961-6. Epub 1997/10/06. PubMed PMID: 9380742; PubMed Central PMCID: PMC23545.

142. Glickman MS, Cox JS, Jacobs WR, Jr. A novel mycolic acid cyclopropane synthetase is required for cording, persistence, and virulence of *Mycobacterium tuberculosis*. *Mol Cell*. 2000;5(4):717-27. Epub 2000/07/06. PubMed PMID: 10882107.
143. Chan K, Knaak T, Satkamp L, Humbert O, Falkow S, Ramakrishnan L. Complex pattern of *Mycobacterium marinum* gene expression during long-term granulomatous infection. *Proc Natl Acad Sci U S A*. 2002;99(6):3920-5. Epub 2002/03/14. doi: 10.1073/pnas.002024599. PubMed PMID: 11891270; PubMed Central PMCID: PMC122624.
144. Domingo-Gonzalez R, Prince O, Cooper A, Khader SA. Cytokines and Chemokines in *Mycobacterium tuberculosis* Infection. *Microbiol Spectr*. 2016;4(5). Epub 2016/10/21. doi: 10.1128/microbiolspec.TBTB2-0018-2016. PubMed PMID: 27763255; PubMed Central PMCID: PMC5205539.
145. Mayer-Barber KD, Sher A. Cytokine and lipid mediator networks in tuberculosis. *Immunol Rev*. 2015;264(1):264-75. Epub 2015/02/24. doi: 10.1111/imr.12249. PubMed PMID: 25703565; PubMed Central PMCID: PMC4339232.
146. Seimon TA, Kim MJ, Blumenthal A, Koo J, Ehrt S, Wainwright H, et al. Induction of ER stress in macrophages of tuberculosis granulomas. *PLoS One*. 2010;5(9):e12772. Epub 2010/09/22. doi: 10.1371/journal.pone.0012772. PubMed PMID: 20856677; PubMed Central PMCID: PMC2939897.
147. Lim YJ, Yi MH, Choi JA, Lee J, Han JY, Jo SH, et al. Roles of endoplasmic reticulum stress-mediated apoptosis in M1-polarized macrophages during mycobacterial infections. *Sci Rep*. 2016;6:37211. Epub 2016/11/16. doi: 10.1038/srep37211. PubMed PMID: 27845414; PubMed Central PMCID: PMC5109032.
148. Cui Y, Zhao D, Barrow PA, Zhou X. The endoplasmic reticulum stress response: A link with tuberculosis? *Tuberculosis (Edinb)*. 2016;97:52-6. Epub 2016/03/17. doi: 10.1016/j.tube.2015.12.009. PubMed PMID: 26980496.
149. Osowski CM, Urano F. Measuring ER stress and the unfolded protein response using mammalian tissue culture system. *Methods Enzymol*. 2011;490:71-92. Epub 2011/01/27. doi: 10.1016/B978-0-12-385114-7.00004-0. PubMed PMID: 21266244; PubMed Central PMCID: PMC3701721.
150. Parida BK, Douglas T, Nino C, Dhandayuthapani S. Interactions of anti-sigma factor antagonists of *Mycobacterium tuberculosis* in the yeast two-hybrid system. *Tuberculosis (Edinb)*. 2005;85(5-6):347-55. Epub 2005/11/03. doi: 10.1016/j.tube.2005.08.001. PubMed PMID: 16263329.

151. Bruckner A, Polge C, Lentze N, Auerbach D, Schlattner U. Yeast two-hybrid, a powerful tool for systems biology. *Int J Mol Sci.* 2009;10(6):2763-88. Epub 2009/07/08. doi: 10.3390/ijms10062763. PubMed PMID: 19582228; PubMed Central PMCID: PMCPMC2705515.
152. Hu H, Tian M, Ding C, Yu S. The C/EBP Homologous Protein (CHOP) Transcription Factor Functions in Endoplasmic Reticulum Stress-Induced Apoptosis and Microbial Infection. *Front Immunol.* 2018;9:3083. doi: 10.3389/fimmu.2018.03083. PubMed PMID: 30662442; PubMed Central PMCID: PMCPMC6328441.
153. Mustafa T, Wiker HG, Morkve O, Sviland L. Differential expression of mycobacterial antigen MPT64, apoptosis and inflammatory markers in multinucleated giant cells and epithelioid cells in granulomas caused by *Mycobacterium tuberculosis*. *Virchows Arch.* 2008;452(4):449-56. Epub 2008/02/13. doi: 10.1007/s00428-008-0575-z. PubMed PMID: 18266005; PubMed Central PMCID: PMCPMC2668550.
154. Danilchanka O, Sun J, Pavlenok M, Maueroeder C, Speer A, Siroy A, et al. An outer membrane channel protein of *Mycobacterium tuberculosis* with exotoxin activity. *Proc Natl Acad Sci U S A.* 2014;111(18):6750-5. Epub 2014/04/23. doi: 10.1073/pnas.1400136111. PubMed PMID: 24753609; PubMed Central PMCID: PMCPMC4020113.
155. Sun J, Siroy A, Lokareddy RK, Speer A, Doornbos KS, Cingolani G, et al. The tuberculosis necrotizing toxin kills macrophages by hydrolyzing NAD. *Nat Struct Mol Biol.* 2015;22(9):672-8. Epub 2015/08/04. doi: 10.1038/nsmb.3064. PubMed PMID: 26237511; PubMed Central PMCID: PMCPMC4560639.
156. O'Connor TJ, Adepoju Y, Boyd D, Isberg RR. Minimization of the *Legionella pneumophila* genome reveals chromosomal regions involved in host range expansion. *Proc Natl Acad Sci U S A.* 2011;108(36):14733-40. Epub 2011/08/30. doi: 10.1073/pnas.1111678108. PubMed PMID: 21873199; PubMed Central PMCID: PMCPMC3169125.
157. Ensminger AW. *Legionella pneumophila*, armed to the hilt: justifying the largest arsenal of effectors in the bacterial world. *Curr Opin Microbiol.* 2016;29:74-80. Epub 2015/12/29. doi: 10.1016/j.mib.2015.11.002. PubMed PMID: 26709975.
158. De Leon JA, Qiu J, Nicolai CJ, Counihan JL, Barry KC, Xu L, et al. Positive and Negative Regulation of the Master Metabolic Regulator mTORC1 by Two Families of *Legionella pneumophila* Effectors. *Cell Rep.* 2017;21(8):2031-8. doi: 10.1016/j.celrep.2017.10.088. PubMed PMID: 29166595; PubMed Central PMCID: PMCPMC5726772.
159. Betts JC, Dodson P, Quan S, Lewis AP, Thomas PJ, Duncan K, et al. Comparison of the proteome of *Mycobacterium tuberculosis* strain H37Rv with clinical isolate

- CDC 1551. *Microbiology*. 2000;146 Pt 12:3205-16. Epub 2000/12/02. doi: 10.1099/00221287-146-12-3205. PubMed PMID: 11101678.
160. Sun J, Singh V, Lau A, Stokes RW, Obregón-Henao A, Orme IM, et al. Mycobacterium tuberculosis nucleoside diphosphate kinase inactivates small GTPases leading to evasion of innate immunity. *PLoS pathogens*. 2013;9(7):e1003499. doi: 10.1371/journal.ppat.1003499. PubMed PMID: 23874203; PubMed Central PMCID: PMC3715411.
161. Khan S, Islam A, Hassan MI, Ahmad F. Purification and structural characterization of Mce4A from Mycobacterium tuberculosis. *Int J Biol Macromol*. 2016;93(Pt A):235-41. Epub 2016/11/05. doi: 10.1016/j.ijbiomac.2016.06.059. PubMed PMID: 27355757.
162. Daleke MH, Cascioferro A, de Punder K, Ummels R, Abdallah AM, van der Wel N, et al. Conserved Pro-Glu (PE) and Pro-Pro-Glu (PPE) protein domains target LipY lipases of pathogenic mycobacteria to the cell surface via the ESX-5 pathway. *J Biol Chem*. 2011;286(21):19024-34. Epub 2011/04/08. doi: 10.1074/jbc.M110.204966. PubMed PMID: 21471225; PubMed Central PMCID: PMC3099717.
163. de Jonge MI, Pehau-Arnaudet G, Fretz MM, Romain F, Bottai D, Brodin P, et al. ESAT-6 from Mycobacterium tuberculosis Dissociates from Its Putative Chaperone CFP-10 under Acidic Conditions and Exhibits Membrane-Lysing Activity. *Journal of Bacteriology*. 2007;189(16):6028-34. doi: 10.1128/JB.00469-07. PubMed PMID: 1791297422312708262related:ppgF0IP32xgJ.
164. Smith J, Manoranjan J, Pan M, Bohsali A, Xu J, Liu J, et al. Evidence for pore formation in host cell membranes by ESX-1-secreted ESAT-6 and its role in Mycobacterium marinum escape from the vacuole. *Infect Immun*. 2008;76(12):5478-87. Epub 2008/10/15. doi: 10.1128/IAI.00614-08. PubMed PMID: 18852239; PubMed Central PMCID: PMC2583575.
165. Refai A, Haoues M, Othman H, Barbouche MR, Moua P, Bondon A, et al. Two distinct conformational states of Mycobacterium tuberculosis virulent factor early secreted antigenic target 6 kDa are behind the discrepancy around its biological functions. *FEBS J*. 2015;282(21):4114-29. doi: 10.1111/febs.13408. PubMed PMID: 26260636.
166. Knodler LA, Vallance BA, Hensel M, Jackel D, Finlay BB, Steele-Mortimer O. Salmonella type III effectors PipB and PipB2 are targeted to detergent-resistant microdomains on internal host cell membranes. *Mol Microbiol*. 2003;49(3):685-704. Epub 2003/07/17. PubMed PMID: 12864852.
167. Franco LH, Nair VR, Scharn CR, Xavier RJ, Torrealba JR, Shiloh MU, et al. The Ubiquitin Ligase Smurf1 Functions in Selective Autophagy of Mycobacterium

- tuberculosis and Anti-tuberculous Host Defense. *Cell Host Microbe*. 2017;21(1):59-72. Epub 2016/12/27. doi: 10.1016/j.chom.2016.11.002. PubMed PMID: 28017659; PubMed Central PMCID: PMC5699477.
168. Ouimet M, Koster S, Sakowski E, Ramkhelawon B, van Solingen C, Oldebeken S, et al. Mycobacterium tuberculosis induces the miR-33 locus to reprogram autophagy and host lipid metabolism. *Nat Immunol*. 2016;17(6):677-86. Epub 2016/04/19. doi: 10.1038/ni.3434. PubMed PMID: 27089382; PubMed Central PMCID: PMC4873392.
169. Mohareer K, Asalla S, Banerjee S. Cell death at the cross roads of host-pathogen interaction in Mycobacterium tuberculosis infection. *Tuberculosis (Edinb)*. 2018;113:99-121. doi: 10.1016/j.tube.2018.09.007. PubMed PMID: 30514519.
170. Qiu S, Cote M. From hitchhiker to hijacker: pathogen exploitation of endosomal phosphoinositides (1). *Biochem Cell Biol*. 2019;97(1):1-9. Epub 2018/05/11. doi: 10.1139/bcb-2017-0317. PubMed PMID: 29746785.
171. Nascimbeni AC, Codogno P, Morel E. Phosphatidylinositol-3-phosphate in the regulation of autophagy membrane dynamics. *FEBS J*. 2017;284(9):1267-78. doi: 10.1111/febs.13987. PubMed PMID: 27973739.
172. Axe EL, Walker SA, Manifava M, Chandra P, Roderick HL, Habermann A, et al. Autophagosome formation from membrane compartments enriched in phosphatidylinositol 3-phosphate and dynamically connected to the endoplasmic reticulum. *J Cell Biol*. 2008;182(4):685-701. doi: 10.1083/jcb.200803137. PubMed PMID: 18725538; PubMed Central PMCID: PMC2518708.
173. De Matteis MA, Wilson C, D'Angelo G. Phosphatidylinositol-4-phosphate: the Golgi and beyond. *Bioessays*. 2013;35(7):612-22. Epub 2013/05/29. doi: 10.1002/bies.201200180. PubMed PMID: 23712958.
174. Matsuoka K, Orci L, Amherdt M, Bednarek SY, Hamamoto S, Schekman R, et al. COPII-coated vesicle formation reconstituted with purified coat proteins and chemically defined liposomes. *Cell*. 1998;93(2):263-75. Epub 1998/05/06. PubMed PMID: 9568718.
175. Blumental-Perry A, Haney CJ, Weixel KM, Watkins SC, Weisz OA, Aridor M. Phosphatidylinositol 4-phosphate formation at ER exit sites regulates ER export. *Dev Cell*. 2006;11(5):671-82. Epub 2006/11/07. doi: 10.1016/j.devcel.2006.09.001. PubMed PMID: 17084359.
176. Sarkes D, Rameh LE. A novel HPLC-based approach makes possible the spatial characterization of cellular PtdIns5P and other phosphoinositides. *Biochem J*. 2010;428(3):375-84. Epub 2010/04/08. doi: 10.1042/BJ20100129. PubMed PMID: 20370717; PubMed Central PMCID: PMC2944655.

177. Akil A, Peng J, Omrane M, Gondeau C, Desterke C, Marin M, et al. Septin 9 induces lipid droplets growth by a phosphatidylinositol-5-phosphate and microtubule-dependent mechanism hijacked by HCV. *Nat Commun*. 2016;7:12203. doi: 10.1038/ncomms12203. PubMed PMID: 27417143; PubMed Central PMCID: PMC4947189.
178. Jin N, Lang MJ, Weisman LS. Phosphatidylinositol 3,5-bisphosphate: regulation of cellular events in space and time. *Biochem Soc Trans*. 2016;44(1):177-84. Epub 2016/02/11. doi: 10.1042/BST20150174. PubMed PMID: 26862203; PubMed Central PMCID: PMC4836390.
179. Behar SM, Martin CJ, Nunes-Alves C, Divangahi M, Remold HG. Lipids, apoptosis, and cross-presentation: links in the chain of host defense against *Mycobacterium tuberculosis*. *Microbes Infect*. 2011;13(8-9):749-56. Epub 2011/04/05. doi: 10.1016/j.micinf.2011.03.002. PubMed PMID: 21458584; PubMed Central PMCID: PMC3130819.
180. Roche PW, Triccas JA, Avery DT, Fifis T, Billman-Jacobe H, Britton WJ. Differential T cell responses to mycobacteria-secreted proteins distinguish vaccination with bacille Calmette-Guerin from infection with *Mycobacterium tuberculosis*. *J Infect Dis*. 1994;170(5):1326-30. Epub 1994/11/01. PubMed PMID: 7963739.
181. Roche PW, Feng CG, Britton WJ. Human T-cell epitopes on the *Mycobacterium tuberculosis* secreted protein MPT64. *Scand J Immunol*. 1996;43(6):662-70. Epub 1996/06/01. PubMed PMID: 8658056.
182. Mustafa T, Wiker HG, Morkve O, Sviland L. Reduced apoptosis and increased inflammatory cytokines in granulomas caused by tuberculous compared to non-tuberculous mycobacteria: role of MPT64 antigen in apoptosis and immune response. *Clin Exp Immunol*. 2007;150(1):105-13. Epub 2007/08/23. doi: 10.1111/j.1365-2249.2007.03476.x. PubMed PMID: 17711491; PubMed Central PMCID: PMC2219281.
183. Reddick LE, Alto NM. Correlative light and electron microscopy (CLEM) as a tool to visualize microinjected molecules and their eukaryotic sub-cellular targets. *J Vis Exp*. 2012;(63):e3650. Epub 2012/05/17. doi: 10.3791/3650. PubMed PMID: 22588091; PubMed Central PMCID: PMC3466960.
184. Bykov YS, Cortese M, Briggs JA, Bartenschlager R. Correlative light and electron microscopy methods for the study of virus-cell interactions. *FEBS Lett*. 2016;590(13):1877-95. Epub 2016/03/25. doi: 10.1002/1873-3468.12153. PubMed PMID: 27008928.
185. Vida TA, Emr SD. A new vital stain for visualizing vacuolar membrane dynamics and endocytosis in yeast. *J Cell Biol*. 1995;128(5):779-92. Epub 1995/03/01. PubMed PMID: 7533169; PubMed Central PMCID: PMC2120394.

186. Guimaraes RS, Delorme-Axford E, Klionsky DJ, Reggiori F. Assays for the biochemical and ultrastructural measurement of selective and nonselective types of autophagy in the yeast *Saccharomyces cerevisiae*. *Methods*. 2015;75:141-50. Epub 2014/12/09. doi: 10.1016/j.ymeth.2014.11.023. PubMed PMID: 25484341.
187. Torggler R, Papinski D, Kraft C. Assays to Monitor Autophagy in *Saccharomyces cerevisiae*. *Cells*. 2017;6(3). Epub 2017/07/14. doi: 10.3390/cells6030023. PubMed PMID: 28703742; PubMed Central PMCID: PMC5617969.
188. Wiens KE, Ernst JD. The Mechanism for Type I Interferon Induction by *Mycobacterium tuberculosis* is Bacterial Strain-Dependent. *PLoS Pathog*. 2016;12(8):e1005809. Epub 2016/08/09. doi: 10.1371/journal.ppat.1005809. PubMed PMID: 27500737; PubMed Central PMCID: PMC4976988.